PRECLINICAL STUDIES OF TELOMERASE INHIBITOR IMETELSTAT IN

NON-SMALL CELL LUNG CANCER

APPROVED BY SUPERVISORY COMMITTEE

John D. Minna, M.D. (Mentor)

Jerry W. Shay, Ph.D. (Chairman)

Rolf A. Brekken, Ph.D.

Michael A. White, Ph.D.

DEDICATION

For Linda, Bob, Mike, Bill, Pauline, Rena, Aaron, Matt, and Elizabeth

# PRECLINICAL STUDIES OF TELOMERASE INHIBITOR IMETELSTAT IN NON-SMALL CELL LUNG CANCER

by

ROBIN ELIZABETH FRINK

DISSERTATION

Presented to the Faculty of the Graduate School of Biomedical Sciences

The University of Texas Southwestern Medical Center at Dallas

In Partial Fulfillment of the Requirements

For the Degree of

DOCTOR OF PHILOSOPHY

The University of Texas Southwestern Medical Center at Dallas

Dallas, Texas

May, 2013

ACKNOWLEDGEMENTS

There are so many people I would like to thank for making this achievement possible. First and foremost, I would like to thank Dr. John Minna, my mentor, for accepting me into his lab and allowing me to pursue my PhD under his guidance. I have learned so much from his example of patience, generosity and diplomacy as he supported me through the challenges and intricacies of graduate school. I would also like to thank my committee members Drs. Jerry Shay, Rolf Brekken and Michael White for their advice, expertise and perspective. I greatly appreciate their open doors and many hours of discussion and suggestions as the project progressed.

This work would not have been possible without the collaboration with Geron Corporation who provided many resources including monetary support. Ning Go and Katia Bassett were especially instrumental with their continual insight and feedback.

I am very grateful for my colleagues in the Minna lab, both past and present, for all of their many hours of discussion, technical guidance, insight, support and friendship. I would especially like to thank Drs. Rachel Greer, Jill Larsen, Michael Peyton, David Shames, and Chunli Shao.

Finally, I would like to thank my loving family for their support and encouragement through this endeavor, especially my parents who nurtured my love of science from an early age, my wonderful husband and best friend Matt, and my beautiful daughter Elizabeth.

PRECLINICAL STUDIES OF TELOMERASE INHIBITOR IMETELSTAT IN NON-SMALL CELL LUNG CANCER

Robin Elizabeth Frink

The University of Texas Southwestern Medical Center at Dallas, 2013

Supervising Professor: John D. Minna, M.D.

## ABSTRACT

Telomerase is expressed in ~90% of all cancers but is not expressed in most somatic cells making it an attractive target for cancer therapy. Telomerase has two essential components, a reverse transcriptase (hTERT) and an RNA template (hTR or hTERC). The RNA template is used by the reverse transcriptase to add the TTAGGG hexameric repeats to elongate telomeres and compensate for the loss of telomeres each cell division caused by the

end replication problem. Imetelstat is an oligonucleotide designed to bind the hTR telomerase template component and inhibit telomerase leading to progressive telomere shortening associated senescence or cell death. The work described here examined the efficacy of imetelstat in a panel of non-small cell lung cancer (NSCLC) cell lines. Imetelstat was tested in a short-term liquid colony formation assay, a 5-day drug response assay, and long-term continuous treatment *in vitro* and *in vivo*.

The panel of over 70 NSCLC cell lines used for this study ranged from 1.5 kb to 20 kb in average telomere length as well as a wide range in telomerase activity, growth rate, NSCLC sub-type, and oncogenotype providing a broad basis for comparison of response to imetelstat. All cell lines tested showed inhibition to telomerase with imetelstat treatment.

In liquid colony formation, a wide range of response to 3 μM imetelstat was seen. Colony formation inhibition ranged from 96% inhibition in HCC44 to H441 which shows a greater than 2-fold increase in colony forming ability in the presence of imetelstat, though not statistically significant.

1 μM imetelstat was given long-term in 8 different cell lines and telomerase inhibition and telomere shortening was observed in all cases. Continuous treatment led to a reduction in growth rate and eventual cell death in all but two cell lines and imetelstat response time varied among the cell lines based on initial telomere length and growth rate. Calu-3 had the fastest response time (11 days or as few as 2 population doublings) to see a change in growth rate and 32 population doublings for cell death in all cells. Calu-3, H1648 and HCC827 all showed reduced growth rate in the presence of imetelstat *in vivo* as well. Imetelstat inhibits

telomerase, shortens telomeres and leads to cell death in many NSCLC cell lines both *in vitro* and *in vivo* supporting the idea of telomerase inhibition for the treatment of lung cancers.

# TABLE OF CONTENTS

LIST OF FIGURES

LIST OF TABLES

LIST OF ABBREVIATIONS

**AC –** adenocarcinoma

**ALDH -** aldehyde dehydrogenase

**ALT** - alternative lengthening of telomeres

**ATCC -** American Type Culture Collection

**AZT** - azidothymidine

**BAA** - BODIPY®-aminoacetate

**BAAA** - BODIPY®-aminoacetaldehyde

**BIBR 1532** - (2-[(E)-3-naphthalen-2-yl-but-2-enoylamino]-benzoic acid)

**BRG1** -Brahma-related gene 1

**CT** - computed tomography

**DEAB** - diethylaminobenzaldehyde

**DMSO** - dimethyl sulfoxide

**DNA** - deoxyribonucleic acid

**EGCG** - epigallocatechin gallate

**EGFR** - epidermal growth factor receptor

**ErbB** - erythroblastic leukemia viral oncogene homolog

**FACS** - fluorescent activated cell sorting

**FBS** - fetal bovine serum

**FISH** - fluorescence in situ hybridization

**HIV** - Human immunodeficiency virus

**hTERT** - human telomerase reverse transcriptase

**hTR** - human telomerase RNA

**IACUC** - Institutional Animal Care and Use Committees

**IC50** - inhibitory concentration that kills 50% of cells

**ITAS** - internal telomerase assay standard

**Kb** - kilobases

**KRAS** - V-Ki-ras2 Kirsten rat sarcoma viral oncogene homolog

**LCC** - large cell carcinoma

**M1** - mortality stage 1

**M2** - mortality stage 2

**MAPK** - mitogen-activated protein kinase

**MM** - mismatch control oligonucleotide for imetelstat

**mRNA** - messenger RNA

**MTS** - (3-(4,5-dimethylthiazol-2-yl)-5-(3-carboxymethoxyphenyl)-2-(4-sulfophenyl)-2H-tetrazolium)

**NCI** - National Cancer Institute

**NOD/SCID** - non-obese diabetic/severe combined immunodeficiency

**NSCLC** - non-small cell lung cancer

**PBS** - phosphate buffered saline

**PCR** - polymerase chain reaction

**PML** - promyelocytic leukemia

**PI** - propidium iodide

**PI3K** - phosphoinositide 3-kinase

**POT1** - Protection of telomeres protein 1

**RAP1** - Ras-related protein 1

**RNA** - ribonucleic acid

**RNase H** - Ribonuclease H

**RO** - reverse order control oligonucleotide for imetelstat

**RPMI** - Roswell Park Memorial Institute medium

**SCC** - squamous cell carcinoma

**SCLC** - small cell lung cancer

**SMARCA4** - SWI/SNF related, matrix associated, actin dependent regulator of chromatin, subfamily a, member 4

**STAT** - signal transducer and activator of transcription

**STELA** - single telomere length analysis

**TIN2** - TRF1-interacting nuclear protein 2

**TITF1** - thyroid transcription factor 1

**TNM** - tumor, node, metastasis classification of tumors

**TP53** - tumor protein 53 kilodaltons

**TPP1** - tripeptidyl peptidase I

**TRAP** - telomeric repeat amplification protocol

**TRF** - terminal restriction fragment

**TRF1** - telomeric repeat-binding factor 1

**TRF2** - telomeric repeat-binding factor 2

# CHAPTER ONE

## TELOMERES, TELOMERASE, AND LUNG CANCER

### 1.1 Telomeres and Telomerase in Cancer

#### *1.1.1 Telomeres*

Telomeres are highly conserved pieces of DNA located at the ends of chromosomes and function to protect the ends of chromosomes from DNA degradation, end-to-end fusion, and double strand DNA break repair (de Lange 2002). Due to the end replication problem, or inability for DNA to be fully replicated during DNA synthesis (Watson 1972), chromosomes shorten by 40-200 base pairs with each cell division (Harley, Futcher et al. 1990; Harley 1991; Counter, Avilion et al. 1992; Levy, Allsopp et al. 1992). Because DNA must be synthesized in a 5'→3' direction, the lagging strand of DNA requires multiple bindings of RNA primers to replicate the DNA resulting in small fragments that are eventually joined together by DNA polymerases. The DNA polymerases are unable to replicate the very end of the lagging strand where the final RNA primer binds, resulting in a small portion of unreplicated DNA which leads to shortening of telomeres with each round of DNA synthesis (Harley 1991; Levy, Allsopp et al. 1992). Telomeres contain non-coding DNA consisting of

the hexameric repeat TTAGGG (in mammals) (Moyzis, Buckingham et al. 1988) that is lost each cell division without losing critical, coding DNA. When the telomeric DNA gets too short on a few chromosome ends, the cells stop dividing and undergo replicative senescence to prevent loss of critical coding DNA (Wright and Shay 2002). This is believed to act as an initial and potent tumor suppressor.

All mammals have the same TTAGGG telomere sequence but other animals vary with their telomere sequences. Telomeres were discovered in *Tetrahymena*, a type of yeast with a repetitive telomere sequence of TTGGGG (Blackburn and Gall 1978). Telomeres in humans begin at 15-20 kb in length and gradually shorten with age (Moyzis, Buckingham et al. 1988; de Lange, Shiue et al. 1990). Other species have varying lengths of telomeres including mice with 40+ kb telomeres and ranging up to 50+ kb in rabbits and tigers (Gomes, Ryder et al. ; Kipling and Cooke 1990; Kelland 2005). Thus, there is likely to be fundamental differences in the role of telomeres among various mammals and in mechanisms regulating cancer and aging, such as between humans and mice, since there is a wide range of telomere lengths in these species (Shay and Wright 2001).

Telomere stability is maintained by the shelterin complex. The shelterin complex is a set of six proteins (TRF1, TRF2, TIN2, TPP1, RAP1, POT1) that bind and protect the telomeres and regulate telomere length (Figure 1.1) (de Lange 2005). TRF1 and TRF2 bind the double stranded portion of the telomere and are necessary to recruit the remaining telomere binding proteins (Zhong, Shiue et al. 1992; Bilaud, Brun et al. 1997; Broccoli, Smogorzewska et al. 1997). TIN2 binds to TRF1 and TRF2 and bridges the two proteins

together (Kim, Beausejour et al. 2004; Ye, Donigian et al. 2004). POT1 binds to the single-stranded portion of the telomere and TPP1 bridges POT1 to TIN2 and the rest of the complex (Ye, Hockemeyer et al. 2004). It has been shown that POT1 is not recruited to the telomere without TPP1 (Hockemeyer, Palm et al. 2007; Xin, Liu et al. 2007). The final shelterin complex protein is RAP1 which binds to TRF2 (Li, Oestreich et al. 2000).

Binding of the shelterin complex to the telomeres maintains structure and prevents the telomere from being recognized as a DNA double-stranded break. The telomere is mostly double-stranded DNA but there is a single-stranded 3' overhang of 50-300 base pairs in length (Wright, Tesmer et al. 1997; Huffman, Levene et al. 2000). This 3' overhang tucks itself back into the double-stranded portion of the telomere forming a lariat structure called the telomere loop or T-loop (Figure 1.1B) (de Lange 2004). The very end of the 3' overhang displaces a small portion of the double-stranded telomere and binds, leaving a small single-stranded section, called the displacement loop or D-loop (Griffith, Comeau et al. 1999). The elimination of the double strand portion of the telomere to create the 3' overhang also contributes to progressive telomere shortening with each DNA replication (Lam, Akhter et al. 2010; Wu, van Overbeek et al. 2010).

There are multiple methods available for measuring telomere length including telomere restriction fragment (TRF) by Southern blot, fluorescence in situ hybridization (FISH, (Lansdorp, Verwoerd et al. 1996), qPCR (Cawthon 2002) and single telomere length analysis (STELA) (Baird, Rowson et al. 2003). TRF is a modified Southern blot that uses restriction enzymes to digest the DNA and then probes for the telomeric sequence on a gel.

This produces a smear on the gel and average telomere length of the sample can be determined. In addition, TRF analysis can provide some information about the shortest telomeres. FISH, or telo-FISH, probes the telomeric sequence of a metaphase spread or interphase cell, allowing for visualization of telomere lengths at the ends of each chromosome. Higher intensity of the signal translates to longer telomeres on a particular chromosome end (Pennarun, Granotier et al. 2008). This provides more quantitative information about the shortest telomeres. qPCR provides a relative average telomere length by measuring and comparing the difference in copy number variation of the TTAGGG repeats to a single gene copy number between a reference DNA sample and the sample of interest. STELA is another PCR based assay that measures the length of telomere of a single chromosome and is very quantitative about how short specific telomere ends can become. Each method has strengths and weaknesses. For this study, TRF was chosen to measure telomere length.

### *1.1.2 Telomerase*

In 1961, Hayflick demonstrated that human embryonic fibroblast cells were not immortal and have a limited ability to divide and this limit has been coined the "Hayflick limit" (Hayflick and Moorhead 1961) or replicative senescence. It has since been shown this limit is due to shortening of telomeres when cells are cultured under adequate conditions. For cells that divide beyond this limit such as during cancer progression and in some highly proliferative somatic cells, an enzyme called telomerase is activated to elongate telomeres.

Telomerase has two components that are necessary and sufficient to lengthen telomeres: the hTERT reverse transcriptase component and the hTR or hTERC RNA template component (Feng, Funk et al. 1995; Harrington, Zhou et al. 1997; Meyerson, Counter et al. 1997; Nakamura, Morin et al. 1997). hTERT extends the ends of the telomeres and uses the hTR RNA template component to add the appropriate hexameric TTAGGG repeats (Figure 1.2). Telomerase activity level is dependent on the expression of hTERT as hTR is universally expressed and hTERT expression correlates with overall telomerase activity (Avilion, Piatyszek et al. 1996; Kilian, Bowtell et al. 1997; Meyerson, Counter et al. 1997; Weinrich, Pruzan et al. 1997; Nakayama, Tahara et al. 1998; Cong, Wen et al. 1999; Horikawa, Cable et al. 1999). Telomerase is active during human fetal development but is suppressed in most somatic cells around 20 weeks of gestation (Ulaner, Hu et al. 1998). Germ-line and stem cells represent some of the few cell types that continue to have active telomerase after development, however this is not constitutive telomerase but rather activated telomerase in transit amplifying cells (Wright, Piatyszek et al. 1996).

### *1.1.3 Telomerase in Cancer*

The shortening of a few telomeres results in the Hayflick limit and cells senescing. This has been termed mortality stage 1 (M1). For cells to continue dividing past the Hayflick limit, they must inactivate tumor suppressor genes such as p53 and pRB that limit their ability to grow. Eventually, most cells that continue to divide beyond M1 will stop dividing after an extended lifespan (20 or 30 additional population doublings) when they reach

mortality stage 2 (M2) or "crisis" (Figure 1.3). Cells that reach crisis have many very short telomeres due to the additional cell divisions between M1 and M2. Telomeres in these cells are generally not long enough to continue to protect chromosomal ends and this results in telomere end fusions and a halt in cell growth and often apoptosis. Very rarely, cells can escape from crisis and continue to divide. For these cells to divide, they require the activation of telomerase to elongate telomeres. Cellular immortalization and cancer progression is a two-stage process where cells must overcome two growth barriers M1-senescence and M2-crisis to become immortal. (Wright, Pereira-Smith et al. 1989; Halvorsen, Leibowitz et al. 1999; Lustig 1999; Reddel 2000; Lin and Yan 2005; Newbold 2005). It was shown that introduction of hTERT alone into human cells before M1 or between M1 and M2 was sufficient to lead to cell immortalization (Bodnar, Ouellette et al. 1998). This indicated that telomere shortening was the cause of both M1 and M2. In addition, the introduction of hTERT into normal human cells did not result in any hallmarks of cancer progression (Morales, Holt et al. 1999; Lee, Choi et al. 2004) suggesting that hTERT is not oncogenic but is only permissive for extended cell proliferation.

Telomerase is active in ~90% of all cancer cells (Kim, Piatyszek et al. 1994) making it an almost universal cancer marker and target for cancer therapeutics. Although the process of how telomerase is reactivated in oncogenesis is not completely understood, hTERT is located on the p-arm of chromosome 5, which is frequently amplified in cancers contributing to increased expression of telomerase in cancers. (Bryce, Morrison et al. 2000; Zhang, Zheng et al. 2000).

While most human tumors activate telomerase to maintain the length of telomeres allowing for unlimited replication potential, about 10% of malignancies develop a method to lengthen telomeres that does not require telomerase activation called alternative lengthening of telomeres or ALT (Bryan, Englezou et al. 1995; Dunham, Neumann et al. 2000). ALT is characterized as a telomere lengthening mechanism that functions similar to homologous recombination. The first indications a cell is undergoing ALT to lengthen telomeres is the absence of any detectable telomerase but the telomeres are not shortening with continued cell division as well as a wide range in telomere length ranging from very short to very long within the cell population as opposed to a smaller range in telomere length in telomerase positive cells (Bryan and Reddel 1997; Feldser, Hackett et al. 2003; Reddel 2003; Newbold 2005). In addition, ALT cells have an increase in what are termed C-circle DNA (Cesare and Griffith 2004; Henson, Cao et al. 2009) and in ALT associated PML bodies (Yeager, Neumann et al. 1999; Grobelny, Godwin et al. 2000; Chung, Osterwald et al. 2012).

### *1.1.4 Targeting Telomerase in Cancer*

Because cells have overcome crisis to reach the stage of activating telomerase, cancers typically have critically short telomeres. Therefore, inhibiting telomerase should lead to cellular senescence or apoptosis with minimal cell divisions and should not affect most somatic cells which do not have active telomerase present. Inhibition of telomerase has been shown to shorten telomeres and lead to apoptosis of cancer cells (Hahn, Stewart et al. 1999; Herbert, Pitts et al. 1999; Zhang, Mar et al. 1999). While there could be some transient

effects on highly proliferative normal stem cells expressing telomerase, there should not be an effect on quiescent stem cells and there is no effect on normal, telomerase silent, human cells in culture.

Most cancers, including pediatric cancers have activated telomerase. As a result, telomerase has become a prognostic marker for some tumors including neuroblastoma patients. Studies have shown that five year event-free survival and five year overall survival show a significant difference when patients with high active telomerase in their tumors are compared to those without telomerase including Stage III and IV patients (Hiyama, Hiyama et al. 1995; Poremba, Willenbring et al. 1999). Some patients with Stage IV disease (IVS) experience very good prognosis with spontaneous regression of tumors without any intervention and many of these patients do not have detectable telomerase activity in their tumors (Hiyama, Hiyama et al. 1995). These studies provide evidence that telomerase is a necessary component of tumor progression and support telomerase as a target for cancer therapy.

Many approaches have been developed to target telomerase as a cancer therapeutic. hTERT is an ideal target for inhibiting telomerase because it is the rate limiting step of telomerase activity and it is the telomerase component not active in most somatic cells. Inhibition of hTERT causes growth arrest, a decrease in telomere length (Herbert, Pitts et al. 1999) and prevents *in vivo* tumor formation (Hahn, Stewart et al. 1999). Azidothymidine (AZT) is a nucleoside analog and reverse transcriptase inhibitor that has been shown to decrease telomerase activity by targeting the active site of hTERT (Strahl and Blackburn

1994; Strahl and Blackburn 1996; Kelland 2005). Another inhibitor of hTERT is epicatechin derivatives EGCG found in green tea as well as synthetic compounds of EGCG such as MST-132, MST-295, MST-199 which have shown potent inhibition of telomerase and subsequent telomere shortening (Naasani, Seimiya et al. 1998; Seimiya, Oh-hara et al. 2002). BIBR 1532 (2-[(E)-3-naphthalen-2-yl-but-2-enoylamino]-benzoic acid) is a non-competitive inhibitor of hTERT that functions similar to HIV reverse transcriptase inhibitors. Although it has shown promise inhibiting telomerase and leading to cellular senescence both *in vivo* and *in vitro*, BIBR1532 most likely will not proceed to the clinic because of weak bioavailability (Bojovic and Crowe ; Roth, Harley et al. ; Damm, Hemmann et al. 2001; Barma, Elayadi et al. 2003; Ward and Autexier 2005).

Telomeres have also been targeted for cancer therapy. Telomestatin, for example, targets the G-quadruplex secondary structure of telomeres disrupting the integrity of the protective loop structure leading to shortened telomeres and cell death (Shammas, Shmookler Reis et al. 2004; Gomez, O'Donohue et al. 2006). However, targeting telomeric structure could lead to side effects of targeting all cells since all cells have telomeres. Telomerase is a target that is almost universally expressed in cancers without targeting normal cells. While an argument can be made that targeting telomerase will also target critical telomerase expressing cells such as stem cells and germ-line cells (Zimmermann and Martens 2007), telomeres in these cells tend to be much longer than neighboring telomerase-negative cells. In addition, almost all cancer therapies currently in use also affect stem cells and medical oncologist are familiar with problems associated with hematological toxicities in standard

chemotherapy. Theoretically, telomerase targeted therapy should halt the growth in short-telomere cancer cells before damage is seen in stem cells and germ-line cells, minimizing side effects of therapy. Since greater than 90% of all human primary cancers have short telomeres, this suggests telomerase inhibition may be effective after a short period of treatment.

*1.1.5 Imetelstat as Cancer Therapy*

Another target for telomerase is the hTR RNA template component of telomerase. In 1995, Feng et al showed that hTR could be targeted with an oligonucleotide sequence that would bind to the hTR template region leading to telomerase inhibition, progressively shortened telomeres and eventual cell death (Feng, Funk et al. 1995). hTR has an eleven nucleotide sequence which serves as the template for the telomerase reverse transcriptase. However, intracellular delivery is a challenge for oligonucleotides. Oligonucleotides cannot cross the cell membrane and require a lipid carrier or transfection agent limiting *in vivo* application. To address this concern, a 13-mer oligonucleotide called imetelstat was developed that has a modified backbone and lipid moiety attached that effectively targets telomerase and solves the transfection problem.

Imetelstat, also known as GRN163L, was created to bind to hTR, the RNA template component of telomerase. The sequence is 5'-Palm-TAGGGTTAGACAA-3' and the backbone is an N3'→P5' thiophosphoramidate. The 3' oxygen is replaced with a 3'amino group (Figure 1.4) connecting the carbon ring and phosphate in the backbone as well as

another oxygen on the phosphate replaced with a sulfur (Pongracz 1999; Asai, Oshima et al. 2003; Herbert, Gellert et al. 2005). The modifications are present to prevent the oligo from being cleaved by RNase H (Sharma, Hsiao et al. 1996; Asai, Oshima et al. 2003). To aid in cellular uptake, a 16-carbon (palmitoyl) chain is covalently attached to the 5' end which facilitates cellular uptake (Herbert, Gellert et al. 2005). Imetelstat is not an anti-sense drug; it is a competitive inhibitor of telomerase activity by competing with the ability of hTR to form the telomerase holoenzyme complex. Because imetelstat is an oligonucleotide, controls can be easily made with alternative sequences to verify specificity and rule out off-target effects.

Imetelstat and imetelstat's precursor GRN163 (same oligo but without the lipid attachment) have been tested preclinically in multiple types of cancer demonstrating telomerase inhibition and telomere shortening in lung (Dikmen, Gellert et al. 2005), breast (Gellert, Dikmen et al. 2006; Hochreiter, Xiao et al. 2006), prostate (Marian, Wright et al. ; Asai, Oshima et al. 2003; Marian and Shay 2009), liver (Djojosubroto, Chin et al. 2005), brain (Marian, Cho et al. ; Ozawa, Gryaznov et al. 2004) and bladder cancers (Dikmen, Wright et al. 2008) as well as multiple myeloma and lymphoma (Akiyama, Hideshima et al. 2003; Wang, Wu et al. 2004).

Although many drugs have been developed to target telomerase, imetelstat is the first telomerase inhibitor to reach clinical testing. Many Phase I and Phase II clinical trials for multiple types of cancer have completed or are currently in progress (Table 1.1). Six Phase I clinical trials determined pharmacokinetics, pharmacodynamics, safety and tolerability of imetelstat alone and in combination with standard chemotherapies for the respective cancer

types including chronic lymphoproliferative diseases, solid tumors, multiple myeloma, non-small cell lung cancer (NSCLC), and breast cancer. For the Phase I trial in NSCLC, patients with advanced or metastatic stage IIIB or IV NSCLC were given three cycles of paclitaxel/carboplatin combination therapy on day 2 of a 21-day cycle along with escalating doses of imetelstat. The trial was altered throughout due to hematological toxicities of imetelstat including neutropenia and thrombocytopenia experienced by many but not all of the patients. Because of these side effects, the patients' blood counts were too low to receive paclitaxel/carboplatin therapy so the imetelstat dosage was reduced.

Imetelstat was recently tested in a Phase II clinical trial for breast cancer in which patients with locally recurrent metastatic breast cancer were randomized to receive paclitaxel with or without imetelstat. Paclitaxel was given on day one and eight of a 21 day cycle and imetelstat on day one. Recently this trial was discontinued due to an interim analysis that found the imetelstat treated arm had a worse progression-free survival prognosis. Other Phase II clinical trials include studies evaluating patients with multiple myeloma and essential thrombocythemia continue.

Imetelstat has moved from the Phase I to a Phase II clinical trial for NSCLC as well. The current NSCLC trial is to evaluate imetelstat as maintenance therapy. Patients with stage IIIB or IV NSCLC were accepted into the trial and given four cycles of paclitaxel/carboplatin chemotherapy. Those that responded were then randomized in a 2:1 ratio into groups receiving bevacizumab as maintenance therapy either with or without imetelstat. The primary end-point of the trial is progression free survival and this was

correlated with initial telomere length. In an initial analysis those patients with the shortest initial telomere length appeared to respond best to the therapy and had a statistically significant increase in progression free survival compared to the control arm. The trial has completed enrollment and official results should be available in the later part of 2013. If the initial analysis holds up, it may suggest selection for patients with the shortest telomeres to be enrolled in future clinical trials.

## 1.2 Lung Cancer

### *1.2.1 Statistics*

Lung cancer is the leading cause of cancer related death for men and women in the United States causing an estimated 160,340 deaths in 2012 and, with an estimated 226,160 new cases in 2012, it is the second most commonly diagnosed cancer among men and women (Figure 1.5). Overall, men have a 1 in 13 chance of developing lung cancer in their lifetime and women have 1 in 16 odds. The 5-year overall survival rate is currently around 16% and has shown minimal improvements in almost 40 years (5 year overall survival in 1975 was 12%) (Siegel, Naishadham et al. 2012). The leading cause of lung cancer is smoking, however, there is a rise in never smokers, especially in females (Stockwell, Goldman et al. 1992; Brownson, Alavanja et al. 1998; Radzikowska, Glaz et al. 2002; Toh, Gao et al. 2006; Sun, Schiller et al. 2007). Smokers have a 10 to 20 fold increased risk of developing lung cancer (Brownson, Alavanja et al. 1998). Smoking status of patients is defined in “pack

years". A person that smokes 1 pack of cigarettes daily for 1 year is a 1 pack year smoker. If a patient smoked 1 pack daily for 10 years, they would be a 10 pack year smoker. If a patient smoked 2 packs of cigarettes daily for 10 years, they would be a 20 pack year smoker.

Only 15% of lung cancers are diagnosed at an early stage and these cases are generally detected incidentally from chest imaging conducted for unrelated reasons. (Raz, Glidden et al. 2007). Most cases are not discovered until patients are symptomatic which does not occur until late stage disease when the cancer is either locally advanced or metastatic (Jett 2012). Unlike breast and prostate cancer, there are no standard early detection methods for lung cancer. However, recent studies have shown that low-dose computed tomography (CT) scans detected 70-80% of early stage lung cancers that were missed by x-rays resulting in a 20% decrease in mortality (Aberle, Berg et al. 2011; Jett 2012).

### *1.2.2 Pathology*

Lung cancer is divided into two main categories based on clinicopathologic features: Small Cell Lung Cancer (SCLC) and Non-small Cell Lung Cancer (NSCLC). All cancer that is not classified as SCLC by default becomes NSCLC. NSCLC can be further divided into adenocarcinoma (AC), squamous cell carcinoma (SCC) and large cell carcinoma (LCC) histologies. Some tumors are not differentiated enough to be categorized in one of the three NSCLC classifications and these tumors are referred to as poorly differentiated, undifferentiated, or simply NSCLC. Histology can play a role in determining a course of

treatment as studies have shown different histologies respond differently to therapy (Triano, Deshpande et al. 2010).

Small cell lung cancer represents 15% of the lung cancer cases and is most prevalent in smokers (Govindan, Page et al. 2006). SCLC tends to occur in the central airways of the lung and tumors are characterized by expression of neuroendocrine markers. While smoking is associated with all types of lung cancer, adenocarcinoma is more prevalent in never smokers and has epithelial origin from peripheral lung (Muscat and Wynder 1995; Brownson, Alavanja et al. 1998; Kreuzer, Kreienbrock et al. 1999; Toh, Gao et al. 2006). Adenocarcinoma expression markers include NapsinA and TITF1. Squamous cell carcinoma is of epithelial cell origin and tends to occur in the central airways of the lung. While adenocarcinoma is more prevalent in non-smokers, squamous cell carcinoma tends to be more common in smokers. p63 can be used to help distinguish squamous cell carcinoma from small cell or adenocarcinoma. Large cell carcinoma is a rare diagnosis (only 5-10% of lung cancers) characterized by larger cells and a higher cytoplasmic-to-nuclear ratio.

### *1.2.3 Tumor Staging*

Tumor staging is determined at diagnosis to describe the severity and extent of the cancer. Stage determination is based on three factors: T class which describes the size and extent of the primary tumor, N class which denotes the extent of involvement of the regional lymph nodes, and M which designates the presence or absence of distant metastasis. All TNM designations are shown in Table 1.2. Once the TNM status has been determined, TNM

ranking combinations are then grouped together and categorized as a stage. Stages range from 0-IV with increasing severity (Table 1.3). Staging is used to determine prognosis and treatment, evaluate treatment results, and to simplify communication between treatment centers (Goldstraw 2010). About 25% of NSCLC diagnosed is Stage I or II, about 35% present with Stage III and about 40% are diagnosed with Stage IV (Gadgeel, Ramalingam et al.).

*1.2.4 Molecular Changes in Lung Cancer*

Three common genetic mutations contributing to the pathogenesis of lung cancer are EGFR, KRAS, and TP53. EGFR is mutated in about 50% of lung cancers (Sharma, Bell et al. 2007). EGFR is a member of the ErbB receptor tyrosine kinase family and forms homodimers and heterodimers with other tyrosine kinase family members that in turn trigger a cascade of signaling events for proliferation, angiogenesis, and prevention of apoptosis (Sharma, Bell et al. 2007). EGFR mutations are most prevalent in adenocarcinomas in female patients and never smokers (Shigematsu and Gazdar 2006; Sharma, Bell et al. 2007).

About 30% of adenocarcinomas have KRAS mutations (Rodenhuis and Slebos 1990) and generally occur in patients with a history of smoking (Ahrendt, Decker et al. 2001). KRAS is downstream of EGFR and mediates cell proliferation, differentiation and apoptosis by interacting with MAPK (mitogen-activated protein kinase), STAT (signal transducer and activator of transcription), and PI3K (phosphoinositide 3-kinase) signaling cascades (Downward 1998; Vojtek and Der 1998; Shields, Pruitt et al. 2000; Downward 2003).

KRAS mutations are oncogenic and contribute to perpetual stimulation of these proliferation pathways (Capella, Cronauer-Mitra et al. 1991; Brandao, Brega et al. 2012). EGFR mutations and KRAS mutations are generally mutually exclusive (Pao, Wang et al. 2005; Shigematsu and Gazdar 2006; Riely, Marks et al. 2009; Suda, Tomizawa et al. 2010).

TP53 is the most commonly mutated gene in all cancers and is mutated in 80% of lung cancers. p53 is a transcription factor that functions as a tumor suppressor gene and regulates many signaling pathways that aid in this process such as apoptosis, senescence, DNA repair and induction of cell cycle arrest (Lane 1992; Levine and Oren 2009; Aylon and Oren 2011). There are many mutations common in p53 that lead to carcinogenesis by no longer mediating these pathways properly.

### *1.2.5 Treatment*

Treatment plans for lung cancer are largely dependent on the stage at which patients are diagnosed. Stage I and II cases generally undergo surgical resection or radiation therapy if the patient is not a candidate for surgery. Stage II patients frequently receive adjuvant chemotherapy after tumor resection with platinum-based doublet chemotherapy (Gadgeel, Ramalingam et al.). Stage III patients usually receive chemotherapy plus radiation therapy while Stage IV patients commonly receive first-line chemotherapy, generally a platinum-based doublet therapy followed by maintenance therapy.

The chemotherapy choices for NSCLC include carboplatin and cisplatin platinum-based chemotherapies and they are generally combined with paclitaxel, docetaxel,

pemetrexed, vinorelbine or gemcitabine (Gadgeel, Ramalingam et al.). In addition to stage, histology may also play a role in determining optimal therapy as different subtypes have been shown to respond better or worse to some chemotherapy. Pemetrexed, for example, has shown little efficacy in squamous cell carcinoma but improved survival in patients with adenocarcinoma (Gadgeel, Ramalingam et al. ; Ciuleanu, Brodowicz et al. 2009; Scagliotti, Hanna et al. 2009).

Maintenance therapy is therapy given after a patient responds to first-line therapy to prevent recurrence. This second line therapy may also involve personalized medicine where patient tumors are genetically profiled for mutations. These mutations can then be exploited by selecting therapies to which tumors are most likely to respond. Some therapies target specific mutations or over-expressing genes. There are several therapies that target EGFR mutations, for example. Gefitinib and erlotinib are EGFR tyrosine kinase inhibitors (TKIs) and have been used in the clinic with promising results. Patients with the appropriate EGFR mutations in their tumors generally respond with tumor regression and achieve remission (Maemondo, Inoue et al. 2010), however incidence of recurrence is alarmingly high. Most tumors eventually mutate to bypass the targeted therapy leading to recurrence with fewer treatment options and poor outcomes (Pao, Miller et al. 2005; Brandao, Brega et al. 2012).

Despite advances in treatment options, minimal improvements have been made in 5-year overall survival of lung cancer patients. Treatment options that show initial promise unfortunately generally lead to recurrence with even worse prognosis. This thesis examines

the option of targeting telomerase in non-small cell lung cancer for improved patient outcome.

"Perhaps the best thing to do is to stop writing introductions and get on with the book."
–*A.A Milne*

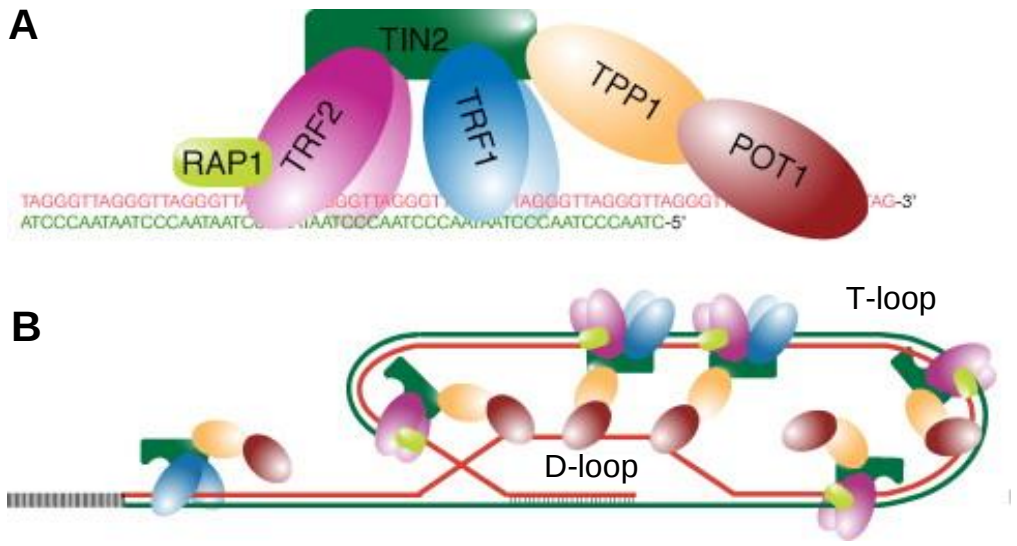


**Figure 1.1 Shelterin Complex at Telomere Ends.** (A) The shelterin complex located at the ends of chromosomes protects the telomere ends. TRF1 and TRF2 bind double stranded telomeric DNA. TIN2 connects TRF1 and TRF2. POT1 binds single stranded portions of telomeric DNA and is connected to the rest of the complex via TPP1 which binds TIN2. (B) The structure of the telomere with shelterin attached. Telomeres loop back forming a T-loop structure. The single-stranded over-hang at the very end of the telomere displaces part of the double-stranded portion forming the D-loop.

Figure adapted from Denchi 2009.

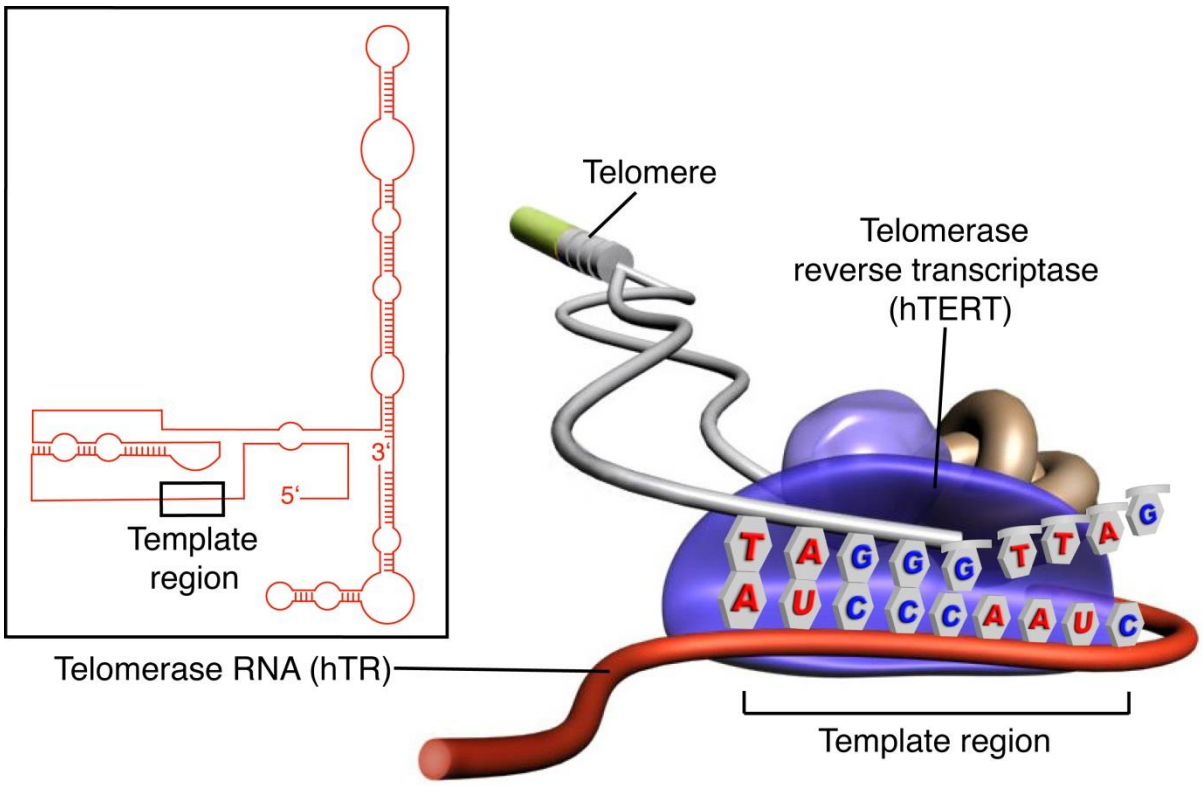


**Figure 1.2 Telomerase Complex.** Active telomerase consists of two components, the hTERT reverse transcriptase and the hTR RNA template. hTERT provides the machinery to elongate the telomeres and uses the RNA template to add the appropriate TTAGGG repeats. Telomerase must have both components to function properly.

Figure adapted from Shay and Wright 2006.

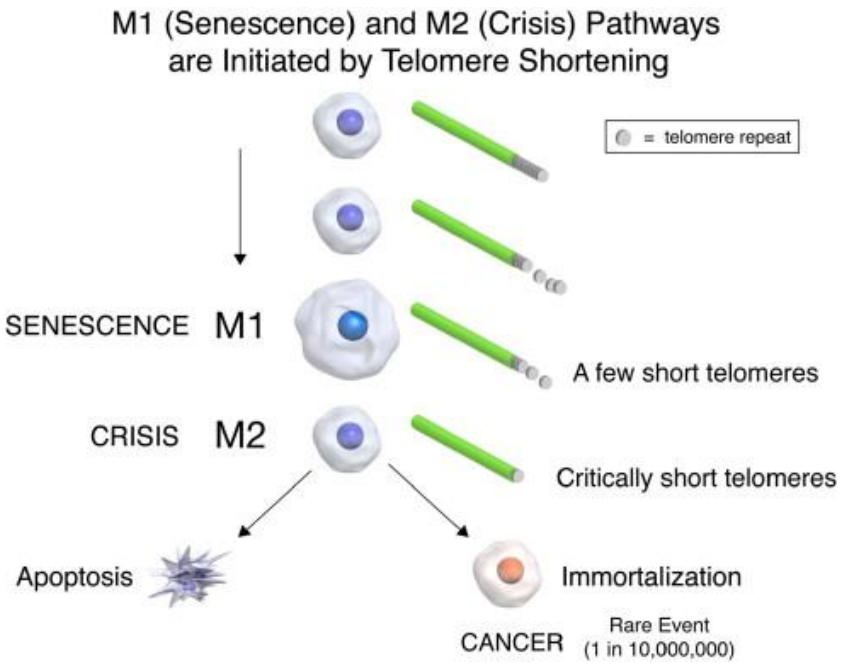


**Figure 1.3 The M1 and M2 Model of Senescence and Cellular Immortalization.** As cells divide, telomeres progressively shorten with each cell division. When a few telomeres become too short, it triggers senescence in the cell (M1). Some cells can overcome the senescence by inactivating tumor suppressor genes and continue to divide eventually reaching M2 or crisis. Very rarely, a cell can escape M2 by activating telomerase to stabilize telomeres and become immortal.

Figure adapted from Shay and Wright 2010.

**A**

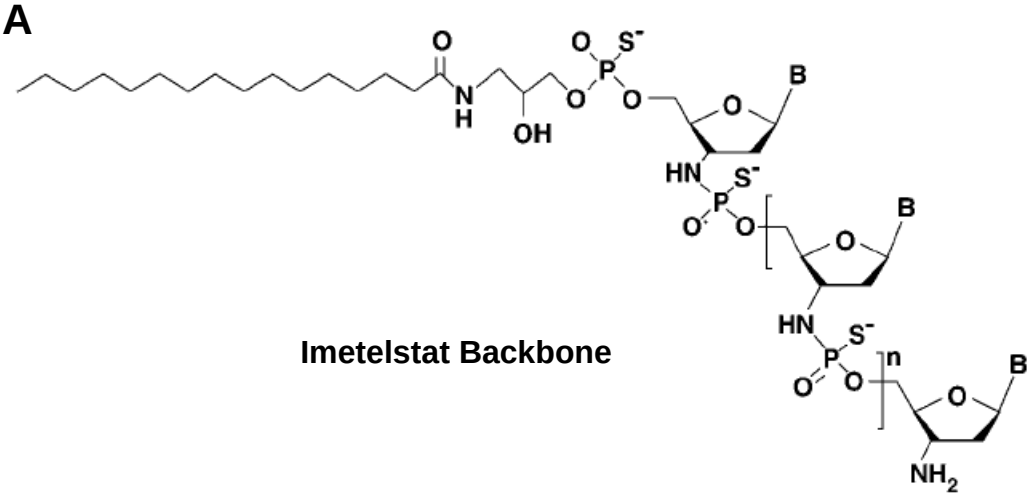


**B**

| Oligo Name | Sequence |
|---|---|
| Imetelstat | 5'-Palm-TAGGGTTAGACAA-3' |
| Mismatch | 5'-Palm-TAGGTGTAAGCAA-3' |
| Sense | 5'-Palm-ATCCCAATCTGTT-3' |

**Figure 1.4 Imetelstat Structure and Imetelstat and Control Sequences.** (A) The backbone structure of imetelstat is a single stranded DNA with modifications. A 16-carbon (palmitoyl) lipid has been added to the 5' end of the oligo as well as an amino and sulphur substitution on the phosphate. (B) Imetelstat, mismatch and sense control sequences. All oligos listed in (B) have the same backbone structure depicted in (A).

(A) was adapted from Herbert, Gellert, et al. 2005.

## Table 1.1 Imetelstat Clinical Trials

| Tumor Type | Phase | Status | Trials | Treatments | Enrollment | Reference |
|---|---|---|---|---|---|---|
| Breast | II | Active, not recruiting | Imetelstat with paclitaxel in locally recurrent or metastatic tumors | imetelstat, paclitaxel | 156 | NCT01256762 |
| Breast | I | Active, not recruiting | Safety study of imetelstat to reverse trastuzumab resistance in Her2+ breast cancer | imetelstat, trastuzumab | 10 | NCT01265927 |
| Breast | I/II | Active, not recruiting | Imetelstat with paclitaxel and bevacizumab in locally recurrent or metastatic breast cancer | imetelstat, paclitaxel, bevacizumab | 35 | NCT00732056 |
| Chronic Lymphoproliferative Disease | I | Active, not recruiting | Safety and dose study of imetelstat in CLD | imetelstat | 48 | NCT00124189 |
| Multiple Myeloma | II | Recruiting | Improvement in response and progression-free survival of imetelstat in previously treated multiple myeloma | standard of care, imetelstat | 48 | NCT01242930 |
| Multiple Myeloma | I | Completed | Safety and dose study of imetelstat in multiple myeloma | imetelstat | 20 | NCT00594126 |
| Myelofibrosis | | Recruiting | Imetelstat for primary or secondary myelofibrosis | imetelstat | 29 | NCT01731951 |
| Myeloma | I | Completed | Safety and dose study of imetelstat and velcade in myeloma | imetelstat, velcade | 40 | NCT00718601 |
| NSCLC | II | Active, not recruiting | Imetelstat as maintenance therapy after initial chemotherapy | imetelstat, bevacizumab | 96 | NCT01137968 |
| NSCLC | I | Completed | Safety and tolerability of imetelstat in combination with paclitaxel and carboplatin in advanced or metastatic NSCLC | imetelstat, paclitaxel, carboplatin | 27 | NCT00510445 |
| Solid Tumors | I | Active, not recruiting | Safety and dose study of imetelstat in solid tumor malignancies | imetelstat | 85 | NCT00310895 |
| Solid Tumors or Lymphoma | I | Recruiting | Maximum tolerated imetelstat dose in young patients with solid tumors or lymphoma | imetelstat | 45 | NCT01273090 |
| Thrombocythemia or Polycythemia Vera | II | Recruiting | Safety and tolerability of imetelstat in thrombocythemia or polycythemia vera | standard of care, imetelstat | 20 | NCT01243073 |

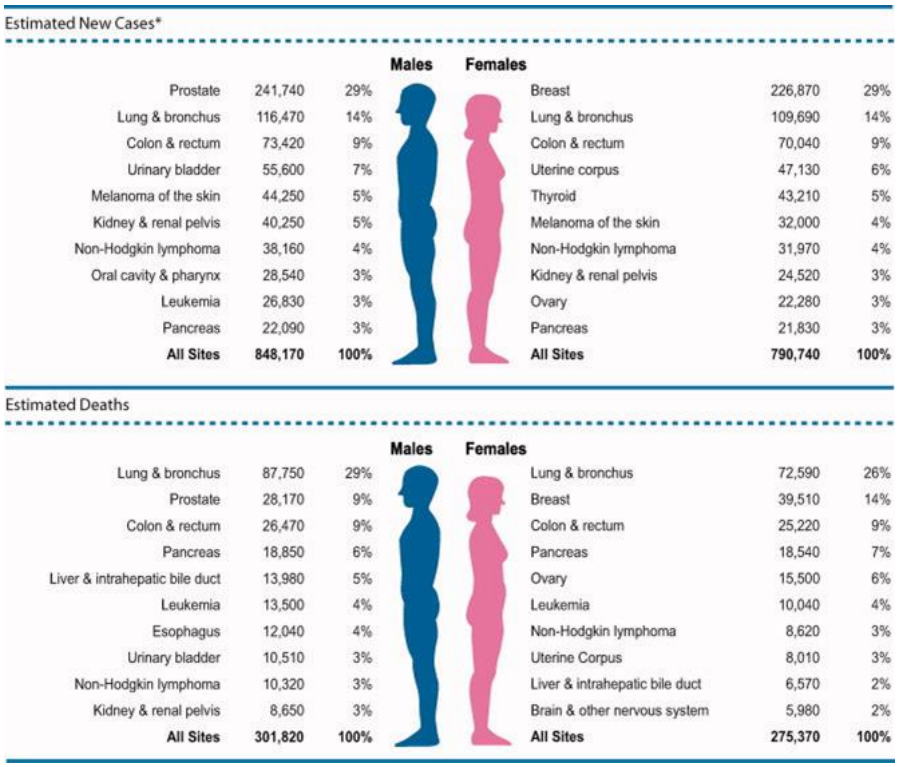

Estimated New Cases*

| | Males | | | Females | | |
|---|---|---|---|---|---|---|
| Prostate | 241,740 | 29% | | Breast | 226,870 | 29% |
| Lung & bronchus | 116,470 | 14% | | Lung & bronchus | 109,690 | 14% |
| Colon & rectum | 73,420 | 9% | | Colon & rectum | 70,040 | 9% |
| Urinary bladder | 55,600 | 7% | | Uterine corpus | 47,130 | 6% |
| Melanoma of the skin | 44,250 | 5% | | Thyroid | 43,210 | 5% |
| Kidney & renal pelvis | 40,250 | 5% | | Melanoma of the skin | 32,000 | 4% |
| Non-Hodgkin lymphoma | 38,160 | 4% | | Non-Hodgkin lymphoma | 31,970 | 4% |
| Oral cavity & pharynx | 28,540 | 3% | | Kidney & renal pelvis | 24,520 | 3% |
| Leukemia | 26,830 | 3% | | Ovary | 22,280 | 3% |
| Pancreas | 22,090 | 3% | | Pancreas | 21,830 | 3% |
| **All Sites** | **848,170** | **100%** | | **All Sites** | **790,740** | **100%** |

Estimated Deaths

| | Males | | | Females | | |
|---|---|---|---|---|---|---|
| Lung & bronchus | 87,750 | 29% | | Lung & bronchus | 72,590 | 26% |
| Prostate | 28,170 | 9% | | Breast | 39,510 | 14% |
| Colon & rectum | 26,470 | 9% | | Colon & rectum | 25,220 | 9% |
| Pancreas | 18,850 | 6% | | Pancreas | 18,540 | 7% |
| Liver & intrahepatic bile duct | 13,980 | 5% | | Ovary | 15,500 | 6% |
| Leukemia | 13,500 | 4% | | Leukemia | 10,040 | 4% |
| Esophagus | 12,040 | 4% | | Non-Hodgkin lymphoma | 8,620 | 3% |
| Urinary bladder | 10,510 | 3% | | Uterine Corpus | 8,010 | 3% |
| Non-Hodgkin lymphoma | 10,320 | 3% | | Liver & intrahepatic bile duct | 6,570 | 2% |
| Kidney & renal pelvis | 8,650 | 3% | | Brain & other nervous system | 5,980 | 2% |
| **All Sites** | **301,820** | **100%** | | **All Sites** | **275,370** | **100%** |

**Figure 1.5 2012 Estimate of New Cancer Cases and Cancer Associated Deaths in the United States for Men and Women.** Prostate and breast cancer are the most commonly diagnosed cancers for men and women, respectively. Lung cancer is the second most commonly diagnosed cancer for both genders. Lung cancer is responsible for the most cancer related deaths in both men and women in the United States annually.

Figure adapted from Siegel, Naishadham et al. 2012.

**Table 1.2 TNM Classification of Lung Cancer Tumors.** Adapted from Goldstraw 2010.

| **T: Primary Tumor** | | |
|---|---|---|
| **TX** | | Primary tumor cannot be assessed, or tumor proven by the presence of malignant cells in sputum or bronchial washings but not visualized by imaging or bronchoscopy. |
| **T0** | | No evidence of primary tumor. |
| **Tis** | | Carcinoma in situ. |
| **T1** | | Tumor ≤3 cm in greatest dimension, surrounded by lung or visceral pleura, without bronchoscopic evidence of invasion more proximal than the lobar bronchus (i.e., not in the main bronchus). |
| | **T1a** | Tumor ≤2 cm in greatest dimension. |
| | **T1b** | Tumor >2 cm but ≤3 in greatest dimension. |
| **T2** | | Tumor >3 cm but ≤7 cm or tumor with any of the following features (T2 tumors with these features are classified T2a if ≤5 cm):<br>Involves main bronchus, ≥2 cm distal to the carina.<br>Invades visceral pleura (PL1 or PL2).<br>Associated with atelectasis or obstructive pneumonitis that extends to the hilar region but does not involve the entire lung. |
| | **T2a** | Tumor >3 cm but ≤5 cm in greatest dimension. |
| | **T2b** | Tumor >5 cm but ≤7 cm in greatest dimension. |
| **T3** | | Tumor >7 cm or one that directly invades any of the following:<br>Parietal pleural (PL3) chest wall (including superior sulcus tumors), diaphragm, phrenic nerve, mediastinal pleura, or parietal pericardium.<br>Tumor in the main bronchus (<2 cm distal to the carina but without involvement of the carina).<br>Associated atelectasis or obstructive pneumonitis of the entire lung or separate tumor nodule(s) in the same lobe. |
| **T4** | | Tumor of any size that invades any of the following:<br>Mediastinum, heart, great vessels, trachea, recurrent laryngeal nerve, esophagus, vertebral body, carina, or separate tumor nodule(s) in a different ipsilateral lobe. |

| **N: Regional Lymph Node** | |
|---|---|
| **NX** | Regional lymph nodes cannot be assessed |
| **N0** | No regional lymph node metastasis |
| **N1** | Metastasis in ipsilateral peribronchial and/or ipsilateral hilar lymph nodes and intrapulmonary nodes, including involvement by direct extension |
| **N2** | Metastasis in ipsilateral mediastinal and/or subcarinal lymph node(s) |
| **N3** | Metastasis in contralateral mediastinal, contralateral hilar, ipsilateral or contralateral scalene, or supraclavicular lymph node(s) |
| **M: Distant Metastasis** | |
| **MX** | Distant metastasis cannot be assessed |
| **M0** | No distant metastasis |
| **M1** | Distant metastasis: |
| **M1a** | Separate tumor nodule(s) in a contralateral lobe; tumor with pleural nodules or malignant pleural (or pericardial) effusion |
| **M1b** | Distant metastasis |

**Table 1.3 Stage Classification of Tumors Based on TNM Status.**
Adapted from Goldstraw 2010.

| | | | |
|---|---|---|---|
| Occult carcinoma | TX | N0 | M0 |
| Stage 0 | Tis | N0 | M0 |
| Stage IA | T1a,b | N0 | M0 |
| Stage IB | T2a | N0 | M0 |
| Stage IIA | T1a,b | N1 | M0 |
| | T2a | N1 | M0 |
| | T2b | N0 | M0 |
| Stage IIB | T2b | N1 | M0 |
| | T3 | N0 | M0 |
| Stage IIIA | T1, T2 | N2 | M0 |
| | T3 | N1, N2 | M0 |
| | T4 | N0, N1 | M0 |
| Stage IIIB | T4 | N2 | M0 |
| | Any T | N3 | M0 |
| Stage IV | Any T | Any N | M1a,b |

# CHAPTER TWO

## MATERIALS AND METHODS

### 2.1 Materials

#### *2.1.1 Cell Lines*

All cell lines used in this study, with the exception of A549, Calu-1, Calu-3, Calu-6, and HOP62 were established by the Minna and Gazdar laboratories and are deposited with the American Type Culture Collection (ATCC) (Gazdar and Minna 1996; Phelps, Johnson et al. 1996). A549, Calu-1, Calu-3, Calu-6 and HOP62 were purchased from ATCC. Cell lines established at the National Cancer Institute are designated with the prefix NCI-H or H and cell lines established at the University of Texas Southwestern Hamon Center for Therapeutic Oncology Research have the prefix HCC (Gazdar, Girard et al. 2010).

#### *2.1.2 Drug Library*

Imetelstat, mismatch control oligo, and sense control oligo were obtained from Geron, Corp (Menlo Park, CA) and stored at -20°C as lyophilized powder or -80°C dissolved

in 0.85% saline. Cisplatin (1 mg/mL; Teva Parenteral), carboplatin (10 mg/mL; Bristol-Myers Squibb), doxorubicin (2 mg/mL; Teva Parenteral), gemcitabine (Eli Lilly and Company), paclitaxel (Bristol-Myers Squibb), vinorelbine (Pierre Fabre Company), and erlotinib (OSI Pharmaceuticals) were purchased at the University of Texas Southwestern Medical Center Campus Pharmacy. Cisplatin, carboplatin, and paclitaxel were stored as received at room temperature. Gemcitabine was dissolved to 38 mg/ml in 0.85% saline and stored at room temperature. Doxorubicin and vinorelbine were stored at 4°C. Erlotinib was dissolved in DMSO to make at 10 μM stocks and stored at 4°C.

## 2.2 Methods

### *2.2.1 Cell Culture*

Cell lines were cultured in RPMI-1640 (Life Technologies Inc) and supplemented with 5% fetal bovine serum (FBS, Life Technologies Inc). Cell lines were maintained in a humidified atmosphere with 5% $CO_2$ at 37°C. All cell lines were authenticated via DNA fingerprinting with the PowerPlex 1.2 kit (Promega) and confirmed to be the same as the DNA fingerprint library maintained by ATCC and/or the Minna and Gazdar laboratories. The cell lines were tested and confirmed free of mycoplasma using the e-Myco kit (Boca Scientific).

*2.2.2 Imetelstat*

Imetelstat was added directly to cell culture media one day after seeding cells to avoid off-target attachment effects of the drug (Jackson, Zhu et al. 2007). For long-term treatment, imetelstat was added two or three times per week as indicated.

*2.2.3 Colony Formation Assay*

Cells were seeded in 6-well plates in triplicate at 500 cells (100 for H1299, 1000 for H441, H1703, and 2000 for H1666 cell lines) per well. Drug was diluted in RPMI-1640 media with 5% FBS and added one day after seeding. Cells were allowed to grow for 14-28 days and end point was determined by colony size. Assay length variation was determined by the inherent doubling time of the cell lines. When 50% of the colonies reached 50+ cells per colony, media was removed and cells were fixed and stained with 50 mg crystal violet in 30% ethanol for 1 hour. After fixing, plates were rinsed with water and imaged using the ChemiDoc XRS+ Imager (Bio-Rad). Colonies were quantified by eye or using the Colony Counting function of Quantity One Software (v4.6.5, Bio-Rad). Assays were repeated at least three times in triplicate and colony counts are averages of all replicates.

### *2.2.4 Drug Response Curve*

#### *2.2.4.1 5-Day Assay*

Cells were plated in 96-well plate format ranging from 500-4000 cells per well, depending on the cell line. Cell number was determined by growth rate and MTS enzymatic activity. For most cell lines, 2000 cells were seeded. Cells were plated on day 0. Drug was added on day 1 in 4-fold dilutions with a maximum dose of 1000 nM for paclitaxel and vinorelbine, 2000 nM for doxorubicin and gemcitabine, 42.5 μM for imetelstat, 808 μM for carboplatin, and 100 μM for cisplatin and erlotinib. Paclitaxel/carboplatin combination was given in a 2:3 wt/wt ratio and listed in terms of paclitaxel, maximum dose 1000 nM paclitaxel. Plates were incubated for four days and relative cell number was determined by incubating for 1 to 3 hours at 37°C in the presence of MTS (Promega, Madison, WI), final concentration 333 μg/ml. Absorbance readings of the plate were obtained at 490 nm using a Spectra Max 190 (Molecular Devices). Each plate contained eight replicates per concentration and was repeated at least 4 times. Drug sensitivity curves and $IC_{50}$s were calculated using in-house software, DIVISA.

#### *2.2.4.2 Colony Formation Dose Response*

Cells were seeded in 6-well plates at 500 cells per well in triplicate. Drug was added the next day. For chemotherapies, drug concentrations mimicked the doses used in the 5-day assay. For imetelstat, 0, 0.1, 0.5, 1, 5, and 10 μM concentrations were used. Cells were

allowed to grow 14-28 days depending on the cell line. Colony formation assays were ended and colony counts were determined as described in the "Colony Formation Assay" methods section. Average colony counts per concentration were graphed to determine the dose response curve.

*2.2.5 Telomerase Detection Assay*

Telomerase activity was measured using the telomerase repeat amplification protocol (TRAP) assay via the TRAPeze Telomerase Detection Kit (Millipore). For cell lines, cell pellets were made with 100,000 cells and resuspended in 100 μl 1x CHAPS lysis buffer. 1 μl (1000 cells) of the cell suspension was used for the PCR reaction to determine telomerase activity. For tumor tissue, 25-50 mg of tissue was covered in 1x CHAPS lysis buffer and homogenized using the Qiagen Tissue-lyzer. 3 μg of tissue lysate was used for the PCR reaction to determine telomerase activity. In both cases, the PCR reaction was run with the TRAPeze kit components and run in the thermal cycler @ 30°C for 30 minutes, 95°C for 15 minutes, and 30 cycles of [30 seconds @ 94°C, 30 seconds @ 59°C and 1 minute @ 72°C]. The product of the PCR reaction was run on a 10% polyacrylamide gel for 2.5-3 hrs at 250 volts. The gel was stained with SYBR green and visualized on the ChemiDoc XRS+ Imager (Bio-Rad). TRAP gels were quantified by measuring the intensity of the bands using Quantity One Software (v4.6.5, Bio-Rad). Relative telomerase activity was calculated as the ∑ (intensities of all bands above the Internal Telomerase Assay Standard (ITAS) band)/ITAS band intensity for each lane.

*2.2.6 Average Telomere Length Determination*

Telomere length was determined using a modified Southern blot (Herbert, Shay et al. 2003). DNA was obtained using the DNeasy kit (Qiagen) in the QiaCube (Qiagen). 1 μg DNA was digested overnight with a mix of equal parts AluI (New England Biosciences), CfoI (Promega), HaeIII (New England Biosciences), HinfI (New England Biosciences), MspI (New England Biosciences), and RsaI (New England Biosciences) restriction enzymes. The digested DNA was run on 0.7% agarose gel for ~16 hrs at 70 volts. The gel was denatured, dried and neutralized. The gel was hybridized with $^{32}P$ radioactive probe to the telomeric sequence, exposed to a phosphor screen, scanned with a PhosphorImager and visualized using ImageQuant software.

*2.2.7 Aldefluor Detection Assay*

Cells were profiled using the Aldefluor Kit (Stem Cell Technologies). Cells were incubated in aldefluor assay buffer with the ALDH substrate BODIPY-aminoacetaldehyde (BAAA) for 45 min at 37°C. Cells capable of catalyzing BAAA to BODIPY-aminoacetate (BAA), a fluorescent product, were considered aldehyde dehydrogenase positive ($ALDH^+$). Cells were profiled and separated into high and low ALDH. Fluorescence activated cell sorting (FACS) gates were established from baseline fluorescence for each cell line determined by incubation in the ALDH inhibitor diethylaminobenzaldehyde (DEAB). DEAB treated samples served as negative controls. Following incubation, the buffer was

removed and cells were re-suspended in fresh assay buffer with 1 μg/ml propidium iodide (PI) to indicate dead cells.

*2.2.8 Cloning Assay*

1000 and 5000 cells were plated in a 10 cm dish and allowed to grow until colonies were visible with the naked eye. Colonies with a wide margin between neighboring colonies were selected. A plastic cloning ring was placed around the colony and 10 μl of trypsin was added to the ring. Cells were trypsinized and transferred to a 24 well dish. When cells reached 80% confluency, they were transferred to a 12-well and then 6-well dish to allow the population to expand.

*2.2.9 Xenograft Treatment Studies*

All mouse work followed an IACUC approved protocol. Cells were trypsinized, neutralized with media and counted in the presence of trypan blue to ensure cell viability. $1x10^6$ cells in 200 μl PBS were injected subcutaneously into the right flank of 6-8 week old female NOD/SCID mice. Treatment began 2 days after cell injection and mice were treated three times per week with 30 mg/kg imetelstat in 100 μl saline or 100 μl of saline alone. Tumors were measured twice weekly using digital calipers. Tumor volumes were calculated using the formula $v = (D)(d^2)(\pi/6)$ where D is the larger measurement and d is the shorter measurement (Euhus, Hudd et al. 1986). The experiment progressed until control mice reached average maximum tumor volume of 2000 $mm^3$.

# CHAPTER THREE

## NON-SMALL CELL LUNG CANCER AND TELOMERASE INHIBITION

### 3.1 Introduction

For new therapies to be developed as cancer treatment, research begins preclinically in the laboratory. New drug target concepts must first be proven effective in preclinical models before they can be tested in the clinic. Many tools have been established to study tumor development and efficacy of new therapy ideas including tumor tissue and animal models (Gazdar, Gao et al. 2010). One of the biggest resources for studying lung cancers are cell lines developed from patient tumors. Many lung cancer cell lines were developed at the National Cancer Institute (NCI) in the labs of Minna and Gazdar (Gazdar and Minna 1996; Oie, Russell et al. 1996; Phelps, Johnson et al. 1996). Cell lines are pure tumor samples and a valuable resource for studying genetics and mutations of tumors (Gazdar, Gao et al. 2010). Over 100 NSCLC cell lines are available for preclinical studies established mostly at NCI (designated with NCI- prefix) or University of Texas Southwestern Medical Center (designated with HCC prefix) (Phelps, Johnson et al. 1996; Gazdar, Girard et al. 2010).

Cell lines are beneficial for drug studies. A panel of over 100 NSCLC cell lines or smaller subsets of cell lines can be tested for drug efficacy to determine the range of sensitivity to a specific therapy. After sensitive and resistant cell lines are determined, many

aspects of the cell lines, such as histology, mutation status, gene expression profiles, and patient data (race, sex, age) can be compared to determine a reason for sensitivity or resistance. Our studies focus on telomere length, telomerase activity and telomerase inhibition to determine the range and efficacy of therapy.

For this study, a panel of over 70 NSCLC cell lines was used. While data is not known for all cell lines, known statistics from this panel include at least 45 lines derived from males and 29 lines derived from females whose age at diagnosis ranged from 25-80 years old. At least 52 lines were derived from Caucasian patients, seven from Black and one from an Asian patient as well as 28 from patients that smoke and at least 3 from never smokers. 52 lines are adenocarcinomas, 4 lines are squamous cell carcinoma and 7 lines are large cell carcinoma. At least 26 lines were derived from primary tumors and 34 lines were derived from metastasis. At least 32 lines received no prior chemotherapy before derivation of the cell line but 14 lines received prior chemotherapy. In addition, 86% of the lines contain p53 mutations, 39% contain KRAS mutations, 18% contain EGFR mutations, and 29% contain STK11 mutations. While some cell lines contain only one of these mutations, many contain two or more of these mutations. One cell line in the panel H2052 however, did not contain any of these four common mutations.

Adult human somatic cell telomeres range from 7-12 kb. Cancer cells go through mortality stage 1 (M1) and mortality stage 2 (M2) before becoming cancer cells. In the process, telomeres shorten to critical lengths before telomerase is activated to overcome M2.

Because of this, telomeres in cancers are much shorter. Telomere lengths vary from cell to cell (Henderson, Allsopp et al. 1996; Lansdorp, Verwoerd et al. 1996; Martens, Zijlmans et al. 1998) and from chromosome to chromosome within the cell (Britt-Compton, Rowson et al. 2006). Because cancer cells have short telomeres, telomerase inhibition should lead to senescence or cell death with minimal cell divisions. Among factors that can contribute to telomere attrition is cigarette smoking (Valdes, Andrew et al. 2005; McGrath, Wong et al. 2007), one reason telomerase targeting therapies could be especially beneficial for the treatment of lung cancer.

Imetelstat is a telomerase inhibitor currently finishing Phase II clinical trials in NSCLC. Imetelstat is a 13-mer oligonucleotide that inhibits telomerase by binding to the hTR RNA template component of telomerase, one of two components necessary for telomerase function. Imetelstat, also known as GRN163L, is not an anti-sense drug. An anti-sense drug binds to mRNA preventing the mRNA from being transcribed into protein. Imetelstat binds to hTR which is a functional RNA and blocks hTR from interacting with hTERT and preventing telomerase from elongating telomeres. To study the efficacy of telomerase therapy in NSCLC, first baseline levels of telomere length, telomerase activity and telomerase inhibition with imetelstat were determined for a panel of about 70 NSCLC cell lines.

## 3.2 Results

### *3.2.1 Range of Telomere Length*

To identify the range of telomere length in lung cancer, we measured telomere length for a panel of non-small cell lung cancer cell lines. Using a modified Southern blot called a TRF, telomere lengths were determined by digesting genomic DNA with a mix of restriction enzymes. Because of the repetitive TTAGGG sequence in telomeres, the telomeric region of the chromosome is not susceptible to restriction enzyme digestion. After the digestion, the remaining DNA was run on a gel and then exposed to a radioactive probe with the telomeric sequence. A molecular weight marker is also run on the gel and used to determine telomere length. Because telomere length varies within a cell line, the telomere on the gel is seen as smear representing the range of telomere length. The darkest part of the smear is the length of telomere in highest concentration and therefore binding the most probe. Average telomere length is determined by the darkest part of the band. Figure 3.1 shows a TRF of a sample of NSCLC cell lines. Calu-3 and H1648 have the shortest telomere length on the gel (1.5 kb and 2 kb, respectively) and H1299 has the longest telomeres on the gel at 19 kb. Telomere length of the entire panel is shown in Figure 3.2 as a waterfall plot indicating the range in telomere length. Telomeres range from 1.5 kb of Calu-3 up to 20 kb of H1703. 80% of the panel has telomeres less than 6 kb, reflecting that most cancer cells have relatively short telomeres.

*3.2.2 Range of Telomerase Activity*

Telomerase activity is measured via the TRAP (Telomere Repeat Amplification Protocol) assay. It is a PCR-based assay that includes a 30 minute incubation step whereby any active telomerase can recognize an internal template as a telomere and elongate the template followed by amplification of the products. The variation in PCR product lengths – the longer the products and more abundant the products, the more active the telomerase – can be quantified to determine relative telomerase activity. Any template not elongated runs as the shortest band and serves as an internal control called ITAS (Internal Telomerase Assay Standard). The intensity of the internal control band is inversely proportional to telomerase activity of the sample. Quantification is calculated by summing the intensities of all bands above the internal control band and dividing the sum by the intensity of the internal control band. Figure 3.3A shows a TRAP gel from a sample of NSCLC cell lines. Lanes 1-4 show 1000, 100, 10 and 0 (lysis buffer only) HeLa cells for control and comparison. 1000 cells were run for each cell line. The length and intensity of the ladder in each lane varies among the different cell lines indicating the variation in telomerase activity among the cell lines. Quantification of the gel is shown in Figure 3.3B depicting graphical representation of the variation of telomerase activity between the cell lines. Relative telomerase activity of the panel is shown in Figure 3.4. 1000 cells were run for each cell line and relative telomerase activity is illustrated with a waterfall plot. Relative telomerase activity ranges from 5.4 to

26.7 for this panel of non-small cell lung cancer cell lines. The results are also listed in Appendix A.

### *3.2.3 Correlation Between Telomere Length and Telomerase Activity*

Figure 3.5 shows average telomere length plotted against relative telomerase activity. This plot indicates there is no direct correlation of the average telomere length and relative telomerase activity of the panel. There is no evidence in the literature supporting a direct correlation between telomerase activity and telomere length (Wang, Sakamoto et al. 2002; Januszkiewicz, Wysoki et al. 2003). Telomere length varies not only from cell line to cell line but also from cell to cell within the cell lines and from chromosome to chromosome within each cell (Lansdorp, Verwoerd et al. 1996; Baird, Rowson et al. 2003). An argument could be made for a correlation between either longest telomere and highest telomerase activity or shortest telomere with highest telomerase activity. High telomerase activity could correlate with longest telomere because more active telomerase activity would allow for more active elongation making telomeres longer. Conversely, high telomerase activity may be necessary for the shortest telomeres to maintain the minimum length for survival and thus high telomerase activity would correlate with shorter telomeres.

*3.2.4 Telomerase Inhibition with Imetelstat*

Previous work (Jackson, Zhu et al. 2007) has shown that imetelstat causes off-target effects that are still poorly understood. When imetelstat is administered *in vitro* at cell seeding, imetelstat inhibits attachment of the cells to the flask. Because of this effect, imetelstat was always administered 24 hours after seeding cells.

To measure efficacy of imetelstat in NSCLC, cell lines were treated with increasing doses of imetelstat for 48 hours and samples were run in a TRAP assay to measure telomerase activity. Previously, this was done in A549 (Dikmen, Gellert et al. 2005) and 1 μM imetelstat was sufficient to inhibit telomerase. 16 more cell lines (H460, H441, H2882, H358, H2009, H2073, H2887, H1648, H2126, H1993, HCC44, H1373, H1703, H838, H661 and H2087) were repeated to determine the range of imetelstat necessary to inhibit telomerase in a panel of NSCLC. Figure 3.6 shows H460 with imetelstat titrations. Collectively, 1 μM to 3 μM imetelstat sufficiently inhibits telomerase in most NSCLC cell lines.

To determine the necessary time frame for telomerase inhibition, 1 μM imetelstat was administered and cells were collected at 24, 48, 72 and 96 hours after imetelstat drugging. Figure 3.7 shows a TRAP of the time course experiment in H358, H2126, and H2882, showing that reduction of telomerase activity is seen within 24 hours of imetelstat treatment and greater reduction is seen at 48 hours. As demonstrated in this gel, 1 μM imetelstat is not sufficient for complete inhibition in all NSCLC cell lines

*3.2.5 Imetelstat Efficacy Across the Panel*

Imetelstat efficacy at 3 μM imetelstat was measured across the panel. Cells were plated in bulk culture and 3 μM imetelstat was added 24 hours later. Cells were allowed to grow in the presence of imetelstat for 48 hours and then harvested for TRAP assay. Figure 3.8 shows a waterfall plot depicting percent residual telomerase activity with 3 μM imetelstat relative to parental telomerase activity for each cell line. All cell lines showed some reduction in telomerase activity in the presence of 3 μM imetelstat. Residual telomerase activity ranged from 60% to 0% telomerase activity compared to parental. Parental inherent telomerase activity was compared to residual telomerase activity in the presence of 3μM imetelstat. No correlation was seen between initial inherent telomerase activity and residual telomerase activity after 48 hours of 3 μM imetelstat treatment (Figure 3.9).

**3.3 Discussion**

Human telomere length is generally 10-15 kb while tumor telomere lengths tend to be much shorter. 80% of the panel is less than 6 kb which is in line with tumors generally having short telomeres. However that does not explain the 20% of NSCLC cell lines in the panel with telomeres longer than 6 kb and ranging up to 20 kb. Telomeres vary from cell to cell within the tumor (Henderson, Allsopp et al. 1996; Lansdorp, Verwoerd et al. 1996; Martens, Zijlmans et al. 1998). When a cell line is established, a tumor resection is placed in

a flask and given media and specific growth factors to help establish the cell line ex vivo. Many cells are potentially lost in the establishment of the cell line and a bottleneck effect can happen (van Staveren, Solis et al. 2009; Gazdar, Gao et al. 2010). In this process, one of a few cells with much longer telomeres could contribute more substantially to the establishment of the cell line resulting in a cell line with much longer telomeres, even though the original tumor overall had a much shorter average telomere length. The same factors could also contribute to the heterogeneity of telomerase activity among the cell lines.

With the methods used for measuring telomere length and telomerase activity in this study, average telomere length did not correlate with relative telomerase activity. As previously mentioned, telomere length varies from cell to cell within a cell line and from chromosome to chromosome within the cell (Britt-Compton, Rowson et al. 2006). While there is no direct evidence in the literature for a correlation between telomere length and telomerase activity, the literature indirectly supports the idea of higher telomerase activity correlating with shorter telomeres. In yeast telomere biology, telomerase appears to have negative feedback via Rap1 and becomes less active with elongation of telomeres (Marcand, Brevet et al. 1999) as well as more active with shorter telomeres because of less Rap1 binding (Bianchi and Shore 2007). In addition, the shortest telomere present, not the average telomere length (as measured here) dictates when a cell will senesce. Telomerase preferentially elongates the shortest telomeres which would support the hypothesis of higher telomerase in cells with shorter telomeres (Hemann, Strong et al. 2001; Teixeira, Arneric et

al. 2004; Sabourin, Tuzon et al. 2007). The method of TRF used to measure average telomere length will not necessarily depict the shortest telomeres of the cell line because the probe will bind the longest and most abundant telomere length. This could mask really short telomeres present in the cells confounding the correlation results. Another method of telomere length measurement such as STELA or telo-FISH could be used to measure more accurately the shortest telomeres for comparison purposes.

Telomerase inhibition was achieved, at least to some degree, in every cell line tested supporting telomerase activity as a viable target using imetelstat. This panel of NSCLC acts as a small representation of the dynamics of tumors in general and the variations of telomere length and telomerase associated characteristics. There is a wide range of telomere length and telomerase activity among the cell lines in the panel analyzed. In addition, there is a wide range in telomerase inhibition. This will allow for investigation into why some lines respond better than others and how to best treat patients with imetelstat to see the greatest efficacy.

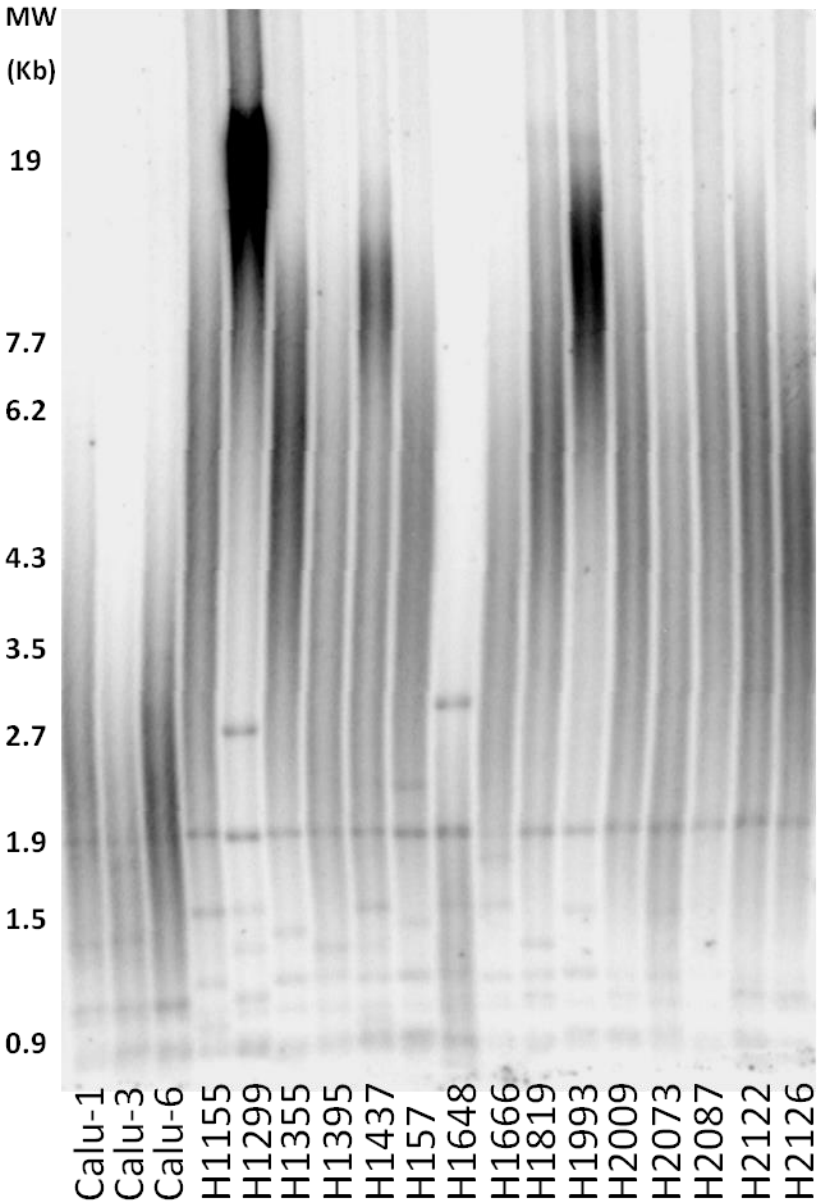


**Figure 3.1 Heterogeneity of Telomere Length in NSCLC**. 1 μg of DNA per cell line was digested and run in TRF assay. A representative sample of NSCLC cell lines is shown illustrating the range in telomere length of the panel. Average telomere length ranges from 1.5 kb (Calu-3) up to greater than 19 kb (H1299) in this gel.

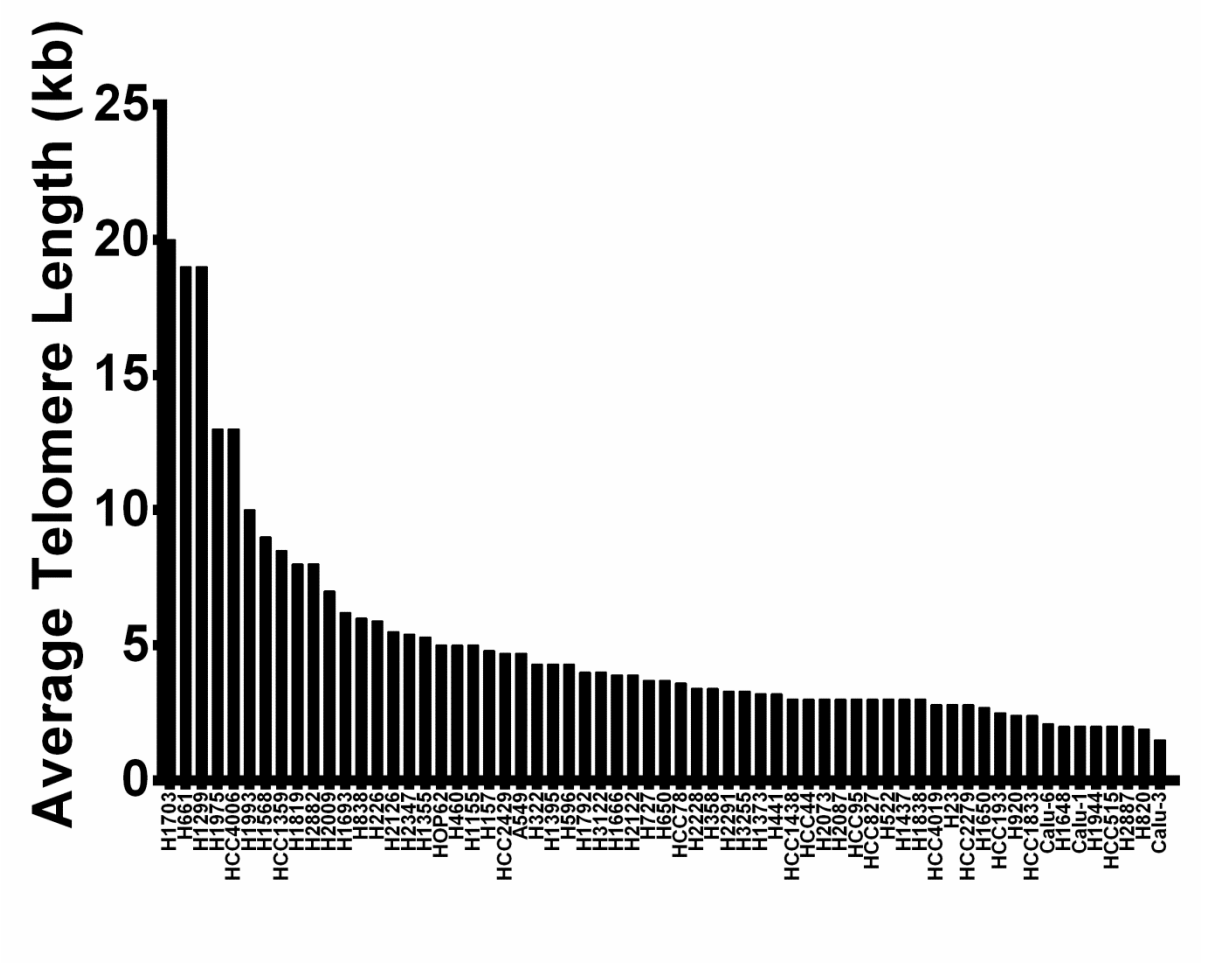


**Figure 3.2 NSCLC Panel Average Telomere Length.** A waterfall plot representing the entire NSCLC panel average telomere length as measured by TRF. The longest telomere length of the panel is 20 kb of H1703 and the shortest average telomere length is 1.5 kb of Calu-3.

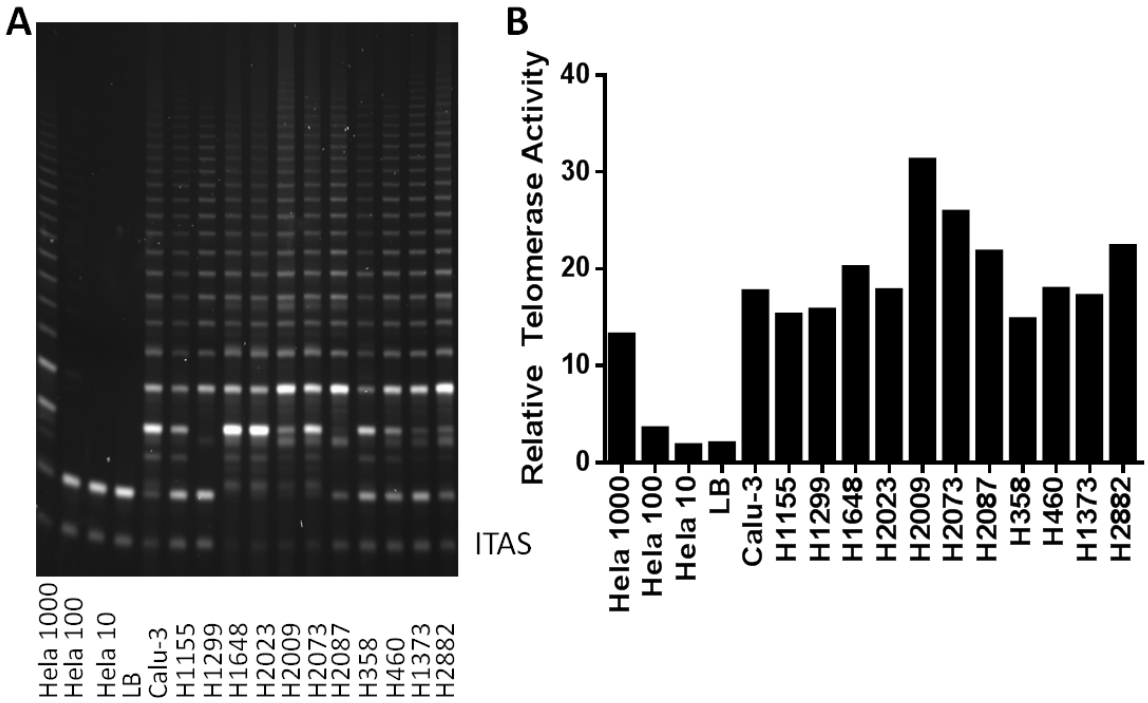


**Figure 3.3 Heterogeneity of Telomerase Activity in NSCLC**. (A) TRAP assay of a representative sample of NSCLC cell lines illustrating the range in telomerase activity of a panel of NSCLC cell lines. Lanes 1-4 are control lanes that show telomerase activity for 1000, 100, 10 and 0 (lysis buffer only) HeLa cells. Lanes 5-16 show 1000 cells per cell line for 12 NSCLC cell lines. (B) Telomerase activity quantified into relative telomerase activity based on the ITAS band. Telomerase activity is inversely proportional to the ITAS band and was determined by summing the intensity of bands above the ITAS band and dividing the sum by the intensity of the ITAS band.

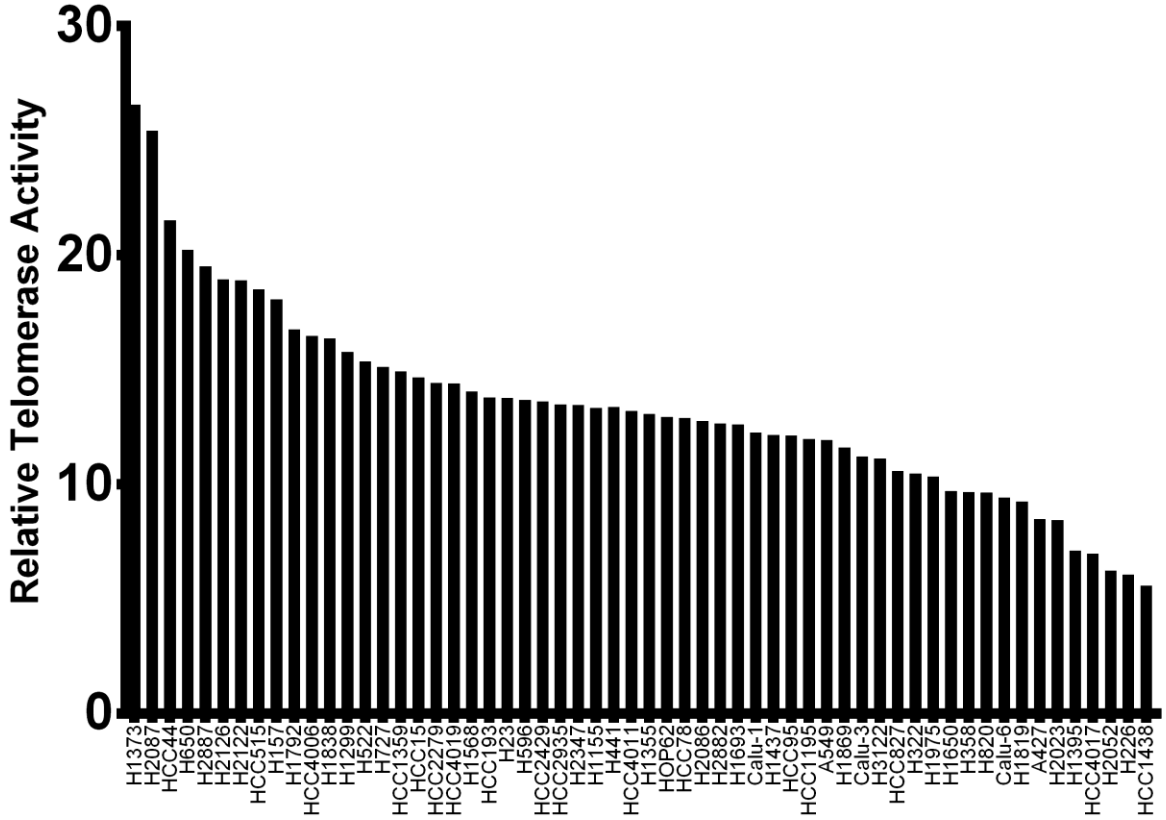


**Figure 3.4 Relative Telomerase Activity of the NSCLC Panel.** Telomerase activity was measured using the TRAP assay with 1000 cells per cell line. Relative telomerase activity is represented as a waterfall plot showing the range in relative telomerase activity. Telomerase activity ranges from 5.4 to 26.7.

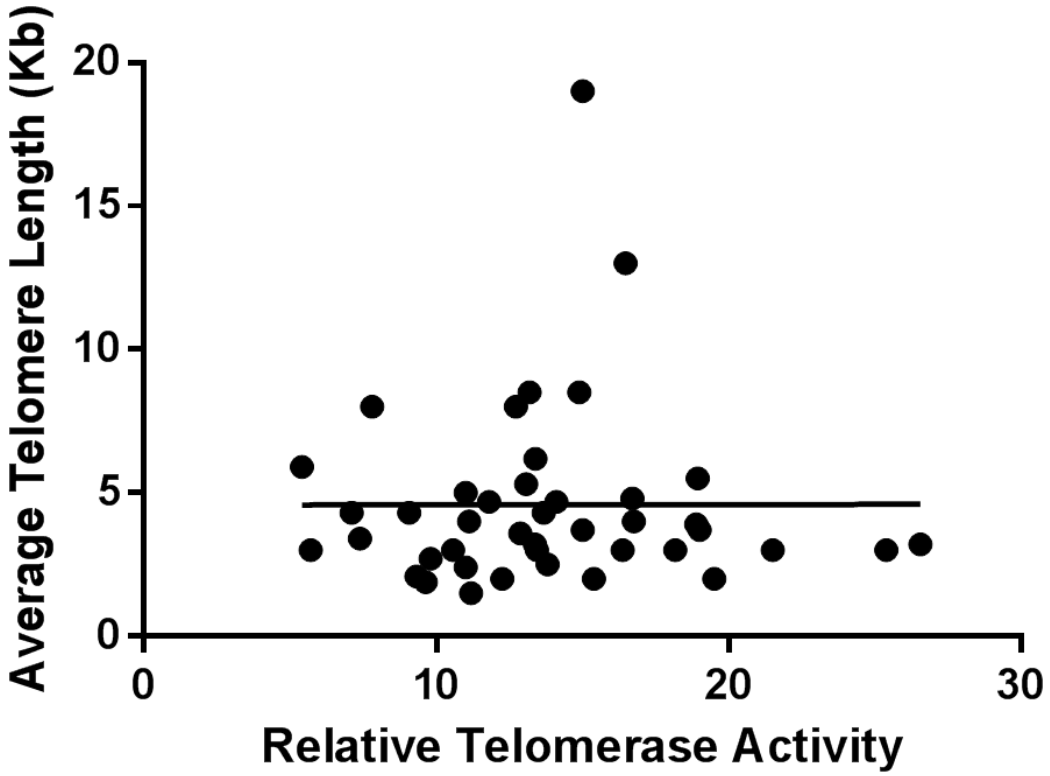


**Figure 3.5 Comparison of Average Telomere Length and Relative Telomerase Activity.** Relative telomerase activity is graphed versus average telomere length indicating there is no correlation between average telomere length and relative telomerase activity ($r^2 = 1.72x10^{-6}$).

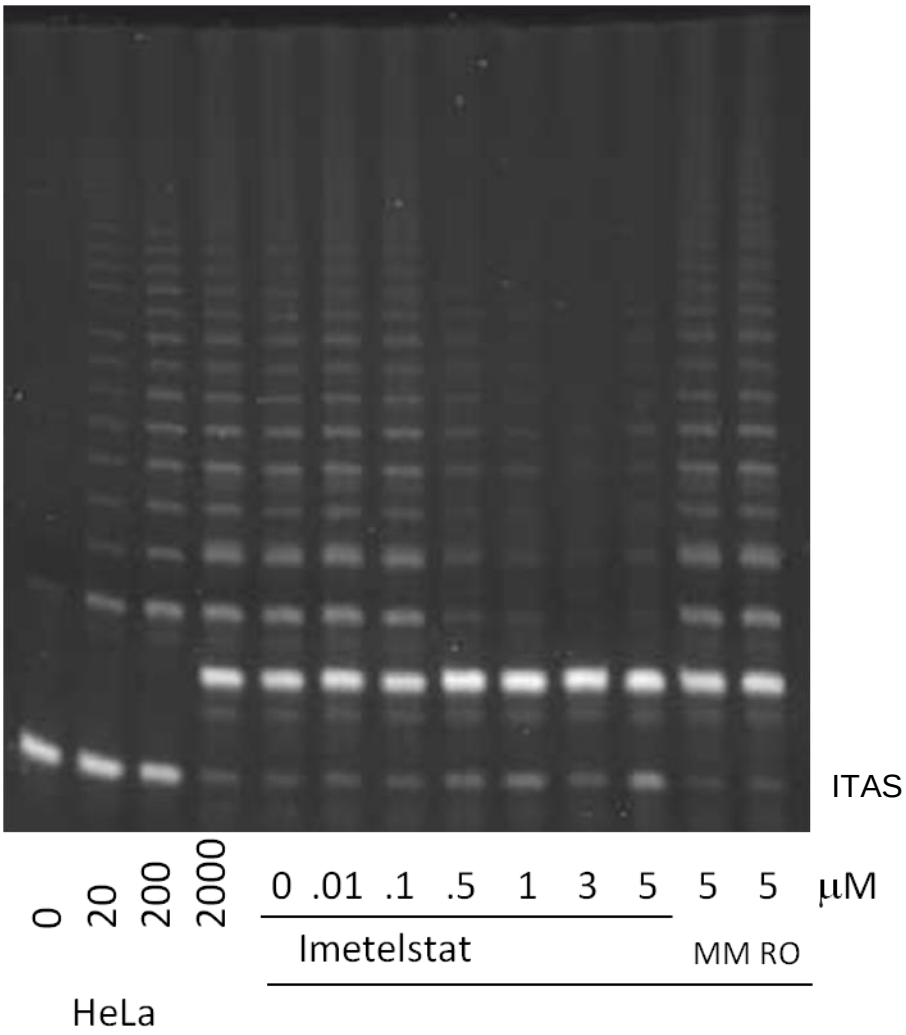


**Figure 3.6 Dose Response of H460 with Imetelstat.** H460 was given 0, 0.01, 0.1, 0.5, 1, 3 and 5 μM imetelstat to determine effective dose of imetelstat necessary to inhibit telomerase. 0.5 μM shows significant reduction in telomerase activity and 3 μM shows near complete inhibition of telomerase activity. 5 μM of Mismatch (MM) or Reverse Order (RO) control show no inhibition of telomerase activity in H460.

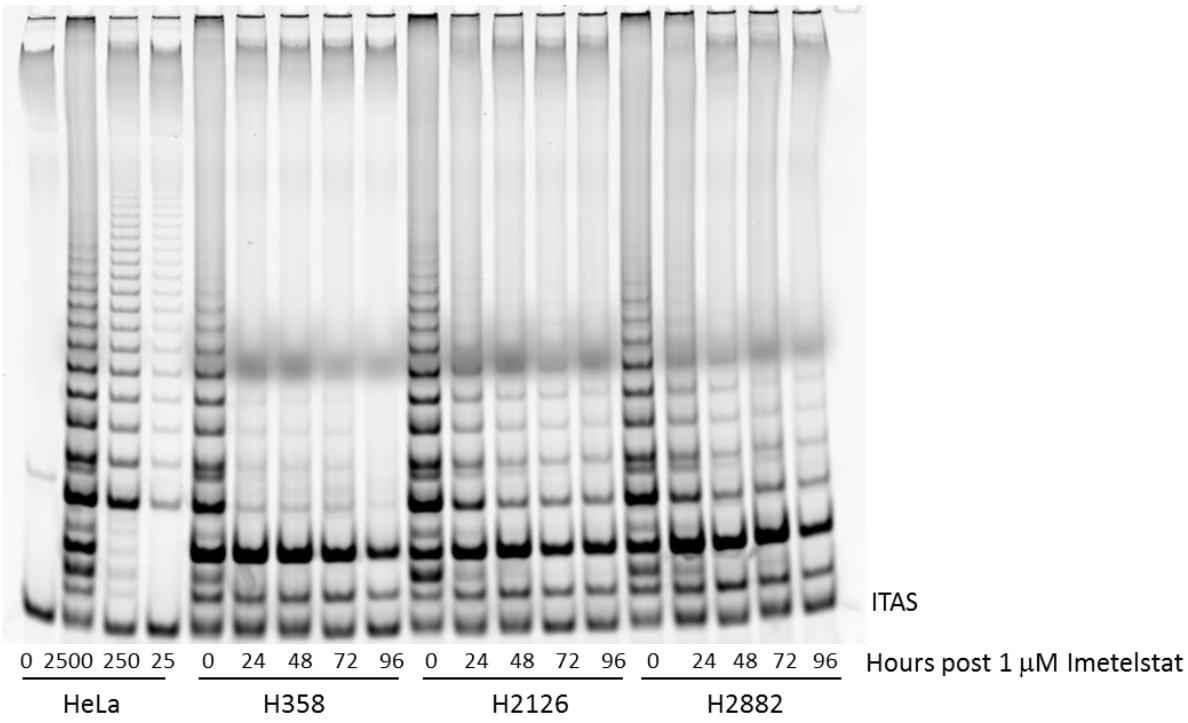


**Figure 3.7 Time Course Analysis with 1 μM Imetelstat.** H358, H2126 and H2882 were given 1 μM imetelstat and cells were collected 24, 48, 72, and 96 hours after administration. TRAP assay was run to determine time frame for dosing. 0 (lysis buffer), 2500, 250, and 25 HeLa cells were run as control (lanes 1-4). 2500 H358 cells (lanes 5-9) shows significant reduction in telomerase activity after 24 hours of exposure to imetelstat and inhibition is maintained through 96 hours. 2500 H2126 cells (lanes 10-14) shows reduced telomerase at 24 hours but peak inhibition at 72 hours. 2500 H2882 cells show peak telomerase inhibition at 48 hours. (lanes 15-19)

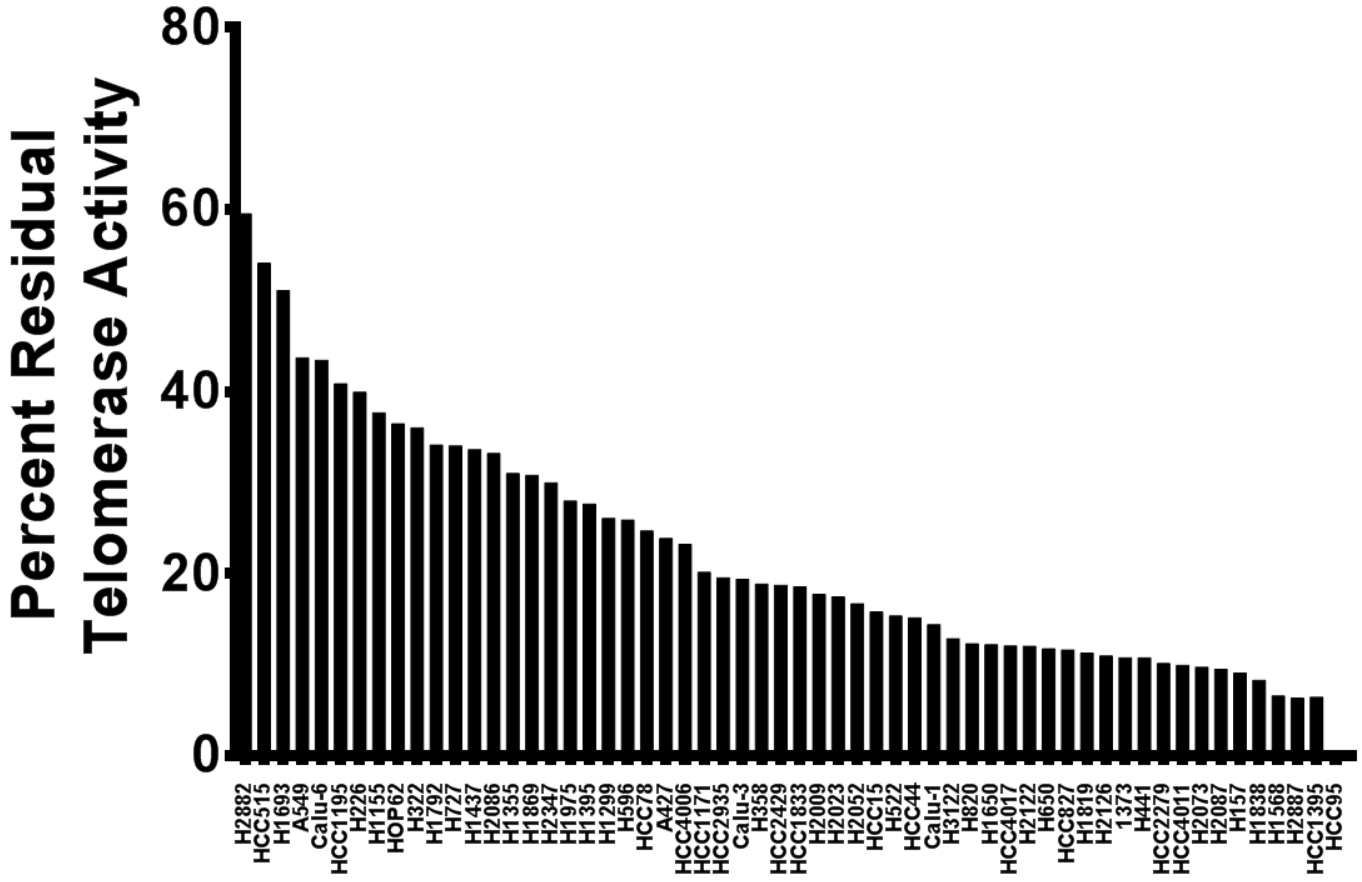


**Figure 3.8 Percent Relative Telomerase Activity Remaining After 3 μM Imetelstat Treatment.** A panel of NSCLC cell lines was given 3 μM imetelstat to determine residual telomerase activity after treatment. Cells were collected after 48 hours of exposure to imetelstat and run in the TRAP assay. The waterfall plot shows the percent of remaining telomerase activity relative to untreated control cells after 3 μM imetelstat treatment.

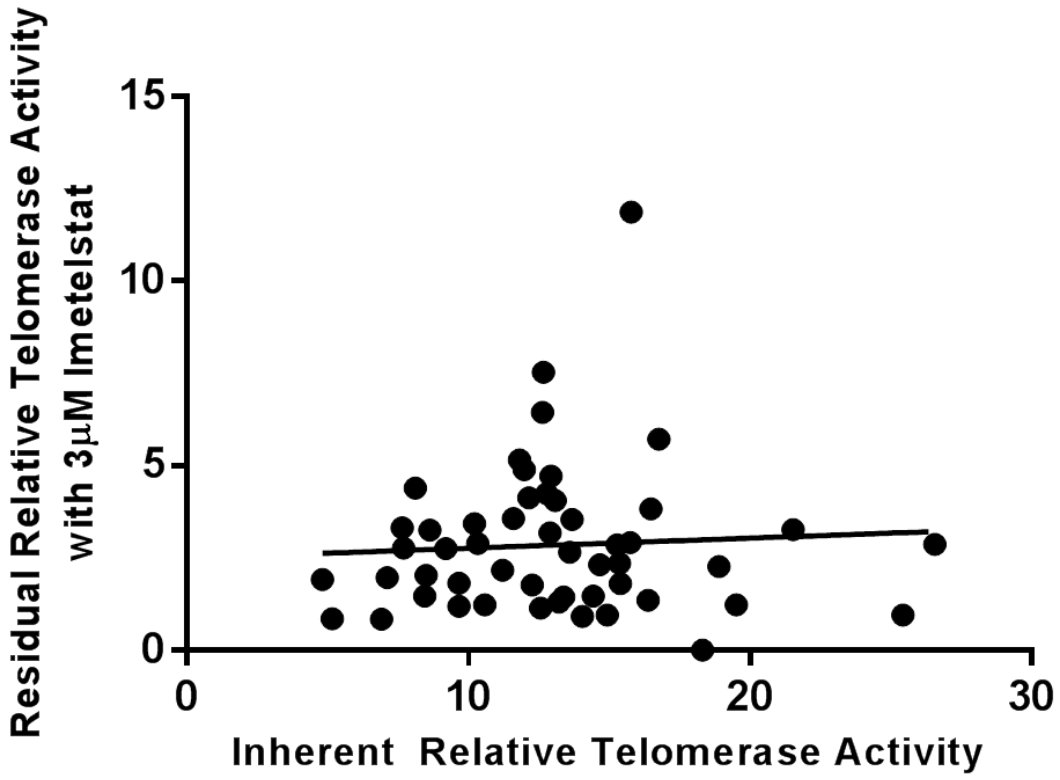


**Figure 3.9 Correlation of Parental Relative Telomerase Activity to Residual Telomerase Activity After 3 μM Imetelstat.** Inherent parental relative telomerase activity graphed versus residual telomerase activity after 3 μM imetelstat to determine correlation of imetelstat ability to inhibit telomerase activity relative to parental telomerase activity. There is not a significant correlation ($r^2 = 0.0037$).

# CHAPTER FOUR

## IMETELSTAT INHIBITION IN CLONOGENIC ASSAY

### 4.1 Introduction

One theory of cancer initiation involves the cancer stem cell theory where by a small subset of cells is responsible for the propagation of the entire tumor. It is hypothesized that cancer stem cells or cancer initiating cells are resistant to most standard chemotherapies. If a tumor is treated with standard chemotherapy and the tumor responds, the tumor commonly recurs. This recurrence is due to either development of resistance to therapy and/or not all cells being susceptible to the chemotherapy. The remaining tumor cells, sometimes not even detectable, could be cancer stem cells which could give rise to new tumors leading to recurrence and/or metastasis. Cancer stem cells have been shown to express telomerase along with the bulk tumor cells and imetelstat is capable of targeting both cell groups (Marian, Cho et al. ; Marian, Wright et al. ; Armanios and Greider 2005; Phatak, Cookson et al. 2007)

One assay for investigating the ability of a single cell to give rise to a colony of cells, a cancer stem cell characteristic, is the liquid colony formation assay. Cells are plated at very low density to minimize cell to cell contact and communication and cells are allowed to grow

for 2-4 weeks. Individual colonies are then counted for quantification. Here, a panel of NSCLC cell lines is examined for response to imetelstat in the colony formation assay. One main objective of this imetelstat study was to find biomarkers that could predict which patients would respond to imetelstat. By screening a large panel of cell lines and determining the range of sensitivity to therapy, many aspects of the cell lines including patient data (race, sex, age, smoking status), histology, mutations, response to other chemotherapies, growth rates, and mRNA expression can be compared to determine parameters that can predict responsiveness of other cell lines to therapy.

## 4.2 Results

### *4.2.1 Colony Formation Screen*

To determine the range of response of NSCLC to imetelstat, a panel of 70 NSCLC cell lines was screened for sensitivity to imetelstat in the liquid colony formation assay. For most cell lines, 500 cells were plated in 6-well format. 3 wells were left untreated and 3 wells were treated with a one-time dose of 3 μM imetelstat. Imetelstat was administered 24 hours after cell plating due to the attachment effects of imetelstat (Jackson, Zhu et al. 2007). Cells were allowed to grow for 2-4 weeks depending on the cell line. Endpoint was determined when at least 50% of the colonies had 50+ cells per colony. Duration was dependent on inherent growth rate of the cell line. At least three plates were plated for each

cell line. Many cell lines were also tested with imetelstat oligo controls to show the sensitivity is imetelstat specific.

A few examples are seen in Figure 4.1. H1373, a responder, shows inhibition in colony formation in the presence of 3 μM imetelstat compared to untreated control. H1373 is not sensitive, however, to 3 μM of mismatch control or 3 μM sense control. H2023 is another responder cell line that shows similar results as H1373 with inhibition in colony formation in the presence of imetelstat but does not respond to either control oligo. H1568 and H460 are both non-responders and show no difference between imetelstat treated and untreated colony forming ability as well as respond to either oligo control. These examples show the response is imetelstat specific and not an off-target effect of the oligo or lipid moiety.

The overall results of the screen of the panel are shown in Figure 4.2 as a waterfall plot. Each column represents the percent colony formation reduction when treated with imetelstat compared to untreated control and was calculated by (1-(average number of colonies with imetelstat/average number of colonies without imetelstat). Response ranged from the most sensitive line HCC44 which showed a 96% colony formation inhibition in the presence of imetelstat to H441 which showed a greater than 2-fold increase in colony forming ability in the presence of imetelstat. However, the colony forming efficiency of H441 is 0.2% (see Appendix A) which is confounding the increase in percent colony forming ability. Using the formula above, H1568, H3122, H1703 and H441 all indicate they grow

better in the presence of imetelstat than without however there is statistically no difference between treated and untreated colony numbers. All results are listed in Appendix A.

The colony formation plates were treated with a one-time dose of 3 μM imetelstat 24 hours after seeding. To ensure this was sufficient treatment, non-responder colonies were harvested at the end of the colony formation assay and tested for telomerase activity. Figure 4.3A shows a TRAP assay of H838, H661, H460 and H441 cell lines with treated and untreated cells from the colony formation assay. In all four cell lines, there is a decrease in telomerase activity in the treated cells at the completion of the assay. Figure 4.3B shows the quantification of the TRAP assay shown in Figure 4.3A. H661 had the highest residual telomerase activity in the presence of imetelstat but it also had the highest levels of telomerase activity in untreated colonies of the 4 cell lines. No responder cell lines could be tested due to lack of treated cells remaining at the end of the assay. These results indicate that a one-time dose of 3 μM imetelstat is sufficient to inhibit telomerase through the duration of the colony formation assay.

### *4.2.2 Colony Formation Titrations with Responders and Non-responders*

The screen was conducted with plating 500 cells and treating with 3 μM imetelstat across the panel. A selection of responders and non-responders were chosen to investigate the range in response with varying doses of imetelstat as well as the range in response to varying cell numbers to determine the robustness of the screen. First, the range of response

to varying doses of imetelstat was examined. HCC44, H1373, H2087, H2023 (responders) and H460, H661, and H1568 (non-responders) were plated for colony formation and were left untreated or treated with 0.1 μM, 0.5 μM, 1 μM, 5 μM, or 10 μM imetelstat. Figure 4.4 shows results for all 7 cell lines. The responders (dotted lines) begin responding with as little as 0.5 μM imetelstat and show greater response with increasing doses. All four cell lines had very few cells, if any, remaining with 10 μM imetelstat treatment. The three non-responders, however, showed less than a 50% reduction in colony formation even with 10 μM imetelstat. Even though the screen was conducted with 3 μM imetelstat, responders can respond with less than 3 μM and non-responders show minimal response with as much as 10 μM imetelstat indicating the responder and non-responder phenotypes extend beyond the 3 μM concentration.

Responders and non-responders were also tested in colony formation with varying numbers of cells to determine if the responder/non-responder phenotype extends to more stringent (fewer cells seeded for non-responders) or less stringent (more cells seeded for responders) colony forming conditions. For the responder cell lines, 500, 1000, and 5000 cells were plated in the presence and absence of 3 μM imetelstat. For non-responders, 500, 100, and 50 cells were plated in the presence and absence of 3 μM imetelstat. Results are graphed in Figure 4.5. H460, H661, and H838, all non-responders, continued to show little response even with as few as 50 cells plated, indicating their lack of response is not dependent on cell number (Figure 4.5A-C). H2882, H1355, and H2023 are all responders

and all three cell lines continued to respond in the presence of imetelstat even with as many as 5000 cells plated in colony formation conditions (Figure 4.5D-F). H1648 and H2085 are both responders with 500 cells plated. With 1000 cells plated for these two cell lines, their response is only about a 50% reduction in colony forming ability. With 5000 cells plated, they show less than 50% reduction in colony forming ability (Figure 4.5G-H). While there is still a decrease in colony forming ability with 5000 cells, they no longer show the high response rate they originally showed with only plating 500 cells. Three different response phenotypes are observed: 1) non-responders remain non-responsive with fewer cells, 2) responders remain sensitive with increased number of cells, and 3) responders become less responsive with increased number of cells. These three response phenotypes indicate the resistant cells have a consistent, stable non-responsive phenotype but the responders have a less stable response phenotype with a range of sensitivity that can change with the number of cells plated in some cell lines.

### *4.2.3 Comparison of Responders and Non-responders*

The ultimate goal was to find biomarkers predictive of response to imetelstat. Many aspects of the cell lines were studied and compared to determine a difference between responders and non-responders. First, patient data was examined. Race of the patient, sex of the patient, age of the patient, and smoking status of the patient were used to compare differences in responsiveness but no correlation was found. Histology of the cancer was also

compared but no correlation was found with response to imetelstat in colony formation (data for cell lines in Appendix A).

Telomere length of the cell lines and inherent relative telomerase activity of the cell lines were both compared to the response rate to imetelstat in colony formation. Figure 4.6A and 4.6B both show a graphical representation of the comparison indicating there is no correlation. Many cell lines were also tested for residual telomerase activity after 3 μM imetelstat treatment. Cells were plated and 3 μM imetelstat was added 24 hours later. Cells were harvested after 48 hours of exposure to imetelstat for TRAP assay. Figure 4.6C shows there is no correlation between residual telomerase activity and response to imetelstat in colony formation. Because cell lines showed a range in telomerase activity reduction with imetelastat in the colony formation assay and imetelstat targets hTR, hTR levels were measured and compared for a correlation to colony formation inhibition. Figure 4.6D shows no correlation between relative hTR levels and colony formation inhibition with imetelstat.

Inherent properties of the cell lines were compared for correlation to sensitivity. Percent colony forming efficiency was determined by counting the number of colonies formed in the control wells and dividing by the number of colonies plated (500 for most cell lines). Colony forming efficiency did not correlate with response to imetelstat, shown in Figure 4.7A. It was hypothesized that doubling time of the cell line could play a role in colony forming ability in the presence of imetelstat versus control. The doubling time of each cell line was determined by counting cells at seeding then allowing the cells to grow to

a confluence of 80-90%. At this point, cells were harvested and total cell number was determined. Population doubling time was calculated with the formula (number of hours from seeding to harvest/[((log N(t) -logN($t_0$))/log2] where N(t) is the number of cells at time of passage and N($t_0$) is the number of cells seeded at previous passage (Bruckova, Soukup et al.). There was no correlation between doubling time and colony formation inhibition with imetelstat.

Aldehyde dehydrogenase (ALDH) has been shown to have higher expression in lung cancer cells with cancer initiating properties compared to bulk tumor (Sullivan and Minna 2010; Sullivan, Spinola et al. 2010). The colony formation assay measures the ability of a single cell to establish a colony and is more probable in cells with cancer initiating properties than cells without. Colony formation inhibition in the presence of imetelstat was compared to percent $ALDH^+$ population but no correlation was found (Figure 4.7C).

Mutation status or oncogenotype of the cell lines was investigated for correlation to sensitivity and resistance to imetelstat in colony formation in the presence of imetelstat. The only mutation that showed a correlation was SMARCA4 (p-value 0.032). However, mutation status of SMARCA4 is not known for all cell lines.

The panel of cell lines has also been tested for sensitivity to many standard and targeted chemotherapies in a 5-day drug response assay. Response to other therapies was compared to response phenotypes to imetelstat. No correlation was seen between sensitivity to imetelstat and sensitivity to other therapies.

mRNA expression data for each cell line was used to correlate responding cell lines to non-responding cell lines to find a mRNA signature predictive of sensitivity. Many signatures were generated but none had statistical significance to reliably predict response. An example is shown in Figure 4.8. If only one cell line changed, the signature changed significantly indicating the weakness of the signature.

**4.3 Discussion**

A wide range of response is seen in NSCLC cell lines to imetelstat in the colony formation assay. Some cell lines are very sensitive with up to 96% inhibition in colony forming ability in the presence of imetelstat ranging to cells that show no difference in colony forming ability in the presence of imetelstat. A one-time does of 3 μM imetelstat is sufficient to inhibit telomerase for the duration of the assay and cells are not sensitive to imetelstat control oligos with mismatched and complimentary sequences.

The sensitive response phenotype is robust across imetelstat doses up to 10 μM. However the response phenotype is not as robust for the cell plating number for the assay. In all non-responder cell lines tested, plating as few as 50 cells showed the same response phenotype. For sensitive cell lines, however, response with up to 5000 cells plated varied. Some cell lines remained sensitive while others became less sensitive with increased numbers of cells.

Response phenotypes of the panel were correlated with many aspects of the cell lines to find predictors of response. No correlation was seen with average telomere length, relative telomerase activity, residual telomerase activity after 3 μM imetelstat, relative hTR levels, percent colony forming efficiency, doubling time of the cell line, or percent $ALDH^+$ population of the cell line.

When response was correlated with mutation status of the cell line, SMARCA4 is the only mutation that indicated a slight correlation. This could be due to the limited availability of mutation status. Mutation status is not known for all cell lines in the panel for this gene. However, SMARCA4 has recently been shown to interact with hTERT, the reverse transcriptase component of telomerase. Interestingly, the interaction has nothing to do with telomerase function at telomeres and instead is involved in the modulating the Wnt/β-catenin pathway (Park, Venteicher et al. 2009). Briefly, hTERT was shown to interact with SMARCA4 to activate Wnt reporters.

The colony formation assay is only 2-4 weeks in length. The proposed mechanism of action of imetelstat is first inhibition of telomerase followed by telomere shortening which should lead to eventual senescence or cell death. The lag time between telomere shortening and subsequent cell death would theoretically take much longer than 2-4 weeks unless the cells possessed very short telomeres. Because average telomere length did not correlate with colony formation response phenotype, this is unlikely the cause of sensitivity. However, telomeres could be measured using STELA or telo-FISH to determine more quantitative

results for shortest telomere present and see if there is a correlation with response to imetelstat in colony formation. However, the recent findings of non-telomerase activity related functions of hTERT suggest the sensitivity seen to imetelstat in the colony formation assay could be related to another function of either hTERT or hTR. Little is currently known about non-telomere lengthening functions of either telomerase component.

mRNA expression was also used to examine responders versus non-responders to create a signature that would predict response. A statistically significant signature could not be developed. The mRNA levels used to develop the signature are base-line inherent levels of the cell lines, irrespective of any therapy. To create a better signature, mRNA levels could be assessed both before and after imetelstat treatment in responders and non-responders to determine changes induced by imetelstat, or lack thereof, that would correlate with sensitivity or resistance. Alternatively, mRNA levels of all cell lines treated with imetelstat could be measured after imetelstat administration and a signature generated based on only these levels. Imetelstat treatment might induce changes that are confounding the results of the current signature.

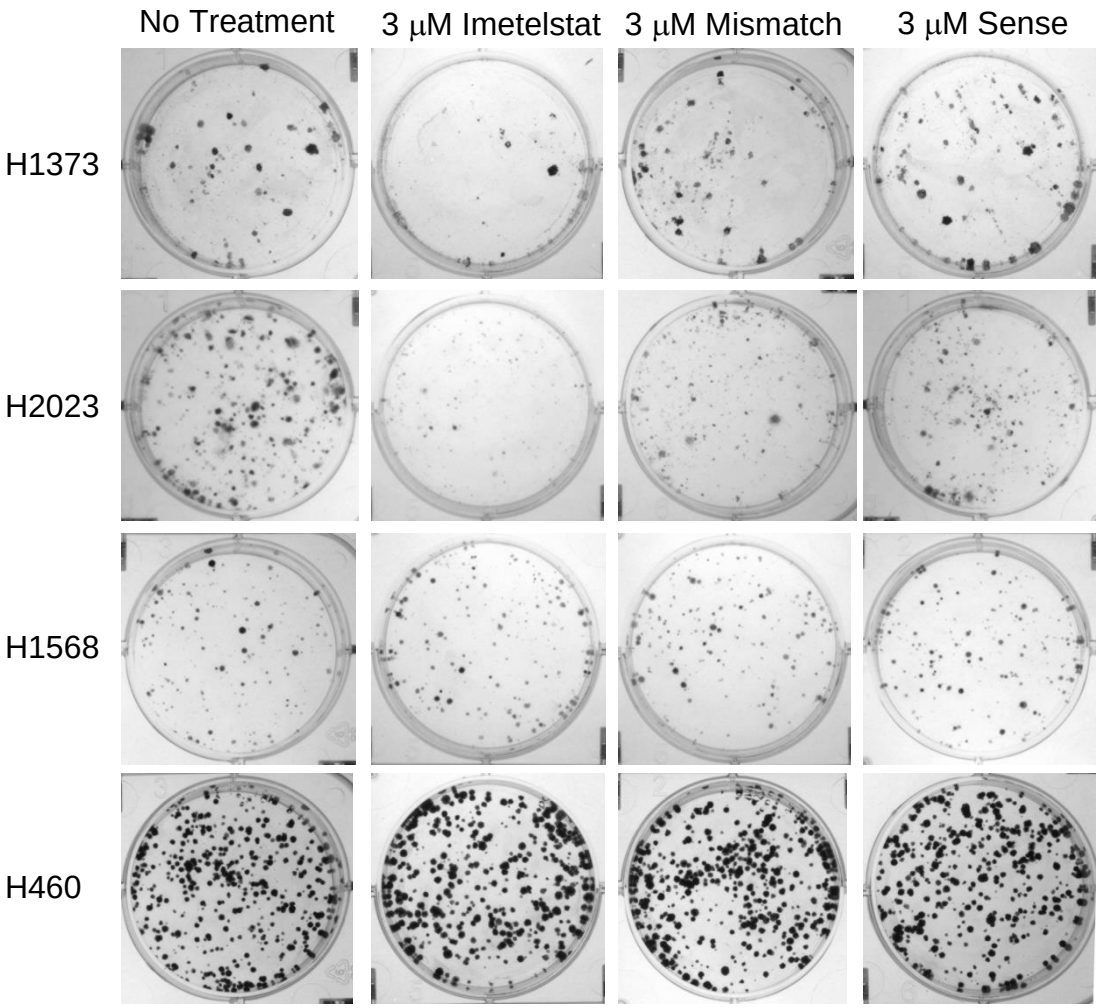


**Figure 4.1 Colony Formation Inhibition with 3 μM Imetelstat.** H1373, H2023, H1568 and H460 were plated in colony formation assay with 500 cells per well. Wells were left untreated or treated with 3 μM imetelstat, 3 μM mismatch control or 3 μM sense control 24 hours after seeding. H1373 and H2023 have reduced colony forming ability in the presence of 3 μM imetelstat but are not sensitive to either control. H1568 and H460 show no difference in colony forming ability in the presence of 3 μM imetelstat or either control.

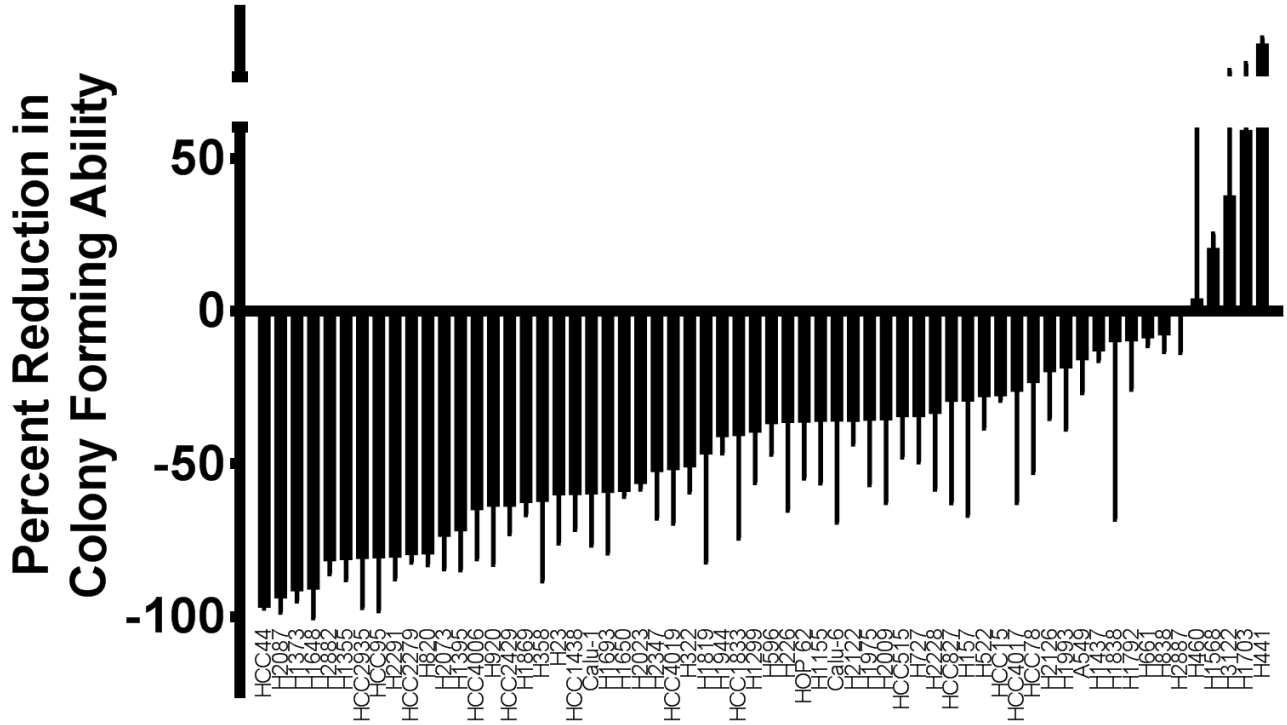


**Figure 4.2 Waterfall Plot of Colony Formation Inhibition with 3μM Imetelstat in NSCLC Panel.** A waterfall plot showing the percent reduction in colony forming ability for a panel of NSCLC cell lines in the presence of 3 μM imetelstat relative to untreated control. Reduction in colony forming ability ranges from 96% in HCC44 to an increase in growth of 194% in H441.

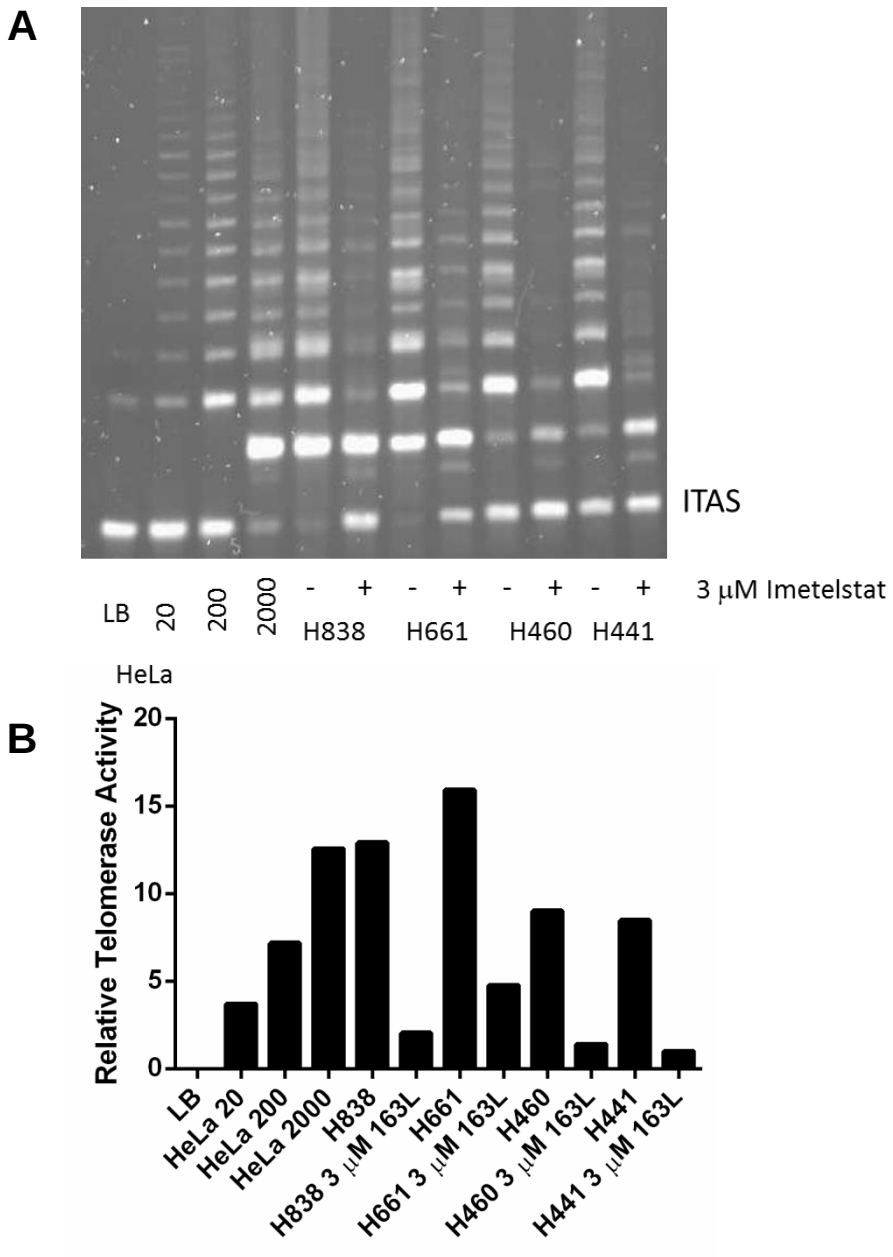


**Figure 4.3 Ability of 3 μM Imetelstat to Inhibit Telomerase for Duration of Colony Formation Assay.** 500 cells of H838, H661, H460 and H441 were plated in colony forming conditions and treated with a one-time dose of 3μM imetelstat 24 hours after plating. At the conclusion of the assay, cells were harvested and tested for telomerase inhibition. (A) TRAP assay depicting telomerase activity after colony formation assay. Lanes 1-4 are control lanes with HeLa cells at 0 (lysis buffer only), 20, 200, and 2000 cells showing increased activity with increased number of cells. Lanes 5-6 show H838 without and with 3 μM imetelstat indicating reduced telomerase activity with imetelstat treatment. Lanes 7-8, 9-10, and 11-12 show H661, H460, and H441 respectively without and with imetelstat. All lines show decreased telomerase activity with imetelstat treatment.

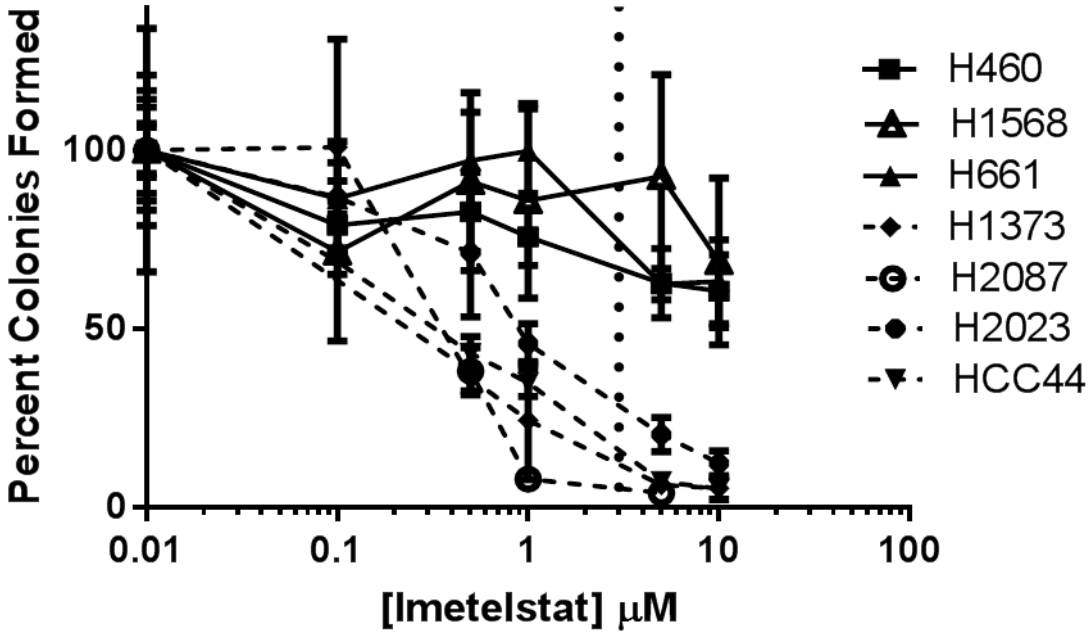


**Figure 4.4 Colony Formation with Imetelstat Titration.** 500 cells per well were plated in triplicate in colony forming conditions for each cell line. 0, 0.1, 0.5, 1, 5, and 10 μM imetelstat was added 24 hours later. Cells were allowed to grow for 2-4 weeks. Colonies were quantified at the end of the assay. Percent colonies formed relative to untreated control cells are shown. H460, H1568, and H661 show less than 50% response with up to 10 μM imetelstat. H1373, H2087, H2023, HCC44 show reduction with 0.5 μM imetelstat and response increases with increased imetelstat doses.

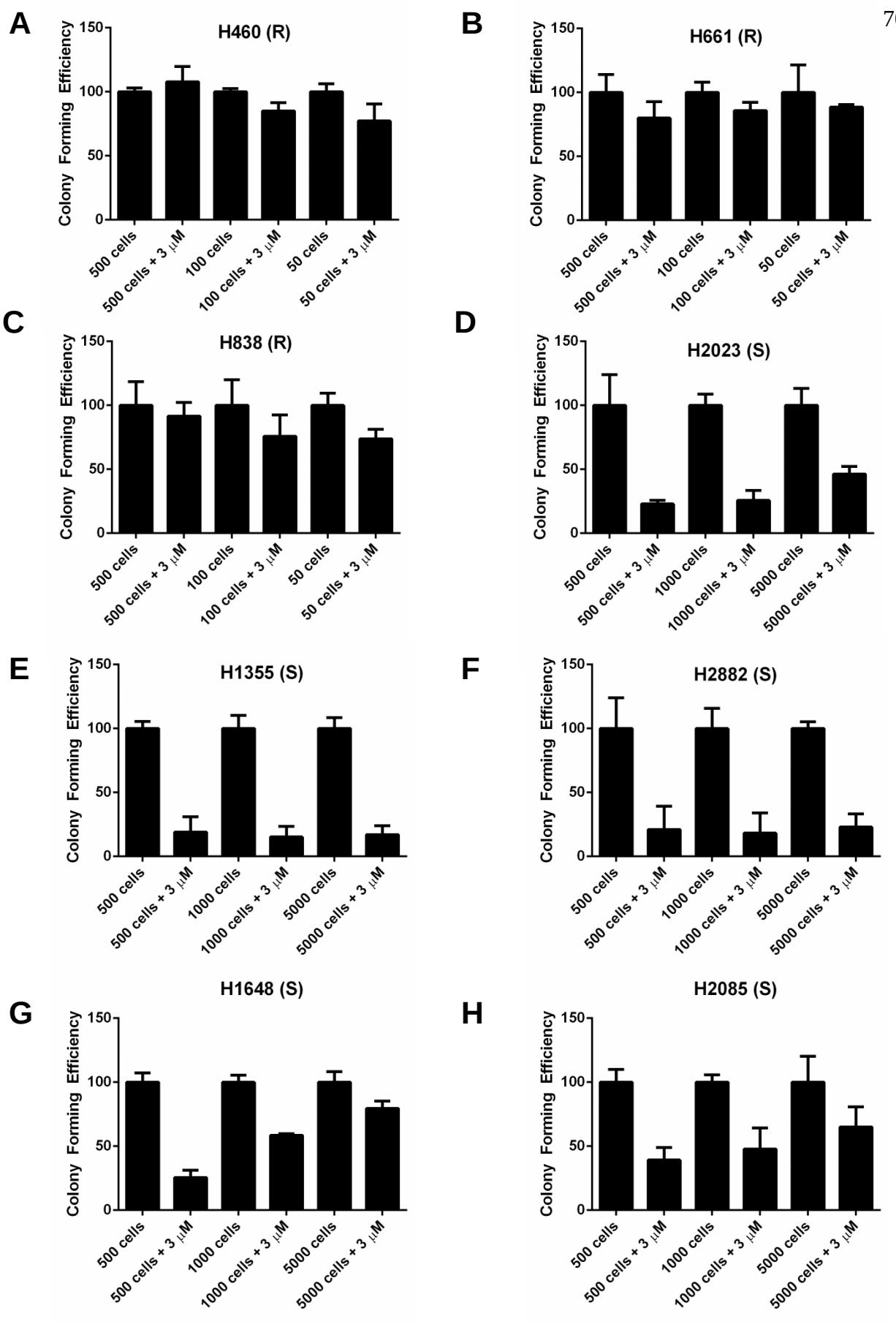
A
H460 (R)
B
H661 (R)
C
H838 (R)
D
H2023 (S)
E
H1355 (S)
F
H2882 (S)
G
H1648 (S)
H
H2085 (S)
Colony Forming Efficiency
150
100
50
0
500 cells
500 cells + 3 μM
100 cells
100 cells + 3 μM
50 cells
50 cells + 3 μM
1000 cells
1000 cells + 3 μM
5000 cells
5000 cells + 3 μM

**Figure 4.5 Colony Formation Cell Number Titrations with 3 μM Imetelstat.** (A-C) 500, 100, and 50 cells of H460, H661, and H838 (all resistant lines in colony formation designated by (R)) were plated in triplicate in colony forming conditions. 3 μM imetelstat was added 24 hours later. Cells were allowed to grow 2-4 weeks followed by staining and quantification. Percent colony forming efficiency relative to control colonies is graphed for each cell line. (D-H) 500, 1000, and 5000 cells of H2023, H1355, H2882, H1648 and H2085 (all sensitive lines in colony formation designated by (S)) were plated in triplicate in colony formation conditions. 3 μM imetelstat was added 24 hours later. Cells were allowed to grow for 2-4 weeks followed by staining and quantification. Percent colony forming efficiency relative to control colonies is shown for each cell line.

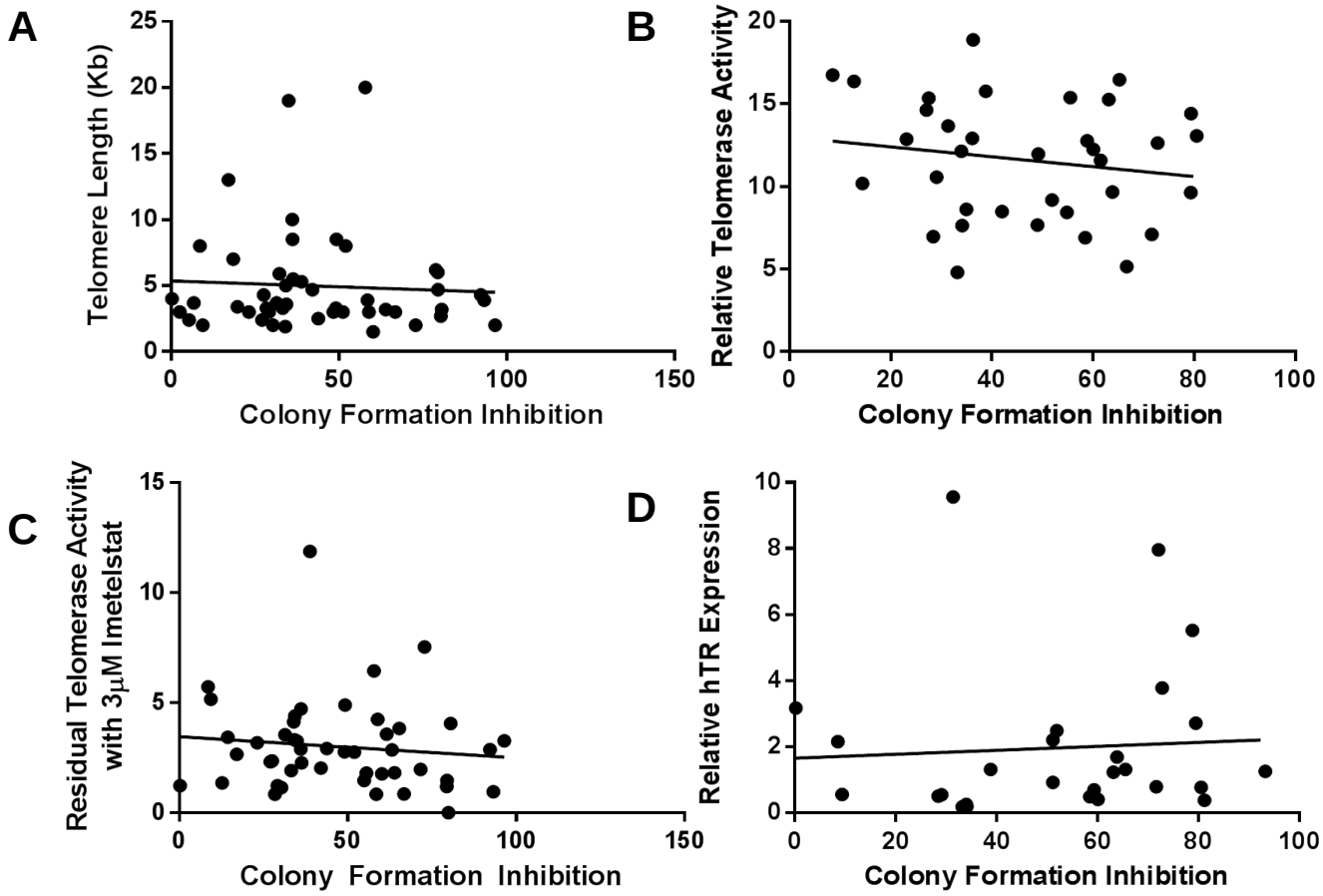


**Figure 4.6 Correlation Between Colony Formation Inhibition with 3 μM Imetelstat and Telomere Length, Telomerase Activity, hTR Expression, and Residual Telomerase Activity.** (A) Percent colony formation inhibition with 3 μM imetelstat versus average telomere length shows no correlation ($r^2$ = 0.0034). (B) Percent colony forming inhibition with 3 μM imetelstat shows no correlation with relative telomerase activity of the cell line ($r^2$ =0.028). (C) 3μM imetelstat induced reduction in colony forming ability shows no correlation with residual telomerase activity after treatment ($r^2$ = 0.013). (D) Imetelstat percent colony formation inhibition does not correlate with relative hTR levels ($r^2$ = 0.004).

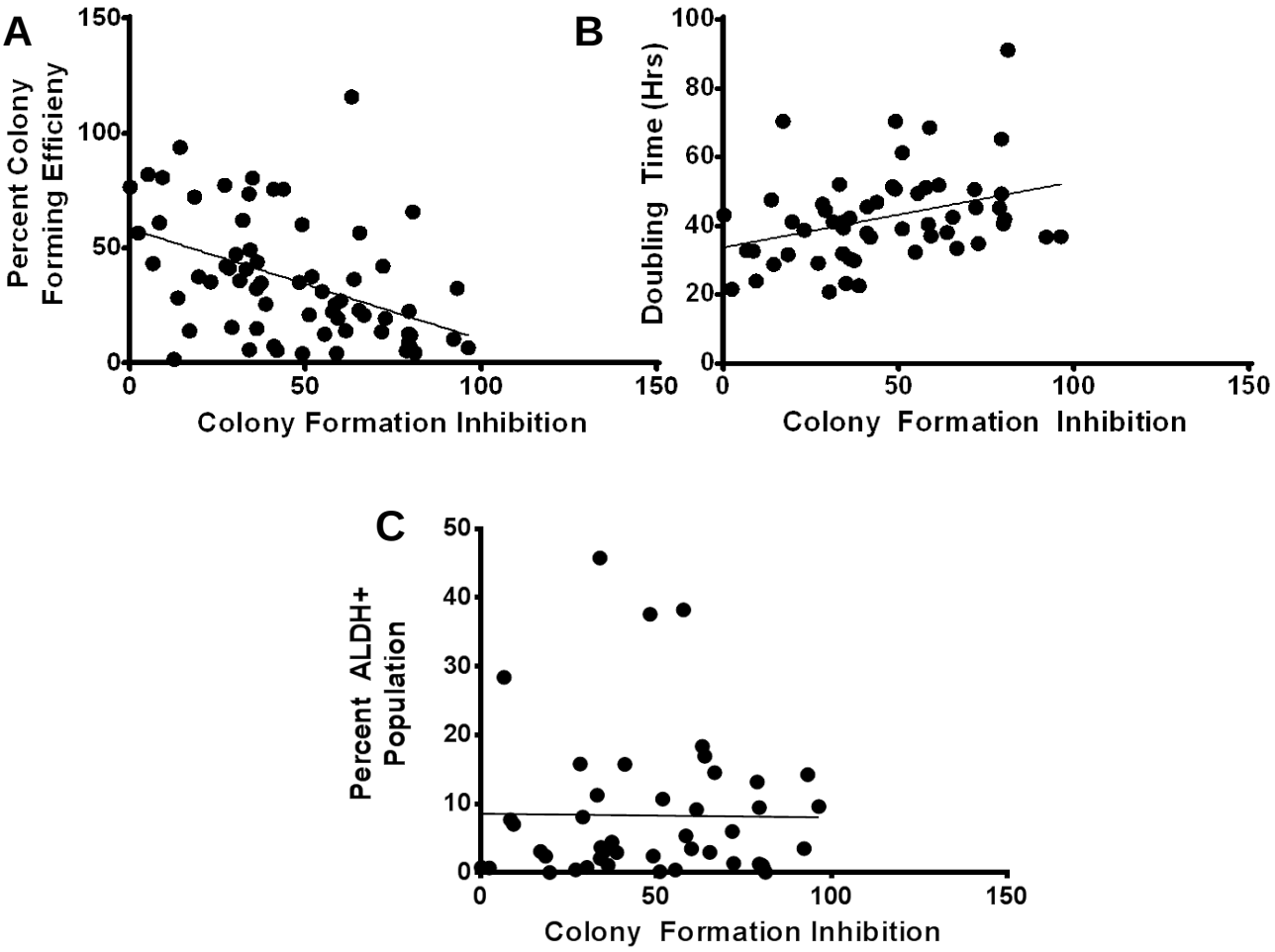


**Figure 4.7 Correlation Between Colony Formation Inhibition with 3 μM Imetelstat and Percent Colony Forming Efficiency, Doubling Time and Percent ALDH$^+$ Population.** (A) Percent colony forming efficiency does not correlate statistically significantly with colony formation inhibition with 3 μM imetelstat ($r^2$ =0.2) (B) Percent colony forming efficiency does not correlate with doubling time of the cell line ($r^2$ = 0.12). (C) Percent ALDH$^+$ population does not correlate with colony formation inhibition with 3 μM imetelstat ($r^2$ = 0.00017).

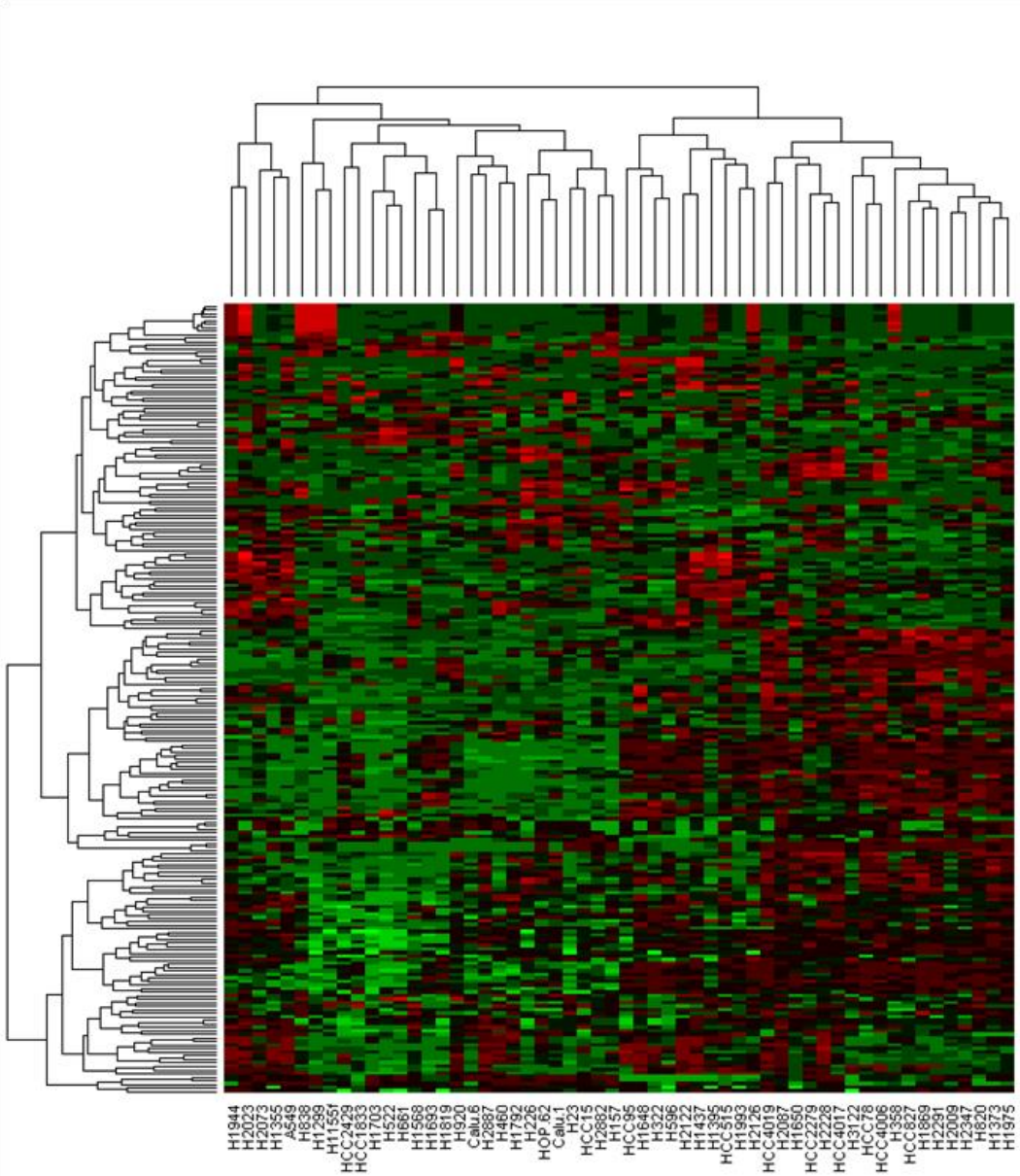


**Figure 4.8 Hierarchical Clustering Analysis of mRNA Expression Data Correlating Responder and Non-responder Phenotypes in Colony Formation.** Example of signature generated to predict response of cell lines to 3 μM imetelstat in colony formation assay. P-value of overall differences between responders and non-responders is not statistically significant ($p = 0.14$).

# CHAPTER FIVE

## LONG-TERM IMETELSTAT TREATMENT

### 5.1 Introduction

For telomerase inhibition to be effective, telomerase must first be inhibited followed by continued cell divisions where telomeres shorten with each division eventually leading the cells to senescence. Using imetelstat in long-term continuous treatment conditions would presumably produce the best results.

Previous work with imetelstat has shown telomerase inhibition and telomere shortening in multiple cancer types. In breast cancer, imetelstat has been shown to inhibit telomerase, shorten telomeres, decrease colony forming ability *in vitro* as well as decrease tumor metastases *in vivo (Gellert, Dikmen et al. 2006; Hochreiter, Xiao et al. 2006)* . In lung cancer, Dikmen, et al showed telomerase inhibition and telomere shortening as well as a decrease in colony forming ability and efficacy *in vivo* with imetelstat. However all of the work completed was only done in A549 lung cancer cell line. The following studies looked at long-term treatment with imetelstat in multiple NSCLC lines to confirm that imetelstat was effective in a range of lung cancer subtypes and telomere lengths.

## 5.2 Results

### *5.2.1 Imetelstat Inhibits Telomerase and Leads to Telomere Shortening*

Previous work by Dikmen, et al demonstrated imetelstat efficacy in the NSCLC cell line A549, but no other cell lines were tested (Dikmen, Gellert et al. 2005). To determine imetelstat efficacy in multiple NSCLC cell lines, imetelstat was administered to H157, H2087 and H1819 cell lines at 1 μM twice weekly. Cells were collected for telomerase activity analysis via the TRAP assay and telomere length analysis via TRF assay periodically during the duration of treatment. Figure 5.1A shows that imetelstat effectively inhibits telomerase long-term. Figure 5.1B is a TRF indicating telomere length with prolonged exposure to imetelstat. With continuous treatment, telomere length gradually shortens in all three cell lines treated. Figure 1A and B collectively demonstrate imetelstat effectively inhibits telomerase and leads to telomere shortening in multiple cell lines indicating imetelstat functions as intended in multiple NSCLC cell lines.

### *5.2.2 Removal of Imetelstat After Long-term Treatment and Telomere Shortening Results in Return of Telomeres*

Long-term imetelstat treatment leads to inhibition of telomerase and gradual telomere shortening. H157 and H1819 were both treated for 40 weeks with imetelstat and telomeres were significantly shortened (Figure 5.2). At this time point, imetelstat was removed from

both cell populations. In both cases, by 2 weeks without treatment, there is a noticeable increase in telomere length compared to 40 weeks of continuous imetelstat treatment. In H157, telomeres returned to parental/pretreatment length in as few as 4 weeks without imetelstat. H1819 also showed elongation of telomeres but at a slower rate. By 8 weeks of treatment, H1819 telomeres have not quite returned to parental/pretreatment length. The difference in telomere length elongation time can be explained by population doubling time. H157 is a very quickly dividing cell line with a population doubling time of 20.8 hours (Appendix A) while H1819 is a much slower growing cell line with a population doubling time of 51.3 hours. Because H157 doubles so quickly, the cell turnover, and therefore telomere extension, happens at a much faster rate leading to telomere elongation within a shorter period of time.

### *5.2.3 Long-term Imetelstat Response Time Dependent on Initial Telomere Length and Cell Line Growth Rate*

Multiple cell lines were treated long-term *in vitro* with 1 μM imetelstat given 3 times per week. Figure 5.3 shows growth curves for many cell lines with and without imetelstat. In most cases, continuous long-term treatment results in an eventual reduction in growth rate followed by cellular senescence and/or cell death indicated by a halt in cell growth and termination of the growth curve. Calu-3 had the shortest initial telomere length measured in the panel at 1.5 kb and as expected, Calu-3 cells had the shortest response time to imetelstat

*in vitro*. Figure 5.3A shows Calu-3 response *in vitro* indicating there is a slow in growth rate in as few as 11 days or 5 versus 2 population doublings in control cells versus imetelstat treated cells, respectively. By 60 days or 32 population doublings in control cells, there were no remaining cells in the imetelstat treated flask. HCC827 initial telomere length was 3 kb and imetelstat treated cells began to show a slow in growth rate at 100 days or about 40 population doublings followed by a relatively quick senescence and cell death at 145 days of treatment or 62 population doublings for control cells and 46 population doublings for treated cells (Figure 5.3B). Figure 5.3C shows the growth curve of H358, initial average telomere length 3.4 kb, with and without imetelstat. H358 cells growth slowed around 60 population doublings (125 days of treatment) and cells senesce and stop dividing by 76 population doublings or 200 days of treatment. H460 growth curve with imetelstat is shown in Figure 5.3D. H460 initial average telomere length is 5 kb and imetelstat treated cells show reduced growth rate by 50 population doublings or 70 days of treatment. The growth curve of treated cells plateaus indicating senescence by 115 days or 60 population doublings. H1648, initial telomere length 2 kb and the second shortest telomere length in the panel, showed similar results. H1648 was repeated twice and growth curves for each replicate are shown in Figure 5.3E-F. Imetelstat treatment was necessary for at least 15 population doublings and complete senescence is seen in both replicates in less than 150 days. H2882 and H2009, initial telomere lengths 9.4 kb and 7 kb respectively, are shown in Figure 5.3G and 5.3H with and without imetelstat. H2882 growth begins to slow compared to untreated control at 70

population doublings however cells continue to divide and grow with up to 1 year of treatment. H2009 shows minimal change in growth rates of treated and untreated cells with only a slight difference beginning at 130 population doublings. Cells were treated up to 1 year with imetelstat.

Figure 5.4 shows morphology changes of the cells with and without long-term imetelstat treatment. HCC827, shown at 126 days of treatment, displays cellular elongation and an increase in the number of vacuoles present. 126 days is about 44 total population doublings for the treated cells and about 20 days before the cells stopped dividing and could not be split again. H1648 cells are shown at 140 days which is about 46 total population doublings for the treated cells and about 10 days before the cells stopped growing and could not be split again. Morphology changes are similar to that seen in HCC827 with elongation of the cells and increased and enlarged vacuoles. H460 is shown at 203 days and displayed negative growth at this time point. Cells were rounding up and detaching from the plate days before leaving minimal cells still attached at the time of the photograph. H358 is shown at 224 days and cells show elongation and increased spindles as well as rounding up and detachment from the plate. H358 cells were not split again after this time point because of lack of cell number and cell growth.

H2887 growth curve with and without 1 μM imetelstat is shown in Figure 5.5A. H2887 initial telomere length is 2 kb and begins to show a decrease in growth rate in imetelstat treated cells in 12 population doublings or 26 days. The growth curve plateaus

shortly after 26 days for the treated cells and cells senesce, however unlike cell lines mentioned above, all of the cells did not eventually detach and apoptosis. Some remain attached in small clusters, as seen in Figure 5.5B at 231 days of treatment. Morphology of the cells has drastically changed. Cells are either elongated with many extra spindles or they are rounded up. Continuous imetelstat treatment was administered even though cells were not split or counted. At 235 days of treatment, or 19 total population doublings of the treated cells, imetelstat was removed and cells were continuously fed with fresh media without drug. At 370 days, cells begin to recover and grow. Cells were split about every 10 days and eventually reached a total of 30 population doublings at 424 days after imetelstat treatment initially started.

### *5.2.4 Long-term Imetelstat Targets Cancer Stem Cell Population*

During multiple time points throughout the long-term imetelstat treatment, cells were plated for colony forming ability. Figure 5.6 shows cell lines with progressive imetelstat treatment in the colony formation assay with 500 cells plated per well. H1648 colony forming ability slows by 56 days with 30% reduction in colony forming ability and minimal colonies form at 91 days (92% reduction in colony forming ability). H358 and H460 show minimal changes in colony forming ability at 56 days, but by 91 days of imetelstat treatment both show a significant reduction in colony forming ability. In all cases, the reduction in colony forming ability correlates with the long-term growth curve of the cell line in the

presence of imetelstat. As the cell growth rate slows and the growth curve begins to plateau, colony forming ability reduces in all cell lines tested.

To determine if imetelstat could target the cancer stem cell population, $ALDH^+$ percentage of the population was measured (Sullivan, Spinola et al. 2010). Figure 5.7 shows H358, H1648, H2009 and H2087 at 70 days of imetelstat treatment. Both H358 and H1648 show a decrease in percent $ALDH^+$ population with continuous imetelstat treatment. At 70 days, H358 treated cells growth curve has not diverged from the untreated control growth curve and no difference can be seen in morphology. H1648 growth is beginning to slow compared to untreated control cells. H2009 and H2087 show no change in percent $ALDH^+$ population.

*5.2.5 Imetelstat Treatment in Combination with Standard Chemotherapy*

In clinical trials, patients must be given at least standard of care. For NSCLC, standard of care is doublet taxel-platinum therapy and in the United States the standard doublet is paclitaxel and carboplatin chemotherapy. The first Phase I clinical trial with imetelstat in NSCLC was paclitaxel/carboplatin doublet chemotherapy with or without imetelstat. However, minimal preclinical work was completed determining the effects of combining imetelstat with standard chemotherapies. To address this, cell lines were treated with either imetelstat concurrently with chemotherapy for short-term assays or treated with long-term imetelstat and periodically treated with chemotherapy after specific time points.

First, H157, H1819 and H2087 cell lines were treated either alone or with 10 μM imetelstat in combination with paclitaxel, carboplatin and a carboplatin/paclitaxel combination given in a 2:3 wt/wt ratio as given in the clinic. The 5-day drug response assay consists of plating the cells in a 96-well plate format on day 0, adding drug on day 1 followed by a 4-day incubation, adding MTS on day 5 and reading on a plate reader. The imetelstat was added at a constant 10 μM for all chemotherapy dosages. The chemotherapy was dosed with a highest concentration of 1000 nM, 808 μM, and 1000 nM for paclitaxel, carboplatin, and paclitaxel/carboplatin (presented in terms of paclitaxel concentration), respectively. Subsequent dosages were determined by four-fold dilutions until the lowest dose of 0.06 nM, 0.06 μM, and 0.06 nM for paclitaxel, carboplatin, and paclitaxel/carboplatin, respectively. The addition of imetelstat to the chemotherapy had no impact on the cell lines sensitivity to chemotherapy.

Many cell lines were treated long-term with 1 μM imetelstat given twice weekly. At multiple time points, H157, H1819, H2087, H2073, H2009, H1648 and H358 were plated in the MTS assay mentioned above with paclitaxel, carboplatin, paclitaxel/carboplatin combination, doxorubicin, gemcitabine, vinorelbine, and erlotinib. No significant changes in sensitivity were seen to the chemotherapies in any cell line with long-term imetelstat compared to untreated parental control cells.

*5.2.6 Imetelstat Treatment in Xenograft Model*

Calu-3, with 1.5 kb average telomeres, has the shortest telomeres found in the NSCLC cell line panel tested. Due to the short telomeres, Calu-3 responded best *in vitro* with the fastest time to senescence with long-term continuous imetelstat treatment. Given this data, it was hypothesized that Calu-3 would respond the fastest *in vivo* as well. Figure 5.8A shows the growth curve of Calu-3 *in vivo*. $1x10^6$ cells were injected subcutaneously into the right flank of 20 mice. 10 mice were given saline 3 times per week and 10 mice were given 30 mg/kg imetelstat 3 times per week. The experiment end point was determined when the control (saline treated) mice reached 2000 $mm^3$, maximum tumor volume allowed by IACUC regulations. The tumors grew for 65 days and at the endpoint, there was a statistically significant difference between the growth curves of treated versus untreated tumors. Figure 5.8B shows the comparison of average tumor mass at the endpoint of experiment and also shows statistically significant difference in tumor volume ($p < 0.008$). H460, H1373, H2073, H1648 and HCC827 were also treated *in vivo* with and without imetelstat. HCC827 (initial average telomere length 3 kb) and H1648 (initial average telomere length 2 kb) tumor growth rates and tumor mass are also shown in Figure 5.8. HCC827 tumors were treated for 54 days before saline treated control group reached maximum tumor burden. The growth curve shows significant difference in growth rates (Figure 5.8C) and the tumor masses show statistically significant difference in size ($p < 0.008$). H1648 control tumors had very different take rates within the treatment groups and

tumor growth for the saline treated control group had a wide range of tumor sizes. At the end of the experiment, saline tumor masses ranged from 0.57 g to 2.77 g. Because of this range, the growth curve for the saline group had large error bars and did not show a statistically significant difference in tumor growth rate. However, average tumor mass at the end of the experiment did show a statistically significant difference with a p value of 0.0067. Three cell lines treated *in vivo* with imetelstat showed a significant response indicated by a significant reduction in tumor mass.

H460, H1373 and H2073 growth curves and tumor masses are shown in Figure 5.9. H460 initial telomere length is 5 kb and was not expected to show a difference in the relatively short-term treatment *in vivo*. H460 cells grow aggressively in a xenograft system so the experiment lasted only 3 weeks before the control tumors reached maximum allowable tumor burden and the mice had to be sacrificed. There was no difference seen in tumor growth rate or tumor mass at the conclusion of the experiment (Figure 5.9A-B). H1373 cells grew almost as quickly as H460 but started with only 3 kb telomere length. 70% of both the treated and untreated tumors became ulcerated. The ulceration led to large differences in tumor size and therefore large error bars. Figure 5.9C-D shows minimal difference in growth rate of treated and untreated tumors and a slight decrease in tumor volume comparing untreated to treated tumors however the difference is not statistically significant. H2073 initial telomere length is 3 kb and *in vivo* tumor growth rates and tumor mass showed no difference between treated and untreated groups (Figure 5.9E-F).

To determine imetelstat efficacy *in vivo*, telomere length and telomerase activity of the tumor xenografts were assessed. Figure 5.10A shows a TRAP assay of tumors with and without imetelstat. 6 μg of protein for Calu-3, H460, H1373 and H2073 treated and untreated tumor samples were run in the TRAP assay to show telomerase activity. Calu-3 shows no telomerase activity in treated or untreated tumor sample. H460, H1373 and H2073 all show telomerase inhibition in the imetelstat treated group indicating imetelstat is reaching its intended target and inhibiting telomerase activity. Figure 5.10B is a TRF of the same tumor samples (Calu-3, H460, H1373, and H2073) with and without imetelstat treatment. All 4 cell lines show a decrease in telomere length in the treated tumor sample. However, all of the telomeres are much longer than the telomere length of the cell line initially injected. Because the tumors are injected into mice and grown *in vivo*, mouse cells help support the tumor and can infiltrate the tumor through vascularization. These cells are then present for DNA extraction and the TRF. Mouse telomeres, however, are much longer than human telomeres, especially human tumor telomeres and can be 40+ kb in length (Kipling and Cooke 1990; Kelland 2005). Telomeres in Figure 5.10B are longer than the cell lines injected, most likely due to contamination of mouse cells in the samples. Nevertheless, telomeres did shorten in all four tumors indicating imetelstat is inhibiting telomerase and causing telomere attrition demonstrating that imetelstat works in an *in vivo* model.

Because H460 cells had longer initial telomeres and eventually responded *in vitro* with prolonged exposure to imetelstat, it was hypothesized that pretreated *in vitro* cells

subsequently injected subcutaneously into mice could show a difference in tumor take rate or tumor growth rate. H460 cells were treated with 1 μM imetelstat three times per week for 12 weeks. $1x10^5$ pretreated cells were injected into 5 mice and $1x10^5$ untreated H460 cells were also injected into 5 mice and tumor growth was monitored. Imetelstat treatment was not continued *in vivo* after tumor injection. Figure 5.11A shows tumor growth rate of pretreated and untreated cells. Initially, there was a lag in tumor formation in the 12 week pretreated tumors. However with continued growth, the pretreated tumor growth rate eventually caught up to the untreated control tumors. $1x10^6$ pretreated and untreated cells were also injected into 5 mice each. Although the $1x10^6$ cells pretreated with 12 weeks of imetelstat did not show as long of a lag between treated and untreated cells for tumor formation, pretreated tumors never reached the growth rate of the untreated tumor cells before the end of the experiment. Because imetelstat treatment was not continued *in vivo*, the pretreated cells had time to reactivate telomerase and stabilize the telomeres. Therefore in the group with $1x10^5$ cells injected, the tumors took longer to form and had longer to recover leading to increased growth rate at the end of the experiment.

**5.3 Discussion**

Imetelstat can effectively inhibit telomerase and lead to telomere shortening resulting in senescence and cell death in multiple NSCLC cell lines *in vitro* and lead to alterations in tumor growth *in vivo*. Once imetelstat treatment has begun, cells must stay in the continuous

presence of imetelstat to ensure constant telomerase inhibition. Figure 5.2 demonstrates how quickly telomere shortening can be negated if imetelstat therapy is removed. 40 weeks of treatment was required in both cell lines to reach the short telomeres shown, but in as few as 2 weeks without imetelstat, telomeres already begin to elongate back to parental length. In addition, Figure 5.5 shows H2887 with long-term imetelstat treatment. The cells begin to slow in growth rate in 12 population doublings and senesce and stop dividing in 19 population doublings. However, with no growth detected, imetelstat was removed and the cells eventually overcame the senescence and morphology changes and recovered. This also emphasizes the importance of continual treatment. Surviving cells can overcome the imetelstat induced senescence if treatment is removed.

Long-term *in vitro* imetelstat treatment leads to reproducible telomere shortening and eventual senescence and cell death in most cell lines tested. H2882 and H2009, however, continue to grow with minimal changes in growth rate up to a year with imetelstat treatment. These two cell lines had the longest initial average telomeres tested at 9.4 kb and 7 kb, respectively, and therefore may simply require much longer treatment time.

Collectively, the *in vitro* long-term studies support the idea that imetelstat therapy time to response is dependent on not only initial telomere length but also growth rate. As expected, Calu-3, with the shortest telomeres tested (1.5 kb), responds in the shortest time frame followed by H1648 with the second shortest telomeres (2 kb). H460 cells have initial telomere length of 5 kb but a doubling time of about 21 hours while HCC827 (initial

telomere length 3 kb) and H358 (initial telomere length 3.4 kb) have doubling times of 44.5 hours and 38 hours respectively. Therefore H460 response time in days is about the same as HCC827 and H358 but there is almost double the turnover in cell divisions in that same time frame.

The hypothesis of imetelstat treatment response time frame depending on both initial telomere length and growth rate also is supported with *in vivo* data. Of the six cell lines tested *in vivo*, H460 (initial telomere length 5 kb), H1373 (initial telomere length 3 kb) and H2073 (initial telomere length 3 kb), did not respond *in vivo*. HCC827 (initial telomere length 3 kb), H1648 (initial telomere length 2 kb) and Calu-3 (initial telomere length 1.5 kb) did respond *in vivo* and together had the shorter telomeres of the lines tested. However, HCC827 (responder), H1373 (non-responder) and H2073 (non-responder) all had initial telomere length of 3 kb and only one of the 3 responded. Figure 5.12 shows the average control saline treated growth curves for all six lines tested *in vivo*. H460, H1373, and H2073 did not respond to imetelstat before tumors reached maximum tumor burden in the mice and the mice had to be sacrificed. As shown in Figure 5.12, these three cell lines also had the fastest tumor growth rates supporting the idea that tumors that grow too quickly do not have time to inhibit telomerase and shorten telomeres before tumors become too big. H1648, HCC827 and Calu-3 all had slower growth rates and did respond to imetelstat in the time frame of the experiment. Growth rate of a cell line *in vivo* can be influenced by many factors, most notably the number of cells injected versus the number of cells that actually

form the tumor. In all cases, $1x10^6$ cells were injected in each mouse, but all one million cells most likely did not contribute to tumor formation and each cell line will be different regarding the number of cells that survive and form the tumor. In the lines that grow slower, fewer cells most likely contributed to the initial tumor and therefore had a higher cell turnover in the mouse before reaching the maximum tumor burden allowing telomeres to shorten further. Imetelstat response is dependent not only shortest telomeres but also slower growing cell lines both *in vitro* and *in vivo*. Additionally, the *in vivo* experiments for the non-responders could be repeated with fewer cells injected. All xenograft studies received $1x10^6$ cells injected subcutaneously. If $1x10^5$ or $1x10^4$ cells were injected for H460, H1373 or H2073, time to maximum tumor burden would be extended and allow for a longer treatment window to possibly provide for long enough exposure to imetelstat to see a difference in growth. However, tumor take rate can decrease with fewer cells injected so number of mice per treatment group should also be increased.

50% of the *in vivo* experiments showed a reduction in tumor burden in the presence of continuous imetelstat therapy. TRAP assay and TRF were conducted from tumor tissue to verify the imetelstat was effectively inhibiting telomerase and shortening telomeres. Figure 5.10A shows that telomerase is inhibited, even in the cell lines that do not show a decrease in tumor burden in the time frame of the assay (H460, H1373, and H2073). Figure 5.10B shows there is a decrease in telomere length in all four cell lines treated with imetelstat. As mentioned in the results section, these assays used tumor tissue that most likely had mouse

cells that infiltrated the tumors. While mice have much longer telomeres than humans, they possess the same telomere sequence and telomerase machinery and therefore are also susceptible to imetelstat treatment. Because there is a detectable reduction in telomerase activity, this indicates that all cells present in the assay, both mouse and human, were affected by the imetelstat and telomerase is inhibited in all cells tested indicating imetelstat is working as proposed. In addition, even though the telomeres are much longer in the TRF gel than the human telomere of the cell line injected, there is still proof of telomere shortening demonstrating imetelstat is not only reaching its target but also having the intended effect of telomerase inhibition and subsequent telomere shortening.

Lastly, H460 did not respond to the initial *in vivo* experiment. Because H460 has longer telomeres than other cell lines tested as well as quickly growing tumors *in vivo*, cells were pretreated to maximize imetelstat exposure before injection into mice. The pretreated cells show a lag time to tumor formation compared to untreated control cells indicating the cells are less able to form tumors compared to the parental control. The $1x10^5$ injection group showed a longer lag time in tumor formation between the pretreated and untreated groups, however by the time the tumors reached maximum tumor burden, the gap between the pretreated and untreated control was minimal. It is hypothesized that the lag time in tumor formation gave the cells the time necessary to reactivate telomerase and begin recovering from imetelstat treatment, similar to what is seen *in vitro* (Figure 5.2). This experiment should be repeated and imetelstat treatment should be given *in vivo* after tumor

injection to ensure the telomerase remains inhibited for the duration of the experiment and then compare tumor forming ability and tumor growth rate.

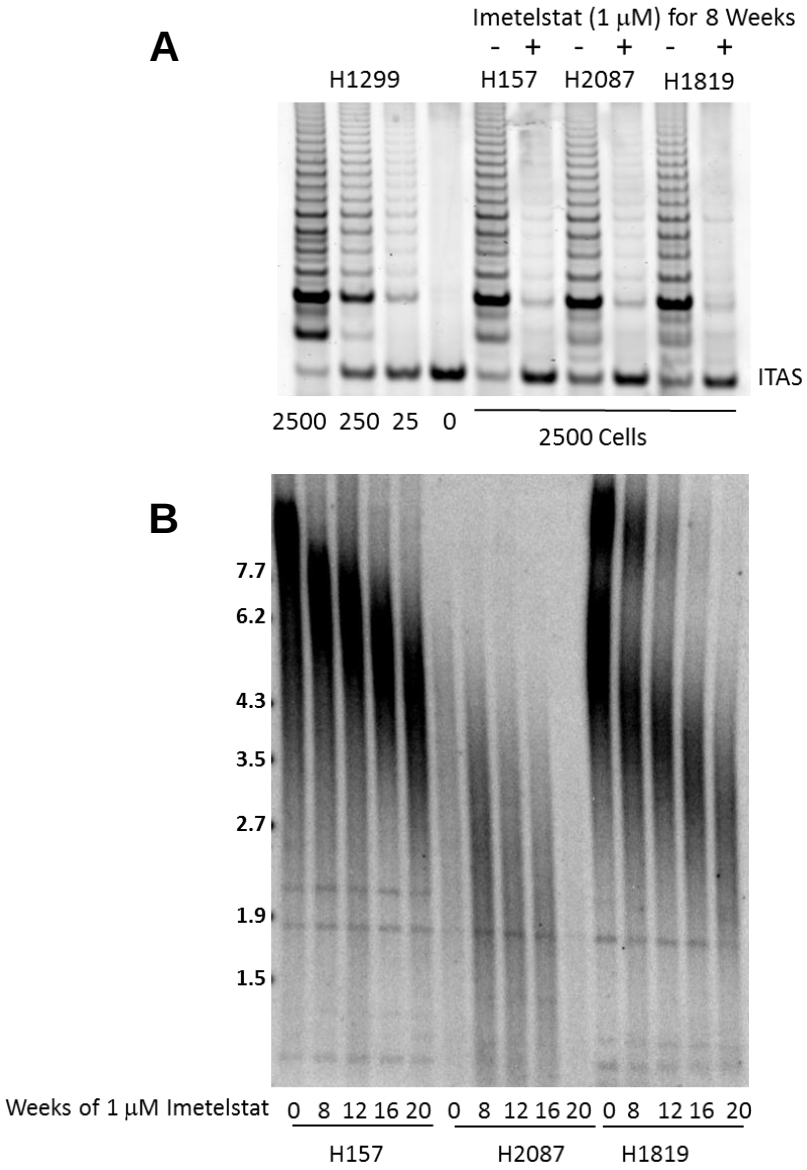


**Figure 5.1 Imetelstat Inhibits Telomerase and Leads to Telomere Shortening in Multiple NSCLC Cell Lines**. (A) H157, H2087 and H1819 were treated with continuous 1 μM imetelstat for 8 weeks and tested for telomerase activity. Lanes 1-4 are control lanes with 2500, 250, 25 and 0 (lysis buffer only) H1299 cells respectively indicating sensitivity of the assay and high levels of active telomerase. Lanes 5-6 are 2500 H157 cells without and with imetelstat, respectively, after 8 weeks. Lanes 7-8 are H2087 and lanes 9-10 are H1819 without and with 1 μM imetelstat. H157, H2087 and H1819 all show inhibition of telomerase with 1 μM imetelstat for 8 weeks. Imetelstat effectively inhibits telomerase long-term in multiple NSCLC cell lines. (B) Telomere length of H157, H2087 and H1819 with continuous 1 μM imetelstat treatment. Telomeres were measured at 0 (parental), 8, 12, 16, and 20 weeks of treatment. Telomeres shorten in all three cell lines with continuous imetelstat treatment.

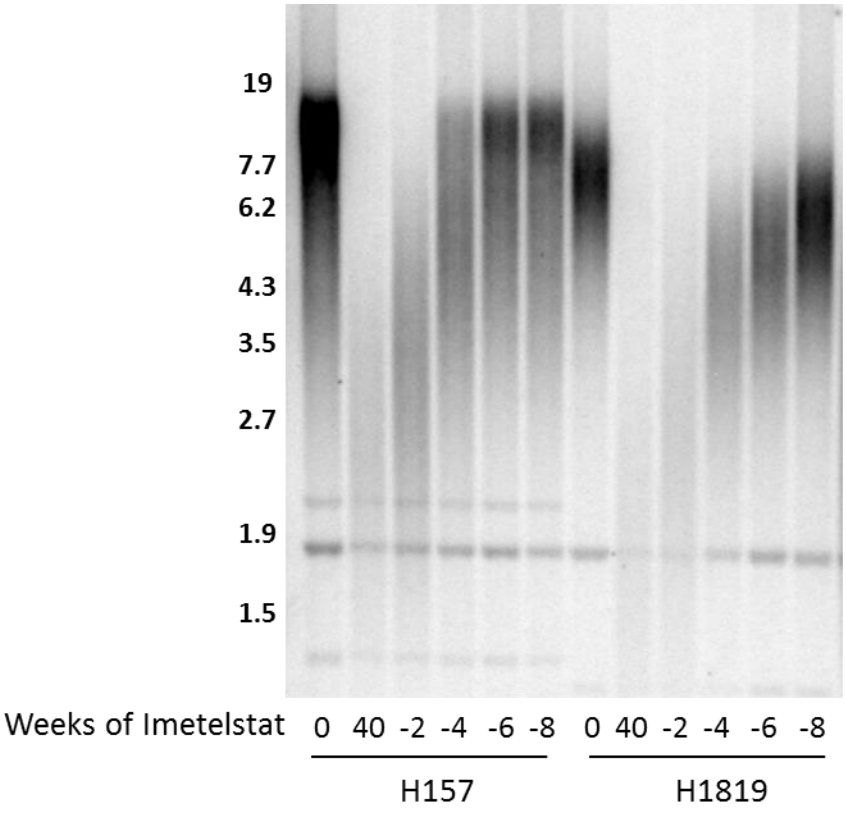


**Figure 5.2 Removal of Imetelstat Results in Progressive Return of Telomere Length.** Lane 1 is parental telomere length of H157 and lane 2 is H157 after 40 weeks of 1 μM imetelstat treatment. After 40 weeks of treatment, imetelstat was removed and cells continued to grow in the absence of imetelstat. Lanes 3-6 are H157 at 2, 4, 6 and 8 weeks after removal of treatment. Lane 7 is parental H1819, lane 8 is H1819 after 40 weeks of treatment, and lanes 9-12 are 2, 4, 6, and 8 weeks after removal of treatment. In both cell lines telomere length returns with removal of imetelstat.

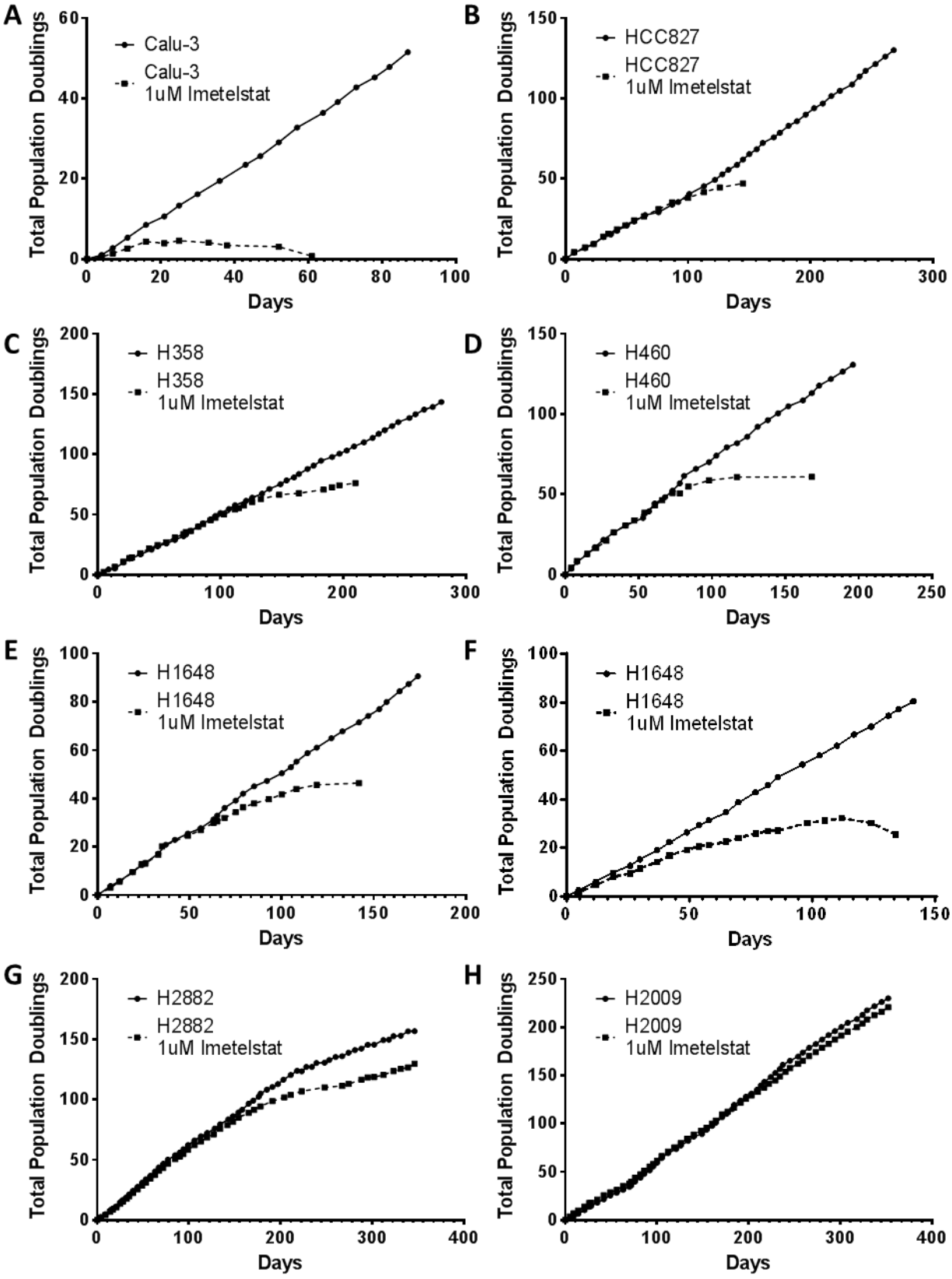
A
Total Population Doublings
Days
Calu-3
Calu-3
1uM Imetelstat
B
HCC827
HCC827
1uM Imetelstat
C
H358
H358
1uM Imetelstat
D
H460
H460
1uM Imetelstat
E
H1648
H1648
1uM Imetelstat
F
H1648
H1648
1uM Imetelstat
G
H2882
H2882
1uM Imetelstat
H
H2009
H2009
1uM Imetelstat

**Figure 5.3 Long-term Imetelstat Treatment Results in Slowed Growth and Eventual Senescence.** (A) Calu-3, initial telomere length 1.5 kb, shows the shortest response time to imetelstat. Growth slows in less than 4 population doublings (11 days) and no cells remained after 60 days. (B) HCC827, initial telomere length 3 kb, shows slowed growth rate at 40 population doublings (100 days) of imetelstat therapy and negative growth by 145 days of therapy. (C) H358 has 3.4 kb initial average telomere length and shows slowed growth rate at 60 population doublings (125 days) and takes about 200 days or a total of 76 population doublings for cells to completely stop dividing. (D) H460 has 5 kb initial telomeres and shows reduced growth rate by 50 population doublings (70 days) and negative growth rate by 115 days and 60 population doublings. (E-F) H1648 has 2 kb initial telomere length. H1648 was treated long-term with two replicates. H1648 growth rate slows with as few as 15 population doublings and shows senescence in both replicates in less than 150 days. (G) Initial telomere length of H2882 is 9.4 kb. H2882 growth slows with 70 population doublings but cells continue to grow with up to 1 year of treatment. (H) H2009 initial telomere length is 7 kb. H2009 growth rate slows slightly after 130 population doublings; however cells continue to grow with up to 1 year of treatment.

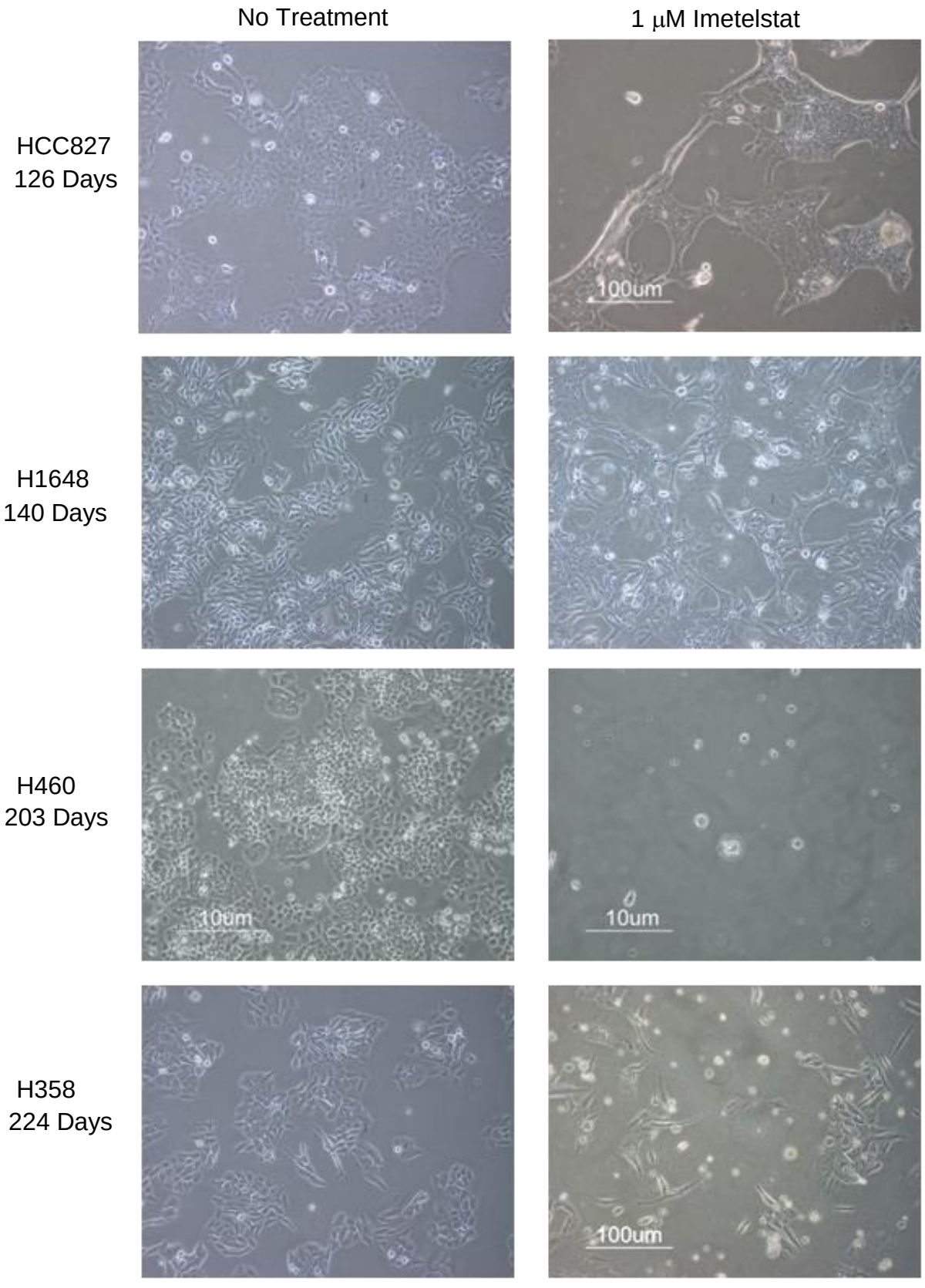
No Treatment
1 μM Imetelstat
HCC827
126 Days
100um
H1648
140 Days
H460
203 Days
10um
10um
H358
224 Days
100um

**Figure 5.4 Morphology Changes with Long-term 1 μM Imetelstat Treatment.** Cells were treated with 1 μM imetelstat three times per week for the designated number of days. The left column is untreated control cells for each line and the right column is cells treated with imetelstat. HCC827, H1648, and H358 cells become elongated and have increased spindles and vacuoles. H460 cell number decreases.

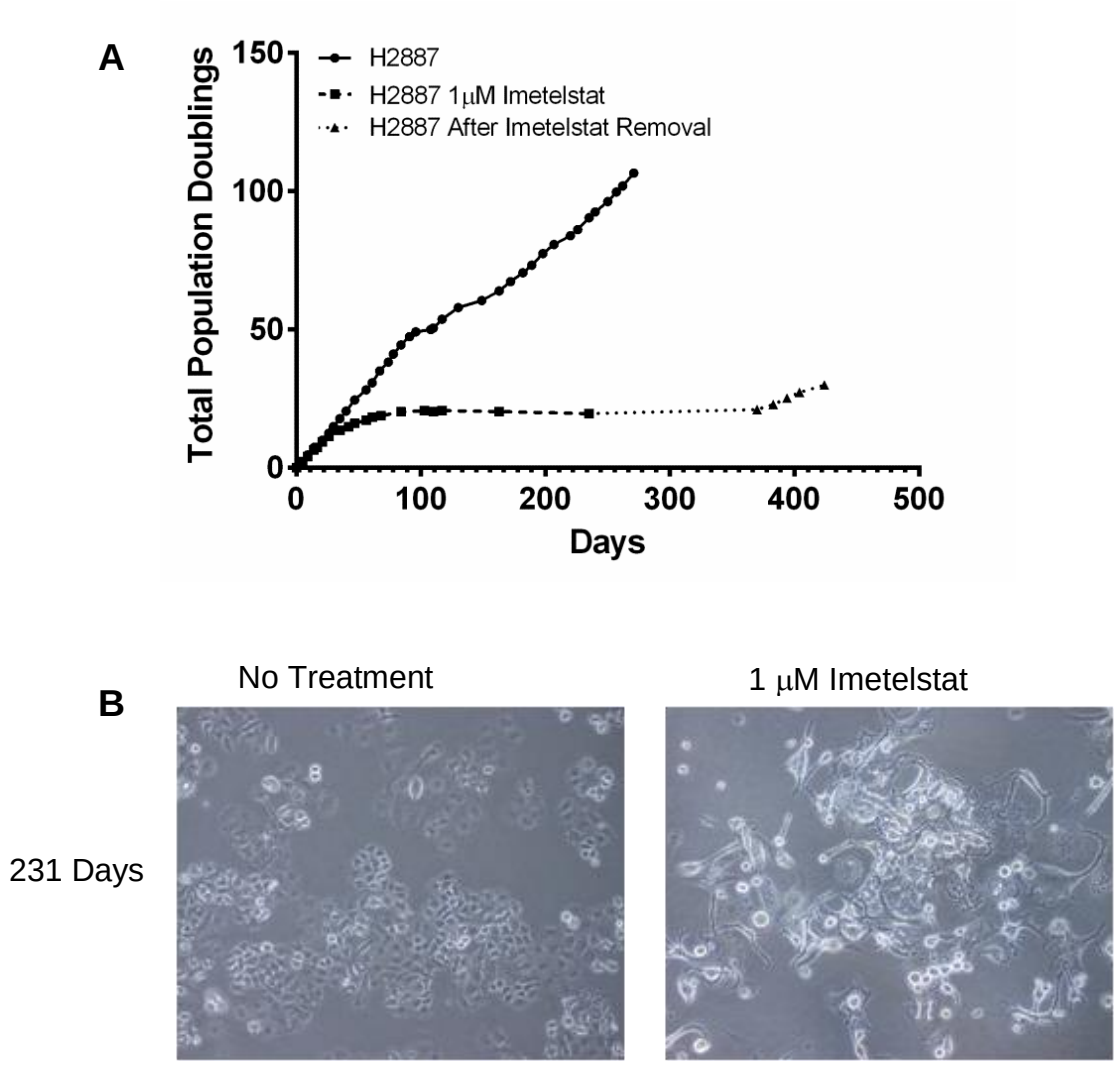


**Figure 5.5 H2887 Long-term Imetelstat Treated Cells.** (A) H2887 was treated long-term *in vitro* with 1 μM imetelstat given three times per week. Treated cells growth slows in 12 population doublings (26 days). Cells continued to survive and imetelstat was removed at 235 days or 19 total population doublings for treated cells. At 370 days, the cells without imetelstat recover. (B) Morphology of H2887 cells at 231 days of treatment. Imetelstat treated cells are elongated and have developed spindles.

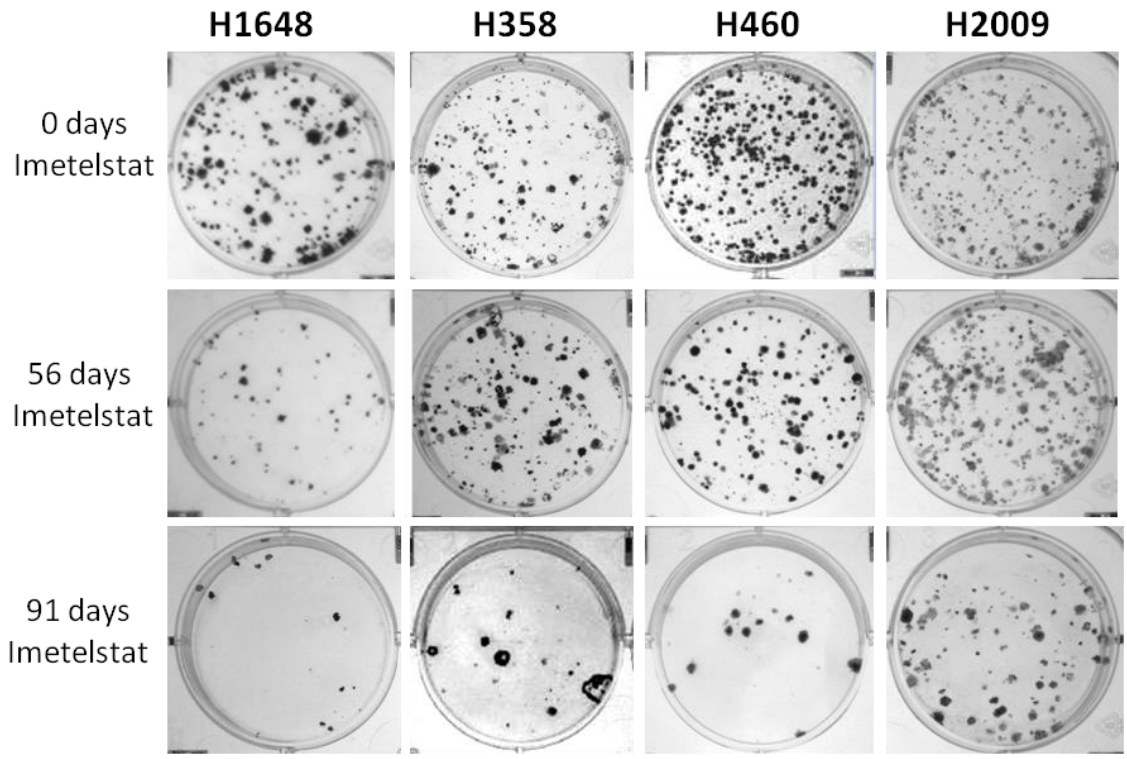


**Figure 5.6 Long-term Imetelstat Treatment Leads to Reduced Colony Forming Ability.** H1648 shows a decrease in colony forming ability by 56 days with a greater reduction seen at 91 days. H358 shows decrease in colony forming ability after 91 days of imetelstat treatment. H460 shows decreased colony forming ability at 56 days with further reduction in colonies by 91 days. H2009 shows a slight reduction in colonies formed after 91 days of imetelstat treatment.

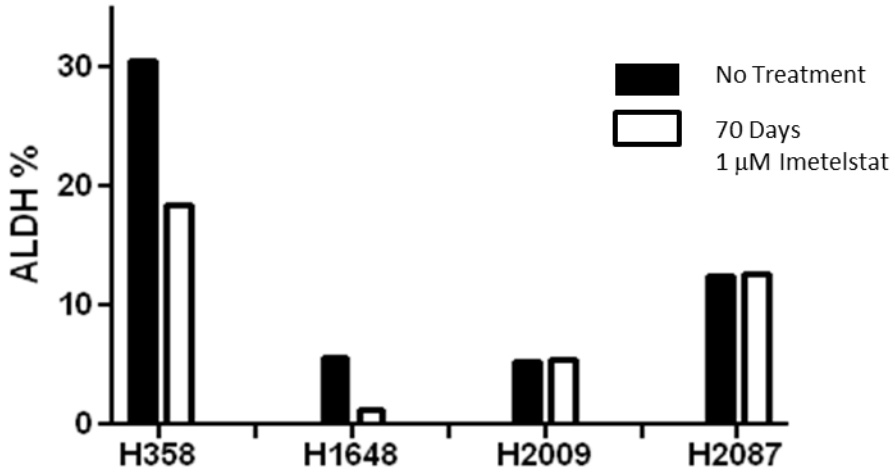


**Figure 5.7 Long-term Imetelstat Treatment Decreases the ALDH$^+$ Population.** H358, H1648, H2009 and H2087 were treated with 1μM imetelstat for 70 days and tested for percent ALDH$^+$ population. The black bars are untreated control cells and the white bars represent imetelstat treated cells. H358 ALDH$^+$ population decreases from 30% to 20% after imetelstat treatment. H1648 ALDH$^+$ population decreases from 6% to 1%. H2009 and H2087 show no change in ALDH$^+$ population with 70 days of imetelstat.

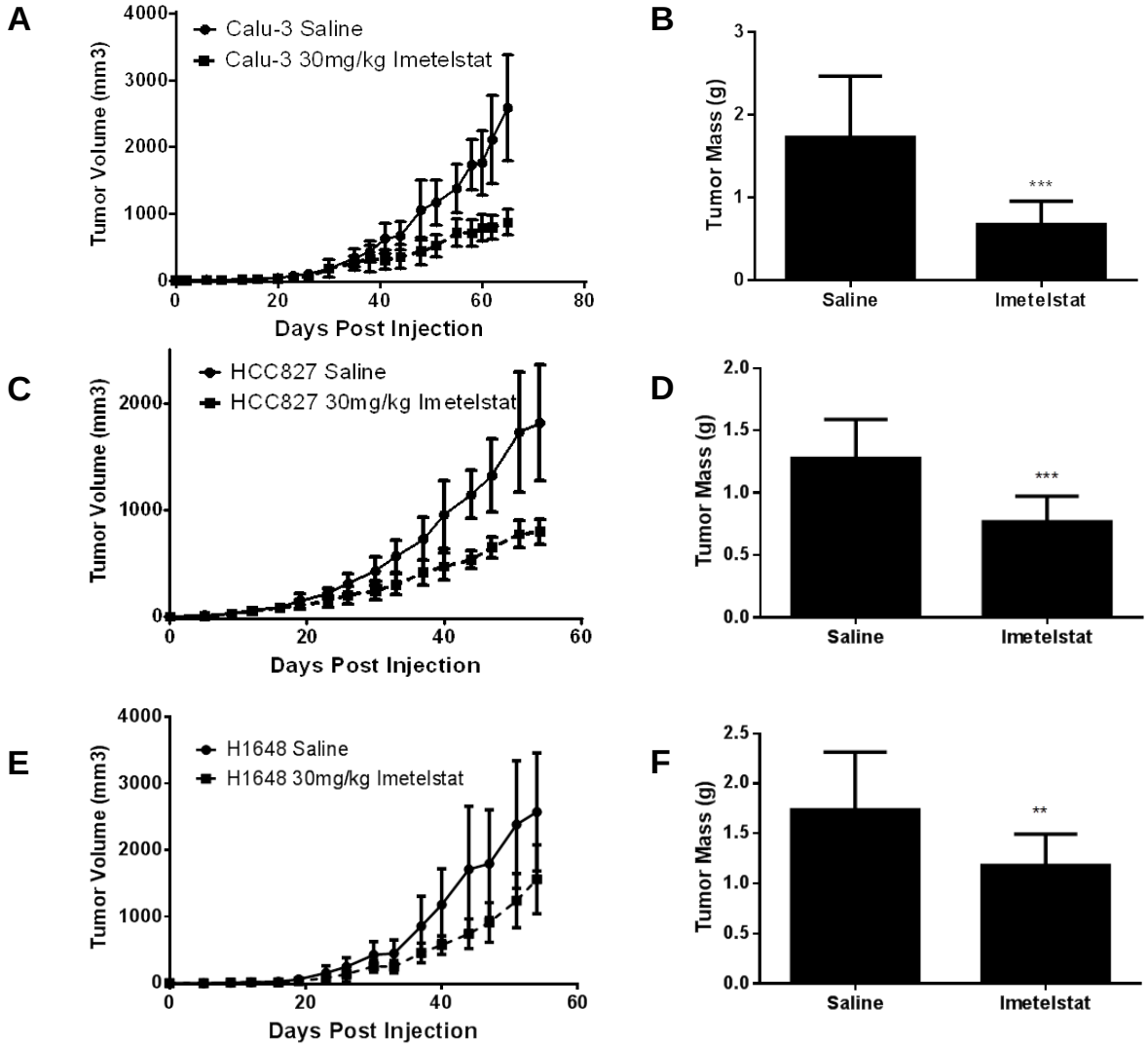


**Figure 5.8 NSCLC Response to Imetelstat *in vivo*.** $1x10^6$ cells were injected subcutaneously into NOD/SCID mice followed by saline (n=10) or 30 mg/kg imetelstat (n=10) given three times per week. Calu-3 (A) and HCC827 (C) show a decrease in tumor growth rate in the imetelstat treated group and significant difference in tumor weights at the conclusion of the experiment (B and D, $p < 0.008$ and $p < 0.008$, respectively). H1648 imetelstat treated tumors growth rate was slower than saline treated but not statistically significant (E). Difference in tumor mass at the conclusion of the experiment was statistically significant (F, $p < 0.0067$).

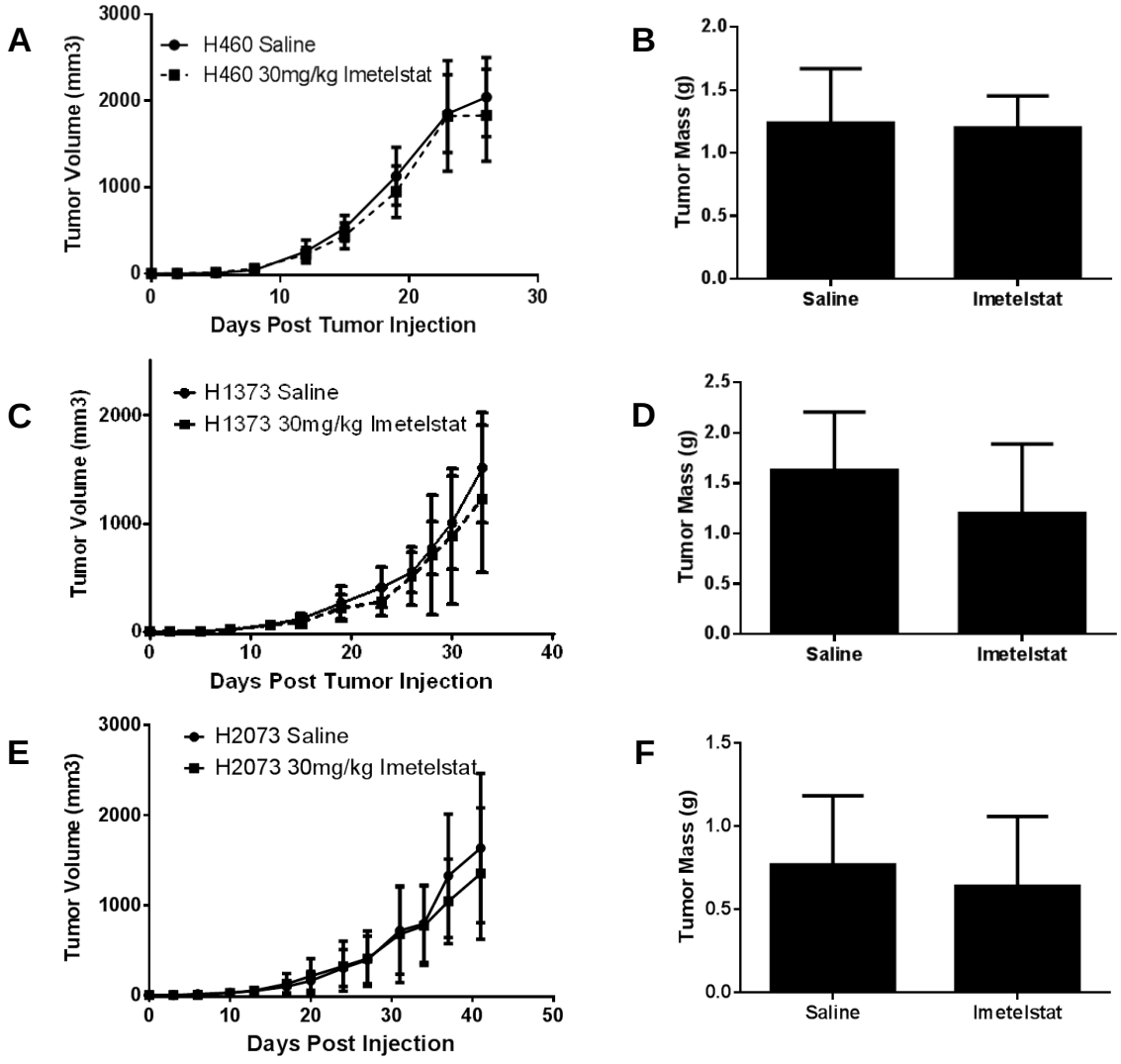


**Figure 5.9 NSCLC with Longer Telomeres and Faster Tumor Growth Rate Show No Response to Imetelstat *in vivo*.** $1x10^6$ cells were injected subcutaneously into NOD/SCID mice followed by saline (n=10) or 30 mg/kg imetelstat (n=10) given three times per week. H460 (A-B), H1373 (C-D) and H2073 (E-F) show no difference in treated versus untreated tumor growth rates or tumor weights at the conclusion of the experiment.

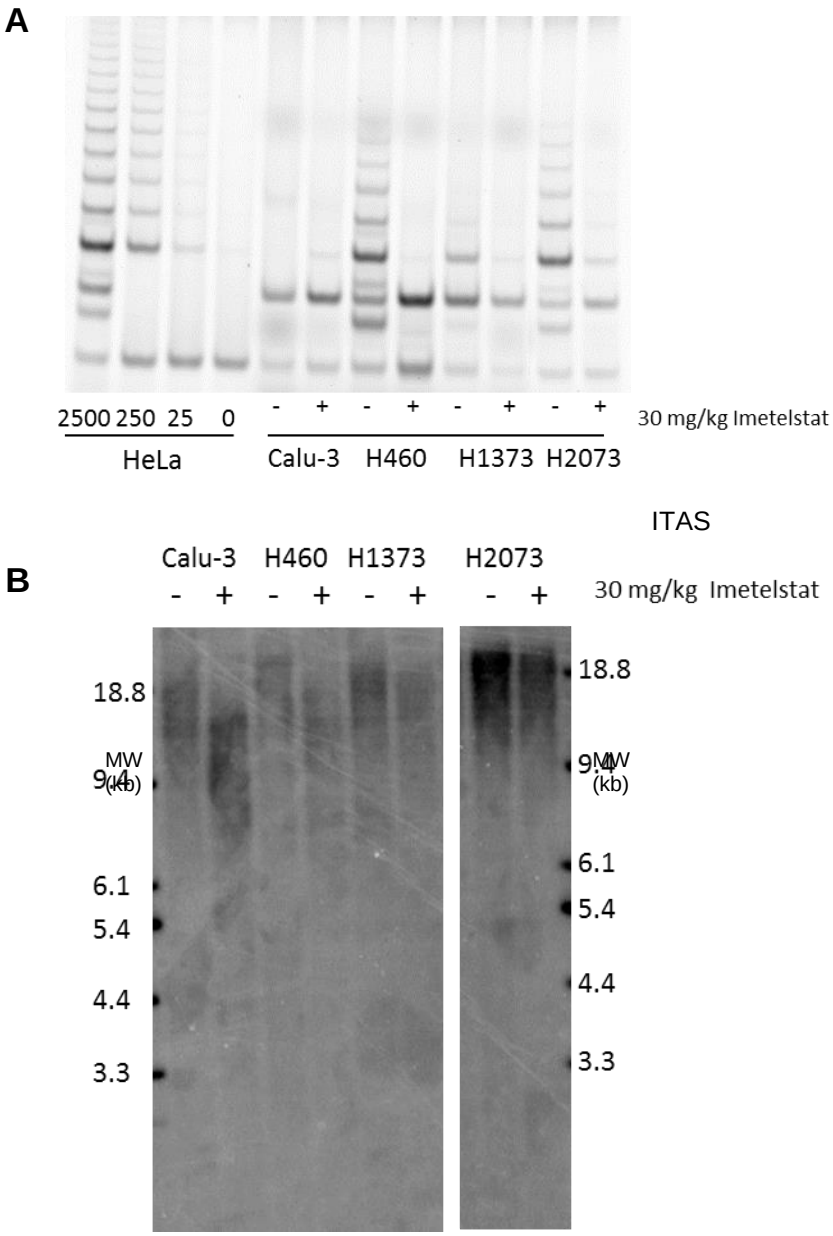


**Figure 5.10 Imetelstat Treatment *in vivo* Inhibits Telomerase and Shortens Telomeres.** (A) Telomerase activity of tumor tissue with and without imetelstat. Lanes 1-4 show 2500, 250, 25 and 0 (lysis buffer only) HeLa cells for control. Lanes 5-6 show 6 μg of Calu-3 saline and imetelstat tumors. Lanes 7-8 show 6 μg of H460 saline and imetelstat treated tumor showing a decrease in telomerase activity in imetelstat treated tumors. Lanes 9-10 and 11-12 show 6 μg of H1373 and H2073, respectively, of saline and imetelstat treated tumors. Both show a decrease in telomerase activity. (B) Telomere length of treated and untreated tumors. Calu-3, H460, H1373 and H2073 are shown without and with 30 mg/kg imetelstat in lanes 1-2, 3-4, 5-6, and 7-8 respectively. All lines show a decrease in telomere length with imetelstat treatment.

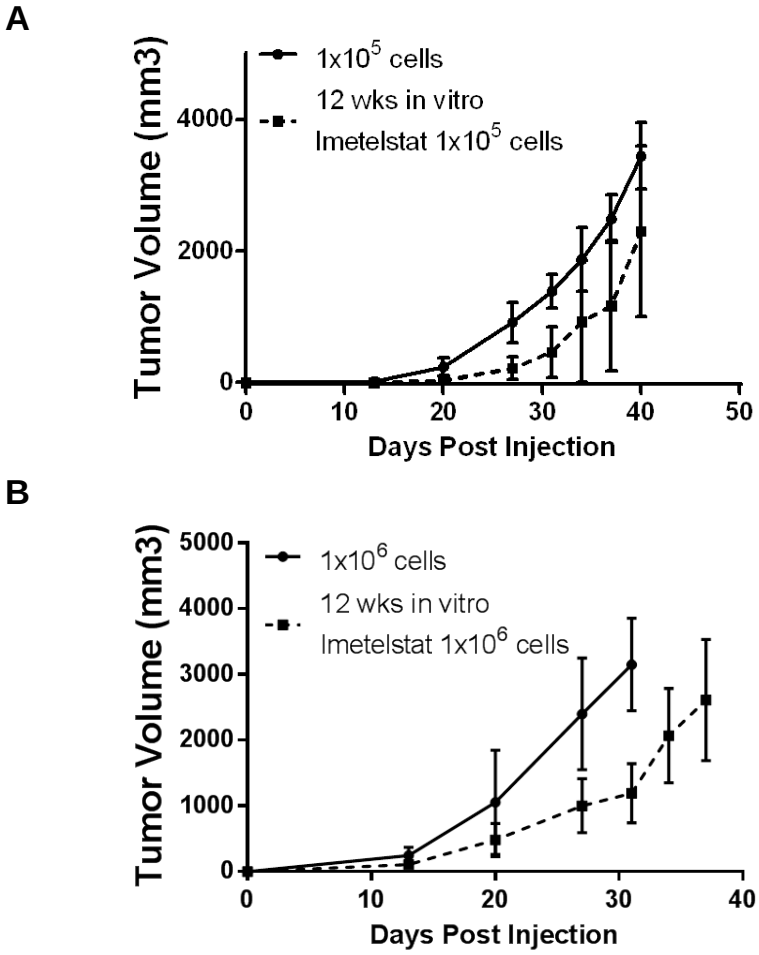


**Figure 5.11 H460 *in vitro* Pretreated Cells Display Slowed Growth Rate *in vivo*.** H460 cells were cultured in tissue culture receiving no treatment or 1μM imetelstat three times per week for 12 weeks. (A) $1x10^5$ H460 untreated (n=5) or 12 weeks pretreated (n=5) cells were injected subcutaneously. (B) $1x10^6$ H460 untreated (n=5) or 12 weeks pretreated (n=5) cells were injected subcutaneously. Both cases show a lag in growth rate for *in vitro* pretreated cells.

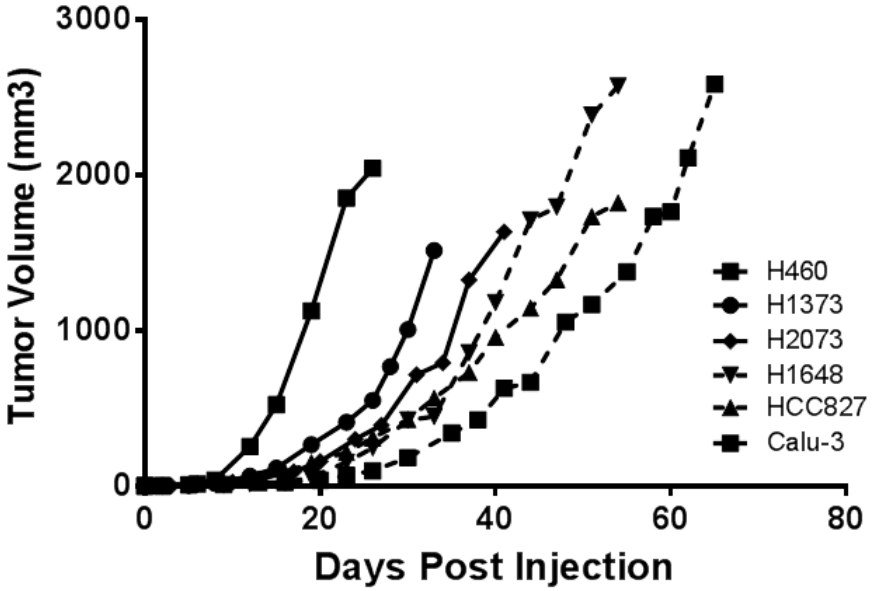


**Figure 5.12 Comparison of Control Tumor Growth Rates.** H460, H1373, H2073, H1648, HCC827 and Calu-3 average control saline-treated *in vivo* growth rates are shown. The three non-responder cell lines: H460 – initial telomere length 5 kb, H1373 – initial telomere length 3 kb and H2073 – initial telomere length 3 kb, had the fastest tumor growth rates and overall longer telomeres than the responders. Responding cell lines: H1648 – initial telomere length 2 kb, HCC827 – initial telomere length 3 kb, and Calu-3 – initial telomere length 1.5 kb, overall had shorter telomeres and slower growth rates than the non-responding cell lines.

# CHAPTER SIX

## SHORT-TERM IMETELSTAT TREATMENT

### 6.1 Introduction

One of the most straight forward and high throughput methods for determining drug sensitivity in a panel of cell lines is a 5-day drug response assay using the MTS reagent. Many cells can be tested quickly and easily with many replicates providing data to determine response phenotypes that can then be used to elucidate mechanisms of sensitivity and resistance.

For imetelstat to be effective, it must first inhibit telomerase and then remain inhibited while the cells continue to divide. If telomerase is sufficiently inhibited, then as cells continue to divide, their telomeres will shorten with every division until the telomeres reach critical length and cause the cells to senesce. Due to the mechanism of action of imetelstat, cells were not expected to respond to imetelstat in a five-day assay but the panel was still screened to determine if there was a range in response to imetelstat.

## 6.2 Results

### *6.2.1 Panel of Cell Lines in 5-day Drug Response Assay*

A panel of 75 NSCLC cell lines was tested in a 5-day drug response assay with 4-fold dilutions of imetelstat concentrations ranging from 2.6 nM- 42.5 μM imetelstat. The assay was conducted in a 96-well plate format and 8 different concentrations of imetelstat were tested in replicates of 8. The plates were repeated at least 4 times per cell line. The number of cells seeded was dependent on inherent growth rate as well as MTS (3-(4,5-dimethylthiazol-2-yl)-5-(3-carboxymethoxyphenyl)-2-(4-sulfophenyl)-2H-tetrazolium) enzymatic activity. For most cell lines, 2000 cells per well were seeded. Cells were plated day 0 and imetelstat was added at 0.0026 μM, 0.01 μM, 0.17 μM, 0.04 μM, 0.66 μM, 2.7 μM, 10.6 μM, and 42.5 μM concentrations on day 1. On day 5, MTS was added per well and plates were incubated at 37°C for 2-4 hours followed by absorbance reading.

Results of the screen are shown in Figure 6.1. Most cell lines show no change in growth for the duration of the 5-day assay with up to 42.5 μM imetelstat. 21 cell lines show a slight response at the highest concentration of imetelstat, however of the 75 cell lines tested, only one cell line was found to be highly sensitive in the short-term five-day assay, H2073 (Figure 6.2).

*6.2.2 H2073 Control Treatment*

H2073 cell line originated from a 47 year old female, 30 pack-year smoker diagnosed with Stage IIIa lung cancer (Phelps, Johnson et al. 1996). The cell line is derived from an adenocarcinoma tumor after a lung resection post neoadjuvant etoposide plus cisplatin doublet chemotherapy treatment. H2073 is the second cell line derived from this patient. H1993 was also derived from the same patient 2.5 months prior to H2073 and was started from a lymph node biopsy before any chemotherapy treatment (Phelps, Johnson et al. 1996). This isogenic pair derived before and after chemotherapy is very useful for studying sensitivity and resistance to many standard and targeted chemotherapies.

H1993 average telomere length is 10 kb while H2073 average telomere length is 3 kb (Figure 6.3A). H1993 and H2073 telomerase activity is similar (Figure 6.3B). Interestingly, H1993 is not sensitive to imetelstat in the five-day MTS assay (Figure 6.3C).

Because imetelstat is an oligonucleotide, oligos with the same backbone, lipid moiety, and sequence length but with altered base pair order easily serve as controls. H2073 is not sensitive to the mismatch control (Figure 6.4A).

The resulting growth curve from the MTS assay with H2073 and imetelstat indicates the $IC_{50}$ is achieved at 0.4 μM imetelstat. However, the growth curve plateaus just under this value. Even with up to 42.5 μM imetelstat, only about 50% of the cells are killed in the five day length of the assay. H2073 was plated in a liquid colony formation assay to see if the sensitive phenotype transcends multiple assays. Figure 6.4B shows H2073 plated in colony

formation conditions and treated with nothing, 3 μM imetelstat, 3 μM mismatch control or 3 μM sense control. While there is a decrease in colony forming ability of H2073 in the presence of imetelstat, there was not a drastic decrease in colony forming ability in the presence of mismatch or sense controls for the 2 week duration of the assay. Collectively, the 5-day drug response assay and colony formation assay demonstrate the sensitivity is imetelstat specific in multiple assays.

*6.2.3 H2073 Long-term Imetelstat Treatment*

Because H2073 achieves only a 50% kill in the 5-day assay but 70% reduction in colony forming ability in the presence of imetelstat, H2073 was treated long-term with 1 μM imetelstat given thrice weekly to determine if a greater than 50% response could be achieved with prolonged treatment. Figure 6.5A shows the results of sustained exposure to 1 μM imetelstat. In the beginning, the growth curve plateaus because there is a 50% reduction in cell number. The rest of the cells remain and continue to grow in the presence of imetelstat. After about 35 days, those susceptible to imetelstat are killed off and removed from the population and the resistant population continues to grow. At 40 days, the cells were split into 3 groups. Group 1 continued to get 1 μM imetelstat and the other two groups received 3 μM and 5 μM imetelstat to determine if the recovery after the initial slowed growth was due to resistance to 1 μM imetelstat. No significant difference in growth rate of the three populations was observed.

Telomere length of H2073 cells was also assessed. Figure 6.5B shows a TRF with parental H2073 at 3 kb, 1 μM imetelstat treated H2073 at 60 days with 2.4 kb telomere and again at 93 days with 2.1 kb as well as 3 μM and 5 μM treated cells at 2.1 kb telomere length. Telomeres shorten with continuous imetelstat exposure indicating the drug is reaching its target and 1, 3, and 5 μM imetelstat treated cells all show similar telomere shortening. This indicates higher telomerase dose does not have a greater effect.

### *6.2.4 H2073 Cloning*

To determine if there are two populations of cells within the H2073 cell line, one susceptible to short-term imetelstat and one resistant to short-term imetelstat, H2073 cells were plated at colony forming density and 10 clones were selected. 7 clones continued to grow and were expanded. Telomere lengths of the 7 clones were 2.3 kb, 2.4 kb, 2.6 kb, 2.9 kb, 3.0 kb, and 3.4 kb (Figure 6.6A). All 7 clones were re-tested in the five-day MTS assay and were expected to be either exquisitely sensitive or completely resistant to imetelstat, however neither was observed (Figure 6.6B). All of the clones displayed the same growth curve in the five-day MTS assay as the parental line – roughly 50% of the cells were killed in the time frame of the assay.

*6.2.5 H2073 hTERT Overexpression*

To determine if the sensitivity of H2073 to imetelstat is dependent on telomerase activity, H2073 was transfected with hTERT to increase telomerase activity and telomere length. Figure 6.7A shows the telomerase activity of H2073 parental, H2073 transfected with pBabe control vector and H2073 transfected with hTERT. Telomerase activity is increased in the cells with additional hTERT compared to parental H2073 or pBabe control vector transfected H2073. All three lines were also tested with 3 μM imetelstat and all three showed reduction in telomerase activity although hTERT transfected H2073 had higher residual telomerase levels after imetelstat treatment, also supporting increased telomerase activity. The parental line, vector control line and hTERT line were all tested in the 5-day MTS assay and all three lines show similar growth curves as the parental H2073 line with $IC_{50}$s of about 0.4 μM for all three lines (Figure 6.7B). All three lines were also tested in the clonogenic assay and all three lines, including the hTERT transfected line, are still sensitive to 3 μM imetelstat, indicating the H2073 sensitivity to imetelstat is not telomerase related (Figure 6.7C).

*6.2.6 H2073 in vivo*

$1x10^6$ H2073 cells were injected into the flank of 20 NOD/SCID mice. 10 mice received saline and 10 mice received 30 mg/kg imetelstat beginning 2 days after cell injection to determine if the initial lag in growth rate seen in *in vitro* transferred to an *in vivo*

model. Figure 6.8A shows the tumor growth rate indicating there is no difference between saline and imetelstat treated mice and there was no difference in tumor weight at the conclusion of the experiment (Figure 6.8B). The initial sensitivity seen in H2073 in the 5-day drug response assay, colony formation assay, and long-term treatment assay is not seen in a mouse model.

### 6.3 Discussion

The proposed mechanism of action of imetelstat is inhibition of the hTR RNA template component of telomerase thereby preventing telomerase from elongating telomeres. To be effective in cancer, imetelstat must first inhibit telomerase, the cells then continue to divide and telomeres shorten without active telomerase eventually leading to telomere shortening associated senescence or cell death. To see this effect, cells must go through multiple cell divisions which takes time. Due to this lag phase, a five-day drug response assay did not seem optimal for testing drug response with this therapy. However, one cell line, H2073, was found sensitive in the 5-day assay.

Discovering one cell line out of 75 tested is sensitive to any drug is not ideal results. First, with such a small population of responders, transfer to the clinic would be for a very rare patient population making it difficult to pursue. In addition, if more than one cell line was found to be sensitive, comparison studies could be conducted to determine what the sensitive lines have in common to elucidate a mechanism of sensitivity. With only one

sensitive line and the hundreds or thousands of mutations, copy number changes, gene expression changes and protein level changes that happen during cancer development, discovering the cause of sensitivity with a sample size of one proves very difficult. However, H2073 has the unique characteristic of having a paired cell line, H1993, which was created from the same patient. This cell line is not sensitive to imetelstat and can be used for comparison purposes. H1993 and H2073 share many of the same oncogenic mutations but also have a wide range of different mutations. Unfortunately, after comparison of differences in gene expression, the sensitivity of H2073 was not elucidated. However, H2073 does have much shorter telomeres than H1993, which would support H2073 responding faster to imetelstat treatment than H1993. Because the shortest telomere, and not the average telomere length, is vital for cell survival (Hemann, Strong et al. 2001), telo-FISH could be used to analyze telomere length for H2073 and the rest of the panel. H2073 may have a very short telomere that leads to early response that is not seen with the TRF method for measuring telomeres.

Cloning of H2073 gives rise to completely isogenic populations of cells. Because only about half of the population appeared to be sensitive to imetelstat, it was presumed that cloning the cells would give rise to very sensitive and very resistant populations. However, with 7 clones, all of the clones showed the same 50% cell viability in the presence of imetelstat in the 5-day drug response assay. This would suggest that either the mechanism of sensitivity to imetelstat is inherent in every cell but only some cells succumb to the treatment

or possibly that in the time necessary to grow up the clones to a larger population, perhaps the cells recapitulate the diversity of the parental population similar to what is seen with culturing cancer stem cell populations (Sullivan, Spinola et al. 2010).

Because H2073 is not sensitive to mismatch control, the sensitivity to imetelstat is presumed to be telomerase specific. The control mismatch oligo has the same backbone modifications and attached lipid moiety as the imetelstat oligo as well as the same GC% content but H2073 is not sensitive to the mismatch control. Over expression of hTERT to increase telomerase activity did not show any change to the response of H2073 to imetelstat in the 5-day assay. This supports the hypothesis that sensitivity of H2073 is off-target and not telomerase related.

H2073 cells were treated long-term in bulk culture with 1 μM imetelstat to see if the 5-day and 2 week colony formation sensitivity transferred to a longer assay. While there was an immediate increase in cell death with continuous exposure to imetelstat, eventually a resistant population continued to grow with a growth curve mimicking untreated control cells. Imetelstat dose was increased to 3 μM and 5 μM to determine if the cells that continued to grow could have developed resistance to 1 μM imetelstat; however there was little change in the growth curve even with an increased dose. One future experiment to aid in determining the mechanism of sensitivity of this cell line would be to repeat the 5-day drug response assay after the long-term imetelstat treatment to see if the resistant population that survived continuous treatment showed the same drug response curve as the parental

population. If the resistant population no longer showed the 50% reduction in cell viability, the parental cells and the long-term treated resistant cells could be compared for differences in mutations, gene expression, and protein expression to determine the cause of the initial sensitivity.

Another follow-up experiment would be to treat the individual H2073 clones each long-term with 1 μM, 3 μM and 5 μM to see if they all display the same initial slowed growth with cell death and eventual outgrowth of a resistant population. If so, the long-term treated resistant populations of each clone could then be compared and assessed for changes in gene expression and protein expression. More samples to compare would aid in the elucidation of the mechanism of sensitivity and whether or not it is telomere and telomerase related.

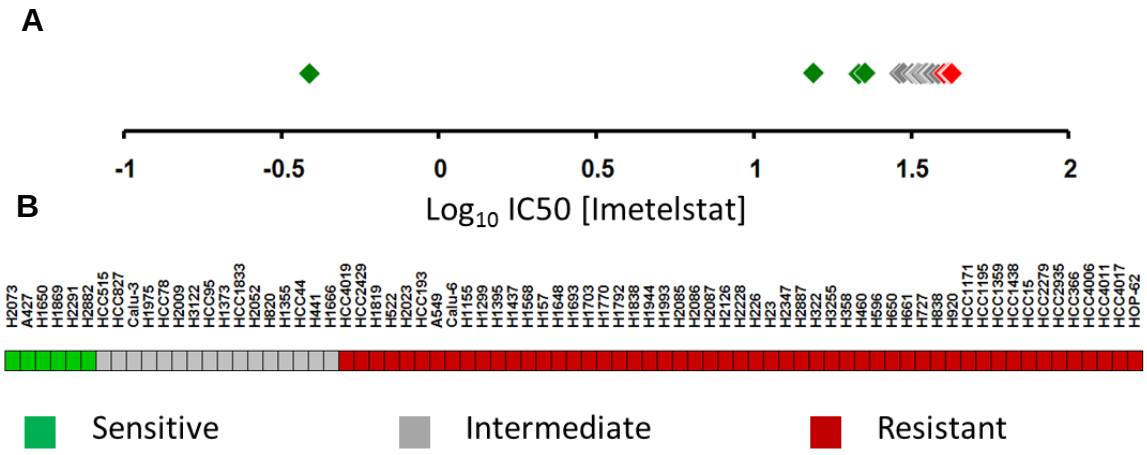


**Figure 6.1 5-day Imetelstat Sensitivity Screen.** (A) Plot of $IC_{50}$ values for 5-day drug response to imetelstat for a panel of 75 NSCLC cell lines. Each diamond represents the average $IC_{50}$ for a cell line with multiple concentration curve assays ($n \geq 4$) per cell line. An algorithm was used to determine there are 3 clusters of $IC_{50}$ values: sensitive (green), intermediate (gray), resistant (red). (B) List of cell lines in order of sensitivity. Each diamond in (A) corresponds with a square in (B) in order.

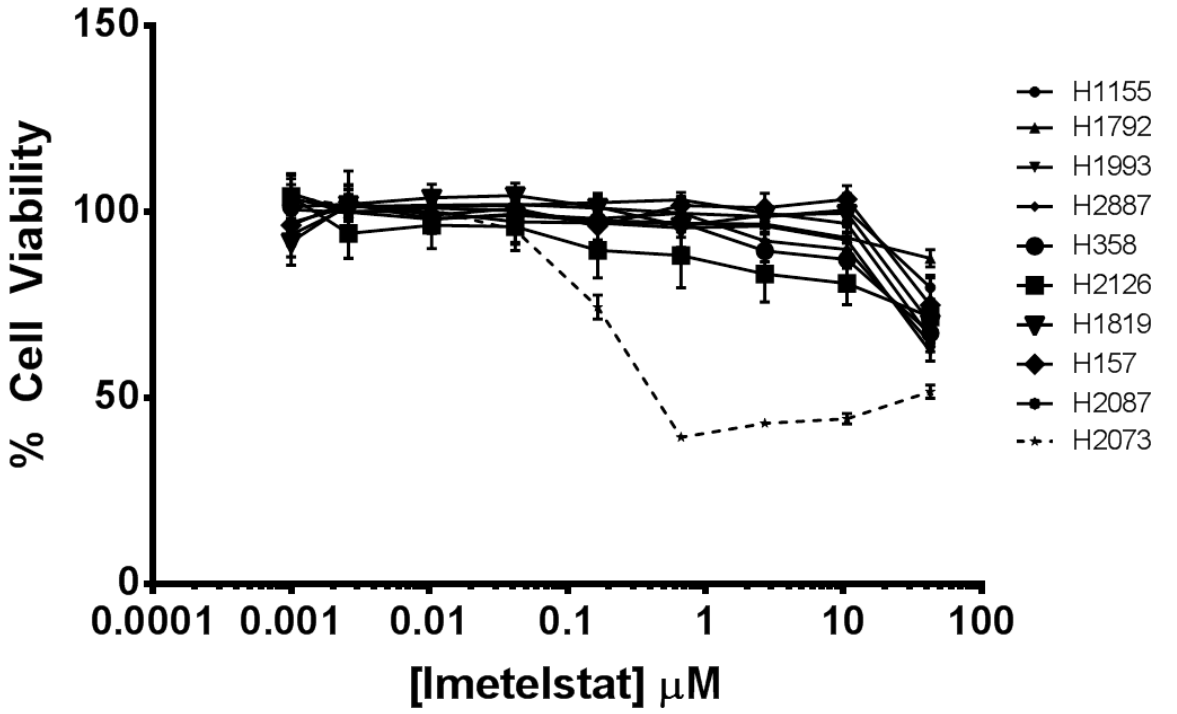


**Figure 6.2 H2073 is the Only NSCLC Cell Line Sensitive to Imetelstat.** Concentration curves for a sample of NSCLC cell lines with imetelstat. Imetelstat dose ranged from 2.6 nM-42.5 μM. Only one cell line, H2073, showed greater than 50% reduction in cell viability with less than 1 μM of imetelstat.

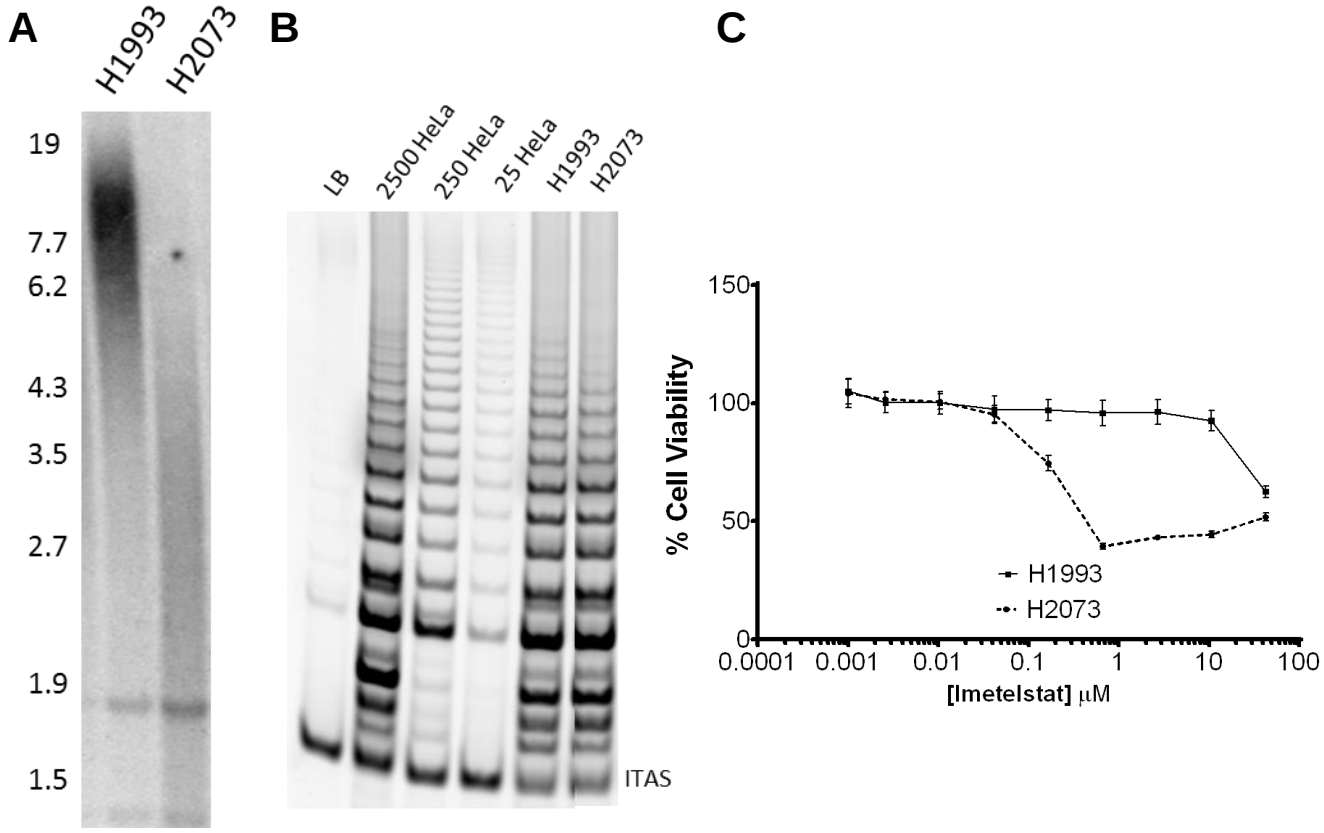


**Figure 6.3 H2073 and H1993 Comparison of Telomere Length, Telomerase Activity and 5-day Response to Imetelstat.** (A) TRF showing telomere length of H1993 (10 kb) and H2073 (3 kb). (B) TRAP assay indicating telomerase activity of H1993 and H2073. Lanes 1-4 are control lanes with 0 (lysis buffer), 2500, 250, and 25 HeLa cells for comparison. Lanes 5 and 6 are H1993 and H2073, respectively. (C) Concentration curve for 5-day drug response assay of H1993 and H2073. H1993 shows no response to imetelstat until the highest concentration tested (42.5 μM) while H2073 has less than 50% cell viability with less than 1 μM imetelstat.

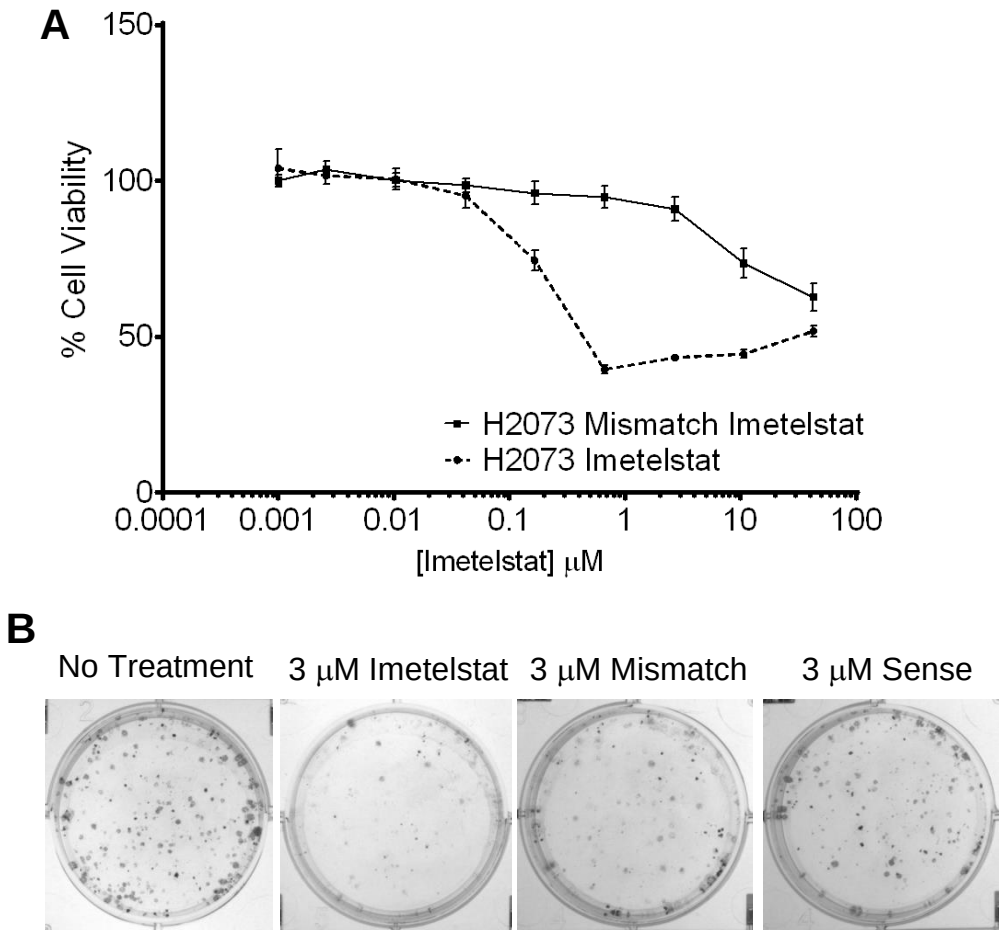


**Figure 6.4 H2073 is Not Sensitive to Imetelstat Control Oligos in 5-day Drug Response or Colony Formation Assay.** (A) Concentration curve for 5-day drug response assay with imetelstat or mismatch control oligo. H2073 shows less than 50% cell viability with less than 1 μM imetelstat but does not respond to mismatch control oligo. (B) 500 H2073 cells were plated in 6-well format. 3 μM imetelstat, mismatch or sense control was added 24 hours later. H2073 shows a 70% reduction in colony forming ability to 3 μM imetelstat but does not show the same sensitivity to mismatch or sense control oligos.

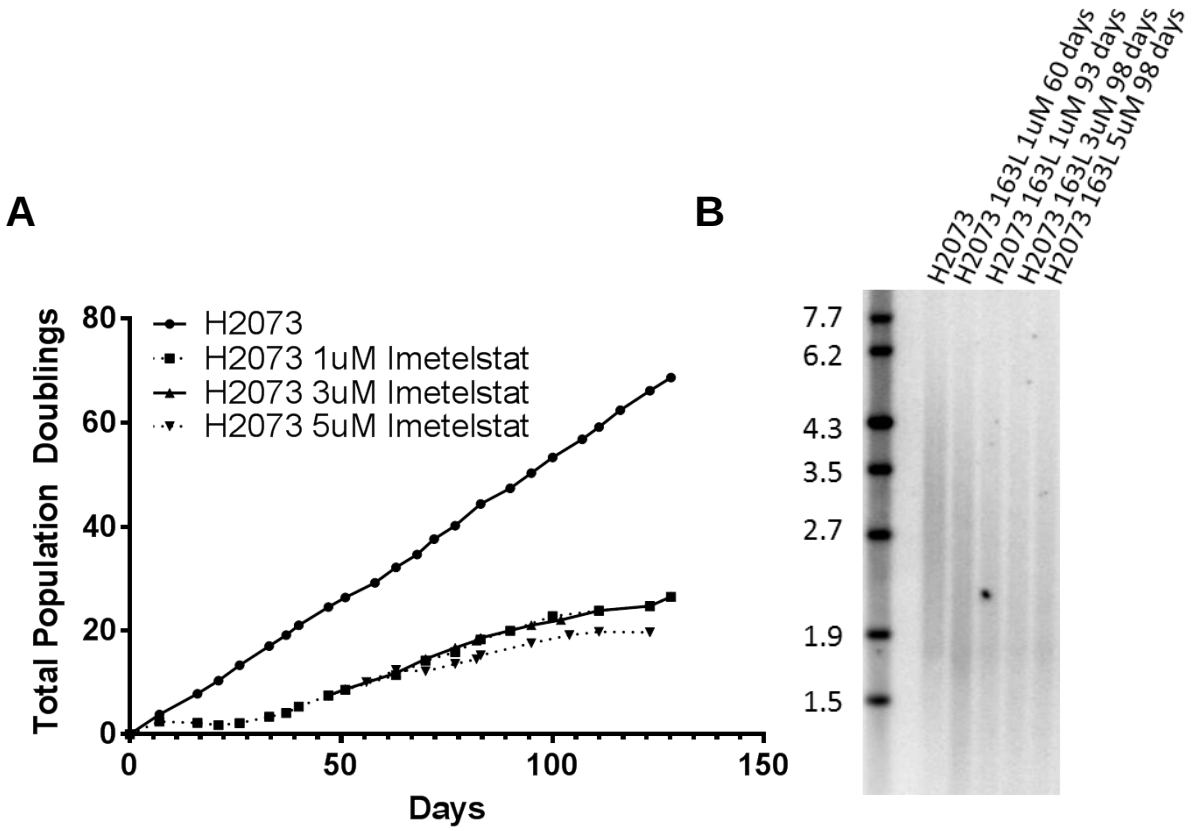


**Figure 6.5 H2073 Long-term Imetelstat Treatment.** (A) H2073 was given 1 μM imetelstat three times per week. Total population doublings is graphed versus days of treatment. At 40 days, treated cells were divided into 3 groups and treatment continued at 1 μM, 3 μM or 5 μM imetelstat. (B) Telomere length of H2073 with continuous imetelstat treatment. Parental H2073 telomeres are 3 kb. At 60 days of treatment, telomeres are shortened to 2.4 kb. 1 μM, 3 μM and 5 μM treatment at 93 and 98 days are all about 2.1 kb.

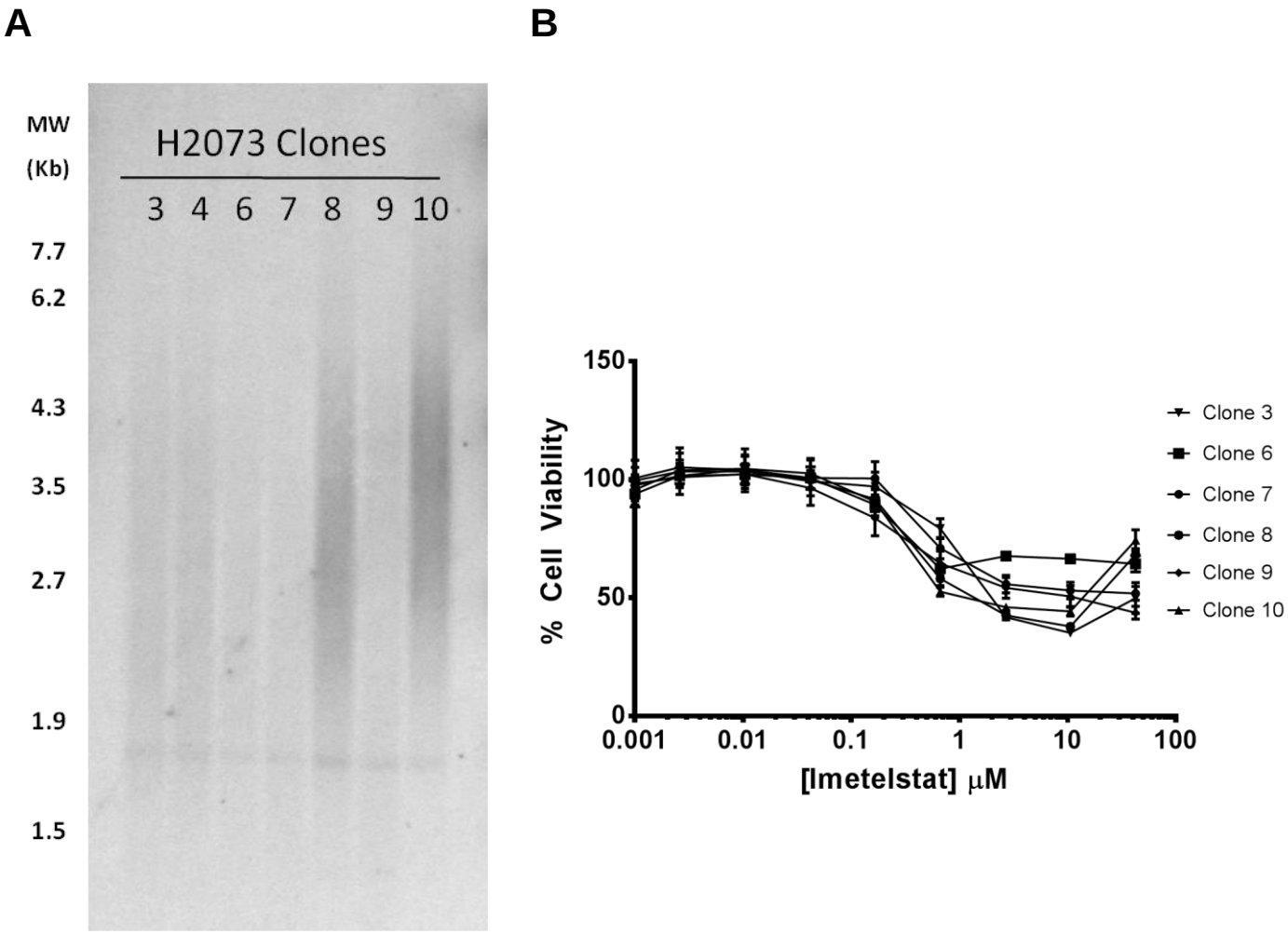


**Figure 6.6 Telomere Lengths and Drug Response for H2073 Clones.** H2073 cells were plated under clonal conditions and single clones were selected and expanded. (A) Telomere length for 7 clones. Telomere length ranges from 2.3 kb to 3.4 kb. (B) H2073 clones were tested in 5-day drug response assay. The drug response curve for all six clones tested mimics the drug response of parental H2073.

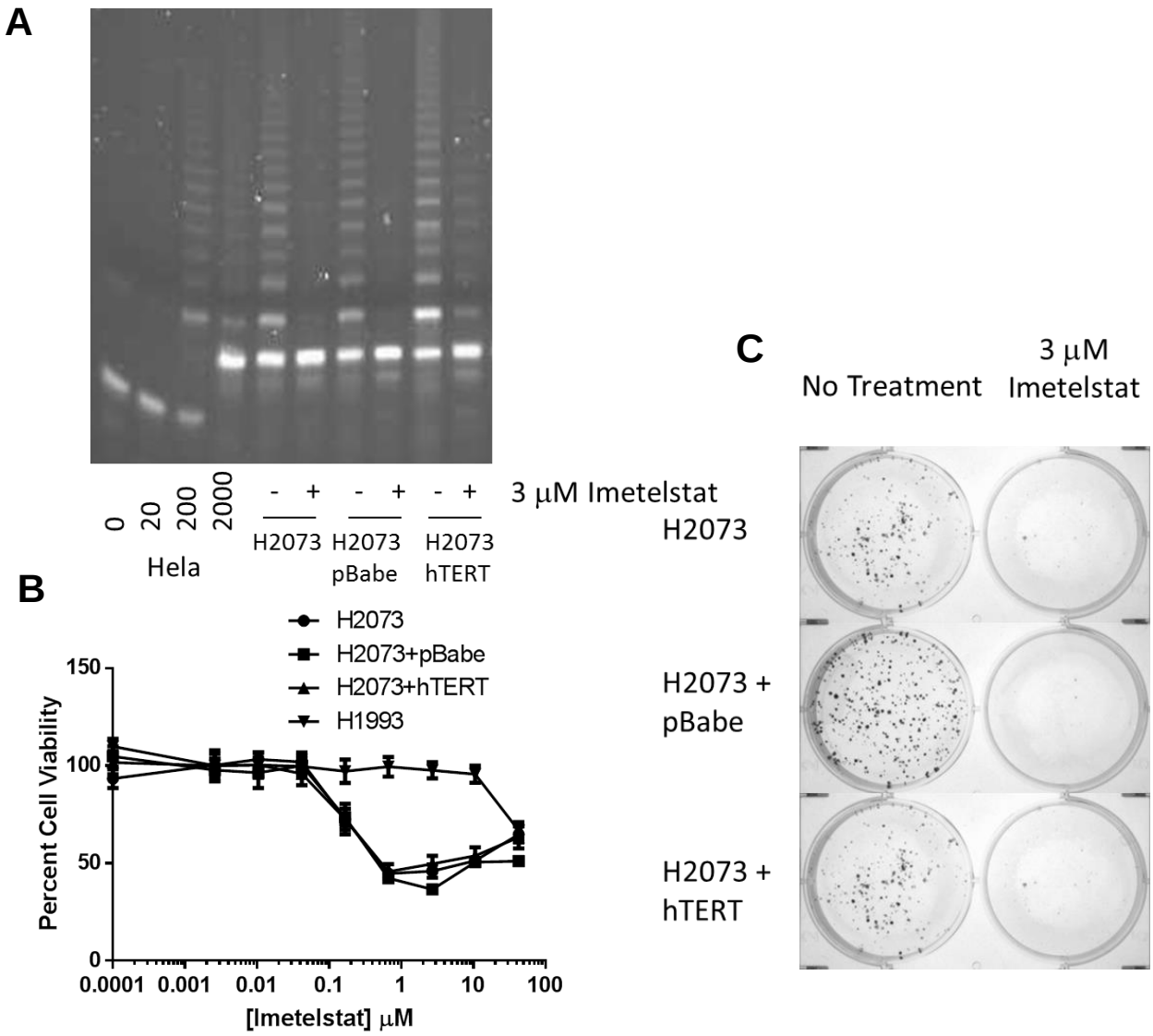


**Figure 6.7 Response of H2073 to Imetelstat with Over Expression of hTERT and Increased Telomerase Activity.** H2073 was transfected with hTERT or pBabe control vector and retested for sensitivity to imetelstat. (A) Lanes 1-4 are 0 (lysis buffer only) 20, 200, and 2000 HeLa cells for control. Lanes 5-6 are parental H2073 without and with 3 μM imetelstat. Lanes 7-8 are H2073 transfected with pBabe control vector without and with 3 μM imetelstat. Lanes 9-10 are H2073 transfected with hTERT without and with 3 μM imetelstat. H2073 hTERT shows increased telomerase activity and less response to 3 μM imetelstat compared to parental H2073. (B) H2073 parental, H2073 pBabe, H2073 hTERT and H1993 (for control) were tested in the 5-day drug response assay. H2073 parental, H2073 pBabe, and H2073 hTERT all show less than 50% cell viability with less than 1 μM imetelstat. (C) 500 H2073 parental, H2073 pBabe, or H2073 hTERT cells were plated in 6-well format. 3 μM imetelstat was added 24 hours later. All 3 H2073 cell variations are still sensitive to 3 μM imetelstat in colony forming conditions.

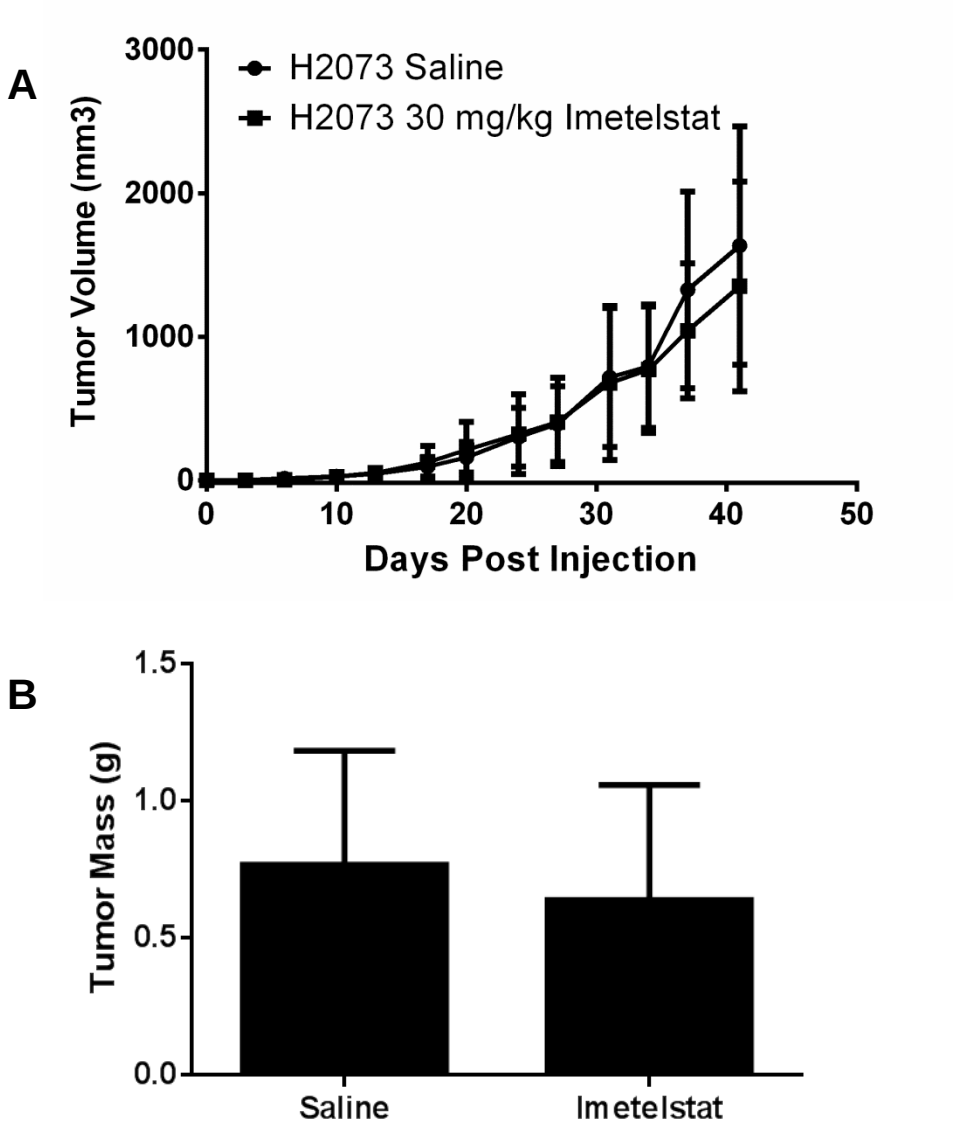


**Figure 6.8 H2073 is Not Sensitive to Imetelstat *in vivo*.** $1x10^6$ H2073 cells were injected subcutaneously into NOD/SCID mice. Mice were treated with saline (n=10) or 30 mg/kg imetelstat (n=10) three times per week starting 2 days after cell injection. (A) Growth curve of mice with saline or imetelstat treatment. There is no difference between treated and untreated growth curves. (B) Tumor weights at conclusion of experiment. There is no difference in tumor weights between treated and untreated groups.

# CHAPTER SEVEN

## DISCUSSION

Telomerase is expressed in 80-90% of lung cancers but is not active in most somatic cells making it an attractive target for cancer therapy. The proposed mechanism of action of telomerase targeted therapy is first inhibition of telomerase followed by subsequent telomere shortening with continued cell divisions leading to eventual senescence and/or apoptosis. Imetelstat is a telomerase inhibitor currently in clinical trials for many cancer types including NSCLC and is currently being tested as maintenance therapy in NSCLC. Given the proposed mechanism of action, maintenance therapy would provide the optimal therapeutic window for telomerase inhibition efficacy. This body of work supports imetelstat therapy in a maintenance setting in NSCLC.

First, tumors typically have very short telomeres because of the process of overcoming mortality stage 1 and mortality stage 2 to become cancerous. Therefore telomerase inhibition should lead to telomere-shortening induced tumor cell senescence or cell death with minimal cell divisions. In addition, lung cancer is responsible for the most cancer related deaths in the United States and smoking is one of the biggest factors in the development of lung cancer. Because cigarette smoking has been shown to correlate with

shorter telomeres (Valdes, Andrew et al. 2005; McGrath, Wong et al. 2007), telomerase targeted therapy has even greater potential in lung cancer patients.

It is important for imetelstat efficacy that once imetelstat treatment has begun, the tumor cells have constant telomerase inhibition as demonstrated by 1) elongation of telomeres in as few as 2 weeks after 40 weeks of therapy to shorten telomeres (Figure 5.2), 2) H2887 cells that responded to imetelstat in as few as 12 population doublings (26 days) but after cellular senescence and 235 days in the presence of imetelstat, imetelstat removal prompted the recovery of the cells and reengagement in active cell growth at 370 days (Figure 5.5) and 3) H460 imetelstat *in vitro* pretreated tumor cells injected into mice demonstrate a lag in tumor formation but recover with no continuous treatment *in vivo* and growth rate reaches untreated control growth rate (Figure 5.11). Current clinical trials administer imetelstat on day 1 and 8 of a 21 day cycle. Given these findings, future clinical trials should ensure that the dosing schedule is sufficient for tumors to always be in the presence of imetelstat so any progress made with telomere shortening is not negated before the next dose.

Imetelstat has the potential to be very beneficial in combination with other targeted therapies. Tumors with EGFR mutations, for example, respond very well to EGFR targeted therapies such as gefitinib or erlotinib initially but universally develop aggressive tumor recurrence and resistance to therapy. Imetelstat could work synergistically with these patients if administered in combination with the EGFR targeted therapy. If imetelstat is

begun when erlotinib or gefitinib is begun and tumors respond to the initial EGFR targeted therapy, imetelstat could be slowly shortening telomeres of the cells and any cells that eventually develop resistance to the EGFR therapy would still be susceptible to the telomere shortening and may not be capable of metastasizing or recurring. HCC827, which responded to imetelstat *in vitro* and *in vivo*, is also an EGFR mutant cell line. This supports the hypothesis that EGFR mutant cells can be susceptible to imetelstat therapy. A future experiment to further support the combination therapy would be to repeat the HCC827 *in vivo* experiments but add erlotinib or gefitinib therapy in combination with the imetelstat. Previous work has shown that HCC827 responds to erlotinib in a mouse model but eventually develops resistance in a dose dependent manner (Zhang, Lee et al.). These experiments lasted about 5 months and tumors took 6-10 weeks to recur after initial response. To determine imetelstat synergism with erlotinib therapy, HCC827 tumors could be established and then tumors divided into 2 groups, those that receive only erlotinib therapy and those that receive erlotinib plus imetelstat therapy. Experiment endpoint would be comparison of time to recurrence in imetelstat treated tumors versus no imetelstat. In the present study, HCC827 tumors showed decrease in tumor growth rates in two months so treating tumors for 5 months with imetelstat should allow time for more cells to reach critical telomere length and prevent tumor recurrence. Alternatively, Calu-3 could be tested for a similar synergistic outcome that exploits the Her2 amplification in the cell line. Calu-3 *in*

*vivo* experiments could be conducted similar to the HCC827 *in vivo* experiments proposed above but erlotinib therapy substituted with lapatinib therapy which targets Her2.

There is no correlation seen between cell lines susceptible to colony formation inhibition with imetelstat (Chapter 4) and cell lines that respond to imetelstat with long-term therapy (Chapter 5). H460 is one of the greatest non-responders with no change in colony forming ability in the presence of imetelstat. However, with long-term imetelstat treatment H460 colony forming ability decreases over time. In addition, H460 *in vitro* imetelstat pretreated cells displayed a lag in tumor development *in vivo* indicating that H460 can respond to imetelstat *in vivo* given enough time. H2882, however, showed minimal changes in growth rate with up to a year of continuous imetelstat treatment but is one of the greatest responders in the colony formation assay in the presence of imetelstat. Given these findings the range in colony formation inhibition in the presence of imetelstat is most likely a non-telomerase related effect of imetelstat and could be due to poorly understood off-target effects of imetelstat (Jackson, Zhu et al. 2007) or be a result of an as yet undetermined function of either hTR or hTERT.

Overall, imetelstat shows great potential as cancer therapy in a maintenance setting with shortest telomeres and slowest growing tumors potentially responding the best to therapy. This thesis supports this dosing regimen with the following findings:

1) Telomere length and telomerase activity varies widely among lung cancers so treating for extended time will increase likelihood of telomere shortening induced senescence or cell death in all tumors (Chapter 3)
2) Long-term continuous imetelstat treatment leads to telomerase inhibition and telomere shortening in multiple NSCLC cell lines both *in vitro* and *in vivo* and response correlates to initial average telomere length and growth rate (Chapter 5)
3) A wide range in response is seen with imetelstat in the colony formation assay, however a cause for the differences in sensitivity and resistance has not been determined (Chapter 4) but the response does not correlate with long-term treatment response (Chapter 5) suggesting response in colony formation assay may not be telomere and telomerase related
4) Only one cell line responds in a 5-day drug response assay and data supports off target effects for the response (Chapter 6)

This data supports further studies of telomerase in a maintenance setting, especially for NSCLC.

# APPENDIX A: IMETELSTAT CELL LINE DATABASE

| Cell Line | Tumor Subtype | Age | Race | Gender | Smoker (Y or N) | Smoking Pack Year |
|---|---|---|---|---|---|---|
| **A427** | | 52 | Caucasian | M | | |
| **A549** | Adenocarcinoma | 58 | Caucasian | M | | |
| **Calu-1** | Muco-epidermoid carcinoma | 47 | Caucasian | M | | |
| **Calu-3** | Adenocarcinoma | 25 | Caucasian | M | | |
| **Calu-6** | Adenocarcinoma | 61 | Caucasian | F | | |
| **H1155** | Large Cell Neuroendocrine | 36 | Caucasian | M | Y | 20 |
| **H1299** | Large Cell Neuroendocrine | 43 | Caucasian | M | Y | 50 |
| **H1355** | Adenocarcinoma | 53 | Caucasian | M | Y | 100 |
| **H1373** | Adenocarcinoma | 56 | Black | M | Y | 30 |
| **H1395** | Adenocarcinoma | 55 | Caucasian | F | Y | 15 |
| **H1437** | Adenocarcinoma | 60 | Caucasian | M | Y | 70 |
| **H1568** | Adenocarcinoma | 48 | Caucasian | F | Y | 60 |
| **H157** | Squamous | 59 | Caucasian | M | Y | |
| **H1648** | Adenocarcinoma | 39 | Black | M | Y | 40 |
| **H1650** | Adenocarcinoma | 27 | Caucasian | M | Y | 10 |
| **H1666** | Adenocarcinoma | 50 | Caucasian | F | | |
| **H1693** | Adenocarcinoma | 55 | Caucasian | F | Y | 80 |
| **H1703** | Adenosquamous | 56 | Caucasian | M | Y | 50 |
| **H1792** | Adenocarcinoma | 50 | Caucasian | M | Y | 30 |

| Cell Line | Tumor Subtype | Age | Race | Gender | Smoker (Y or N) | Smoking Pack Year |
|---|---|---|---|---|---|---|
| **H1819** | Adenocarcinoma | 55 | Caucasian | F | Y | 80 |
| **H1838** | Adenocarcinoma | | | F | | |
| **H1869** | Squamous | 58 | Caucasian | M | Y | 50 |
| **H1944** | Adenocarcinoma | 62 | Caucasian | F | Y | 40 |
| **H1975** | Adenocarcinoma | | | F | | |
| **H1993** | Adenocarcinoma | 47 | Caucasian | F | Y | 30 |
| **H2009** | Adenocarcinoma | 68 | Caucasian | F | Y | 30 |
| **H2023** | Adenocarcinoma | 26 | Caucasian | M | | |
| **H2052** | Mesothelioma | 65 | Caucasian | M | Y | 40 |
| **H2073** | Adenocarcinoma | 47 | Caucasian | F | Y | 30 |
| **H2085** | Adenocarcinoma | 45 | | M | | |
| **H2086** | Adenocarcinoma | | | M | | |
| **H2087** | Adenocarcinoma | 69 | Caucasian | M | Y | 60 |
| **H2122** | Adenocarcinoma | 46 | Caucasian | F | Y | 30 |
| **H2126** | Adenocarcinoma | 65 | Caucasian | M | | |
| **H2228** | Adenocarcinoma | | | F | | |
| **H226** | Squamous Mesothelioma | | | M | | |
| **H2291** | Adenocarcinoma | | | | | |
| **H23** | Adenocarcinoma | 51 | Black | M | Y | 40 |
| **H2347** | Adenocarcinoma | 54 | Caucasian | F | | |

| Cell Line | Tumor Subtype | Age | Race | Gender | Smoker (Y or N) | Smoking Pack Year |
|---|---|---|---|---|---|---|
| **H2882** | NSCLC | 61 | | F | | |
| **H2887** | NSCLC | 31 | | M | | |
| **H3122** | NSCLC | | | | | |
| **H322** | Adenocarcinoma | 52 | Caucasian | M | Y | 60 |
| **H3255** | Adenocarcinoma | 47 | Caucasian | F | N | |
| **H358** | Adenocarcinoma | | Caucasian | M | | |
| **H441** | Adenocarcinoma | 33 | | M | | |
| **H460** | Large Cell | | | M | | |
| **H522** | Adenocarcinoma | 60 | Caucasian | M | Y | 60 |
| **H596** | Adenosquamous | 73 | Caucasian | M | | |
| **H650** | Adenocarcinoma | | | M | | |
| **H661** | Large Cell | 43 | Caucasian | M | | |
| **H727** | Carcinoid-endocrine | 65 | Caucasian | F | Y | 60 |
| **H820** | Adenocarcinoma | 53 | Caucasian | M | | |
| **H838** | Adenocarcinoma | 59 | Caucasian | M | Y | 80 |
| **H920** | Adenocarcinoma | 44 | Caucasian | M | Y | 75 |
| **HCC1171** | NSCLC (poorly diff) | 58 | Caucasian | M | | |
| **HCC1195** | Adenocarcinoma (mixed) | 47 | Black | M | | |
| **HCC1359** | Large Cell | 55 | Black | F | | |

| Cell Line | Tumor Subtype | Age | Race | Gender | Smoker (Y or N) | Smoking Pack Year |
|---|---|---|---|---|---|---|
| **HCC1438** | Large Cell | 43 | Black | M | | |
| **HCC15** | Squamous | 55 | Black | M | | |
| **HCC1833** | Adenocarcinoma | 69 | Caucasian | F | | |
| **HCC193** | Adenocarcinoma | 71 | Caucasian | F | | |
| **HCC2279** | Adenocarcinoma | 52 | Asian | F | | |
| **HCC2429** | NSCLC (poorly diff) | | | F | | |
| **HCC2935** | Adenocarcinoma | 39 | Caucasian | M | N | |
| **HCC366** | Adenosquamous | 80 | unknown | F | | |
| **HCC4006** | Adenocarcinoma | | Caucasian | M | N | |
| **HCC4011** | Adenocarcinoma | 53 | Caucasian | M | | |
| **HCC4017** | Large Cell | 62 | Caucasian | F | | |
| **HCC4019** | Adenocarcinoma | 40 | Caucasian | M | | |
| **HCC44** | Adenocarcinoma | 54 | Caucasian | F | | |
| **HCC515** | Adenocarcinoma | 39 | Caucasian | F | | |
| **HCC78** | Adenocarcinoma | 55 | Caucasian | M | | |
| **HCC827** | Adenocarcinoma (BAC features) | 38 | Caucasian | F | | |
| **HCC95** | Squamous | 65 | Caucasian | M | | |
| **HOP62** | Adenocarcinoma | | | F | | |

| Cell Line | Telomere Length (kb) | Telomerase Activity (RTA) | SD | Residual Telomerase with 3uM Imetelstat | MTS IC50 | SD | % CFE | SD | Cell # Plated for CF |
|---|---|---|---|---|---|---|---|---|---|
| **A427** | | 8.5 | | 0.24 | 23 | 15.0 | 5.4 | 1.7 | 500 |
| **A549** | 4.7 | 11.9 | 0.1 | 0.44 | 42.5 | 0.0 | 80.7 | 23.1 | 500 |
| **Calu-1** | 2 | | | 0.14 | 42.5 | 0.0 | 27.2 | 3.2 | 500 |
| **Calu-3** | 1.5 | 11.2 | 0.0 | 0.19 | 32.0 | 11.0 | no colonies | | |
| **Calu-6** | 2.1 | 9.3 | 1.6 | 0.43 | 42.5 | 0.0 | 5.7 | 2.3 | 500 |
| **H1155** | 5 | 11.0 | 3.3 | 0.38 | 42.5 | 0.0 | 80.5 | 19.0 | 500 |
| **H1299** | 19 | 15.0 | 1.2 | 0.51 | 42.5 | 0.0 | 25.6 | 6.5 | 100 |
| **H1355** | 5.3 | 13.1 | | 0.31 | 28.5 | 8.4 | 65.8 | 15.4 | 500 |
| **H1373** | 3.2 | 26.6 | | 0.11 | 35 | 6.0 | 10.4 | 3.2 | 500 |
| **H1395** | 4.3 | 7.1 | | 0.28 | 42.5 | 0.0 | 13.6 | 3.2 | 500 |
| **H1437** | 3 | 10.4 | 1.7 | 0.34 | 42.5 | 0.0 | 93.9 | 9.9 | 500 |
| **H1568** | 9 | 14.0 | | 0.07 | 42.5 | 0.0 | 23.4 | 3.3 | 500 |
| **H157** | 4.8 | 16.7 | 3.6 | 0.09 | 42.5 | 0.0 | 47.3 | 13.6 | 500 |
| **H1648** | 2 | | | | 41.9 | 1.4 | 5.7 | 4.1 | 500 |
| **H1650** | 2.7 | 9.8 | 2.9 | 0.12 | 21.5 | 2.4 | 25.5 | 2.5 | 500 |
| **H1666** | 3.9 | | | | 38.8 | 4.6 | 5.3 | 2.4 | 2000 |
| **H1693** | 6.2 | 13.4 | 1.1 | 0.51 | 42.5 | 0.0 | 22.4 | 3.5 | 500 |
| **H1703** | 20 | | | | 41.3 | 1.8 | 16.8 | 10.6 | 1000 |
| **H1792** | 4 | 16.8 | | 0.34 | 42.5 | 0.0 | 61.1 | 7.5 | 500 |

| Cell Line | Telomere Length (kb) | Telomerase Activity (RTA) | SD | Residual Telomerase with 3uM Imetelstat | MTS IC50 | SD | % CFE | SD | Cell # Plated for CF |
|---|---|---|---|---|---|---|---|---|---|
| **H1819** | 8 | 8.5 | 1.8 | 0.11 | 38.9 | 4.9 | 35.2 | 21.7 | 500 |
| **H1838** | 3 | 16.4 | | 0.08 | 41.6 | 1.8 | 1.6 | 0.6 | 500 |
| **H1869** | | 11.6 | | 0.31 | 21.5 | 1.0 | 14.0 | 1.7 | 500 |
| **H1944** | 2 | | | | 42.5 | 0.0 | 75.6 | 13.1 | 500 |
| **H1975** | 13 | 10.3 | | 0.28 | 32.3 | 5.6 | 32.4 | 5.4 | 500 |
| **H1993** | 10 | | | | 42.5 | 0.0 | 72.3 | 11.9 | 500 |
| **H2009** | 7 | | | 0.18 | 33.5 | 4.7 | 34.9 | 8.2 | 500 |
| **H2023** | | 8.4 | | 0.17 | 42.3 | 8.7 | 31.2 | 3.7 | 500 |
| **H2052** | | 6.9 | 2.2 | 0.17 | 36.8 | 7.3 | 20.8 | 3.0 | 500 |
| **H2073** | 3 | | | 0.10 | 0.4 | 0.3 | 42.1 | 6.4 | 500 |
| **H2085** | | | | | 42.5 | 0.0 | 4.3 | 1.3 | 500 |
| **H2086** | | 12.8 | | 0.33 | 42.5 | 0.0 | 4.2 | 2.2 | 500 |
| **H2087** | 3 | 25.4 | | 0.10 | 42.5 | 0.0 | 32.5 | 16.3 | 500 |
| **H2122** | 3.9 | 18.9 | | 0.12 | 42.5 | 0.0 | 44.0 | 9.8 | 500 |
| **H2126** | 5.5 | 15.1 | 5.4 | 0.11 | 42.5 | 0.0 | 37.5 | 6.3 | 500 |
| **H2228** | 3.4 | | | | 40.2 | 3.9 | 62.1 | 13.0 | 500 |
| **H226** | 5.9 | 5.4 | 0.9 | 0.40 | 42.5 | 0.0 | 40.8 | 17.1 | 500 |
| **H2291** | 3.3 | | | | 22.5 | 7.8 | 22.5 | 7.2 | 500 |
| **H23** | 2.8 | 13.8 | | | 42.5 | 0.0 | 21.0 | 3.1 | 500 |
| **H2347** | 5.4 | 11.3 | 3.0 | 0.30 | 41.4 | 2.2 | 37.6 | 10.2 | 500 |

| Cell Line | Telomere Length (kb) | Telomerase Activity (RTA) | SD | Residual Telomerase with 3uM Imetelstat | MTS IC 50 | SD | % CFE | SD | Cell # Plated for CF |
|---|---|---|---|---|---|---|---|---|---|
| **H2882** | 8 | 12.2 | 1.0 | 0.60 | 22.5 | 9.4 | 19.4 | 10.0 | 500 |
| **H2887** | 2 | 19.5 | | 0.06 | 42.5 | 0.0 | 76.6 | 6.7 | 500 |
| **H3122** | 4 | 9.3 | 1.7 | 0.13 | 30.6 | 10.0 | 7.0 | 2.9 | 500 |
| **H322** | 4.3 | 8.4 | 1.8 | 0.36 | 42.5 | 0.0 | 60.3 | 11.9 | 500 |
| **H3255** | 3.3 | | | | | | no colonies | | |
| **H358** | 3.4 | 7.4 | 3.2 | 0.19 | 42.5 | 0.0 | 36.4 | 12.0 | 500 |
| **H441** | 3.2 | 13.4 | | 0.11 | 36.3 | 5.8 | 0.2 | 0.1 | 1000 |
| **H460** | 5 | | | | 37.3 | 8.0 | 56.6 | 23.0 | 500 |
| **H522** | 3 | 18.2 | 4.0 | 0.15 | 39 | 4.2 | 42.2 | 2.2 | 500 |
| **H596** | 4.3 | 13.7 | | 0.26 | 42.5 | 0.0 | 35.8 | 10.7 | 500 |
| **H650** | 3.7 | 19.0 | 3.1 | 0.12 | 42.5 | 0.0 | 12.5 | 2.1 | 500 |
| **H661** | 19 | | | | 40.3 | 5.0 | 43.3 | 6.7 | 500 |
| **H727** | 3.7 | 15.0 | 2.8 | 0.34 | 42.5 | 0.0 | 73.6 | 14.8 | 500 |
| **H820** | 1.9 | 9.7 | | 0.12 | 31.9 | 11.0 | 12.7 | 6.4 | 500 |
| **H838** | 6 | | | | 42.5 | 0.0 | 82.1 | 10.5 | 500 |
| **H920** | 2.4 | | | | 42.5 | 0.0 | 56.6 | 13.6 | 500 |
| **HCC1171** | | | | 0.20 | 42.5 | 0.0 | 28.4 | 2.7 | 500 |
| **HCC1195** | | 12.0 | | 0.41 | 42.5 | 0.0 | 4.1 | 2.2 | 500 |
| **HCC1359** | 8.5 | 14.9 | | 0.06 | 42.5 | 0.0 | no colonies | | |

| Cell Line | Telomere Length (kb) | Telomerase Activity (RTA) | SD | Residual Telomerase with 3uM Imetelstat | MTS IC50 | SD | % CFE | SD | Cell # Plated for CF |
|---|---|---|---|---|---|---|---|---|---|
| **HCC1438** | 3 | 5.7 | 1.3 | | 42.5 | 0.0 | 19.4 | 4.4 | 500 |
| **HCC15** | | 14.7 | | 0.16 | 42.5 | 0.0 | 77.4 | 6.5 | 500 |
| **HCC1833** | 2.4 | 10.6 | 4.8 | 0.19 | 36.4 | 4.6 | 75.6 | 23.1 | 500 |
| **HCC193** | 2.5 | 10.2 | 5.1 | | 42.3 | 0.3 | 7.3 | 3.1 | 500 |
| **HCC2279** | 2.8 | 14.4 | | 0.10 | 42.5 | 0.0 | 8.7 | 1.6 | 500 |
| **HCC2429** | 4.7 | 14.1 | 1.0 | 0.19 | 41.4 | 1.1 | 115.9 | 15.0 | 500 |
| **HCC2935** | | 12.1 | 2.6 | 0.20 | 42.5 | 0.0 | 14.0 | 4.6 | 500 |
| **HCC366** | | | | | 42.5 | 0.0 | no colonies | | |
| **HCC4006** | 13 | 16.5 | | 0.23 | 42.5 | 3.9 | 22.9 | 2.0 | 500 |
| **HCC4011** | | 13.2 | | 0.10 | 42.5 | 1.3 | low | | 500 |
| **HCC4017** | | 7.2 | 0.4 | 0.12 | 42.5 | 0.0 | 41.2 | 10.0 | 500 |
| **HCC4019** | 2.8 | 13.8 | 0.9 | | 40.0 | 2.9 | 21.0 | 3.1 | 500 |
| **HCC44** | 3 | 21.5 | | 0.15 | 37 | 5.0 | 6.6 | 1.3 | 500 |
| **HCC515** | 2 | 15.4 | 6.4 | 0.54 | 32.0 | 6.7 | 49.3 | 8.0 | 500 |
| **HCC78** | 3.6 | 12.9 | | 0.25 | 32.3 | 9.4 | 35.3 | 10.5 | 500 |
| **HCC827** | 3 | 6.4 | 3.6 | 0.12 | 30.0 | 8.7 | 15.6 | 7.5 | 500 |
| **HCC95** | 3 | 13.4 | 4.4 | 0.00 | 34.0 | 1.6 | 12.1 | 5.3 | 500 |
| **HOP62** | 5 | 12.9 | | 0.36 | 42.5 | 0.0 | 15.0 | 3.2 | 500 |

| Cell Line | % CFI | SD | Doubling Time | SD | % ALDH+ | SD |
|---|---|---|---|---|---|---|
| **A427** | 42.0 | 15.3 | 36.6 | 6.3 | | |
| **A549** | 9.4 | 26.7 | 23.9 | 2.6 | 7.03 | 4.76 |
| **Calu-1** | 60.1 | 17.0 | 49.8 | 14.9 | 3.46 | 1.52 |
| **Calu-3** | | | 40.1 | 6.3 | | |
| **Calu-6** | 34.1 | 24.7 | 31.9 | 4.7 | 2.06 | 2.91 |
| **H1155** | 35.0 | 13.3 | 23.2 | 2.0 | 2.99 | 3.13 |
| **H1299** | 38.8 | 7.7 | 22.5 | 3.4 | 2.93 | 0.73 |
| **H1355** | 80.6 | 2.1 | 48.8 | 20.5 | 0.60 | 0.71 |
| **H1373** | 92.2 | 8.2 | 36.7 | 7.0 | 3.48 | 1.99 |
| **H1395** | 71.7 | 13.1 | 50.5 | 9.4 | 5.98 | 1.94 |
| **H1437** | 14.4 | 5.7 | 28.7 | 3.8 | | |
| **H1568** | -21.7 | 21.8 | 42.5 | 9.7 | | |
| **H157** | 30.3 | 25.6 | 20.8 | 2.4 | 0.76 | 1.31 |
| **H1648** | 80.3 | 12.2 | 41.9 | 10.2 | 1.02 | 0.25 |
| **H1650** | 58.5 | 5.9 | 40.4 | 4.0 | 5.34 | 1.26 |
| **H1666** | 78.8 | 20.4 | 45.2 | 10.5 | 13.17 | 8.67 |
| **H1693** | 57.8 | 22.7 | 51.1 | 18.3 | 38.20 | 9.26 |
| **H1703** | -84.1 | 90.3 | 47.9 | 13.5 | 27.70 | 0.00 |
| **H1792** | 8.5 | 16.2 | 32.6 | 3.0 | 7.68 | 4.13 |

| Cell Line | % CFI | SD | Doubling Time | SD | % ALDH+ | SD |
|---|---|---|---|---|---|---|
| **H1819** | 48.3 | 6.3 | 51.3 | 12.5 | 37.57 | 7.49 |
| **H1838** | 12.7 | 33.5 | 71.8 | 8.7 | | |
| **H1869** | 61.5 | 17.9 | 51.8 | 21.5 | 9.17 | 0.79 |
| **H1944** | 41.0 | 11.4 | 37.8 | 6.6 | | |
| **H1975** | 36.1 | 5.4 | 42.2 | 7.9 | 3.56 | 4.08 |
| **H1993** | 18.5 | 7.7 | 31.6 | 5.5 | 2.38 | 3.70 |
| **H2009** | 37.4 | 22.4 | 29.8 | 8.3 | 4.42 | 2.36 |
| **H2023** | 54.8 | 11.8 | 32.3 | 3.4 | | |
| **H2052** | 66.7 | 11.9 | 33.4 | 4.0 | 14.53 | 3.07 |
| **H2073** | 72.1 | 13.9 | 45.3 | 7.0 | 1.35 | 1.56 |
| **H2085** | 81.2 | 11.3 | 91.1 | 38.3 | 0.05 | 0.01 |
| **H2086** | 58.9 | 41.7 | 68.5 | 12.0 | | |
| **H2087** | 93.2 | 5.2 | 51.0 | 4.8 | 14.23 | 7.46 |
| **H2122** | 36.3 | 20.5 | 31.6 | 8.4 | 1.08 | 0.33 |
| **H2126** | 19.7 | 9.2 | 41.1 | 10.0 | 0.00 | 0.00 |
| **H2228** | 32.2 | 28.5 | | | | |
| **H226** | 33.2 | 23.4 | 52.0 | 13.3 | 11.25 | 3.75 |
| **H2291** | 79.5 | 5.3 | | | | |
| **H23** | 51.1 | 19.5 | 39.1 | 3.6 | 0.14 | 0.14 |
| **H2347** | 51.9 | 4.8 | 38.6 | 6.6 | 10.70 | 0.57 |

| Cell Line | % CFI | SD | Doubling Time | SD | % ALDH+ | SD |
|---|---|---|---|---|---|---|
| **H2882** | 72.8 | 24.6 | 34.8 | 6.0 | | |
| **H2887** | 0.2 | 7.0 | 43.1 | 7.8 | 0.76 | 0.77 |
| **H3122** | -31.5 | 30.7 | 48.5 | 8.8 | | |
| **H322** | 49.1 | 12.2 | 50.6 | 6.7 | | |
| **H3255** | | | | | 6.92 | 5.01 |
| **H358** | 63.9 | 17.5 | 38.0 | 9.8 | 16.92 | 7.29 |
| **H441** | -194.2 | 62.5 | 46.5 | 8.3 | 4.41 | 1.40 |
| **H460** | 2.5 | 23.2 | 21.5 | 2.8 | 0.67 | 0.17 |
| **H522** | 27.5 | 7.8 | 48.1 | 4.3 | | |
| **H596** | 31.4 | 24.1 | 41.1 | 7.7 | | |
| **H650** | 55.5 | 4.1 | 49.4 | 3.0 | 0.39 | 0.54 |
| **H661** | 6.7 | 17.9 | 32.7 | 7.9 | 28.40 | 4.67 |
| **H727** | 34.0 | 5.2 | 41.0 | 3.3 | 45.75 | 6.15 |
| **H820** | 79.4 | 4.2 | 65.2 | 27.9 | 9.47 | 6.79 |
| **H838** | 5.3 | 25.4 | 26.4 | 2.0 | | |
| **H920** | 65.5 | 13.6 | 42.5 | 7.4 | | |
| **HCC1171** | 13.8 | 1.4 | 47.5 | 7.8 | | |
| **HCC1195** | 49.2 | 30.2 | 70.4 | 13.9 | 2.36 | 0.77 |
| **HCC1359** | | | 62.8 | 2.1 | | |

| Cell Line | % CFI | SD | Doubling Time | SD | % ALDH+ | SD |
|---|---|---|---|---|---|---|
| **HCC1438** | 59.3 | 3.9 | 37.0 | 4.1 | | |
| **HCC15** | 27.1 | 2.4 | 29.1 | 9.3 | 0.40 | 0.00 |
| **HCC1833** | 43.8 | 18.4 | 46.8 | 2.8 | | |
| **HCC193** | 41.1 | 23.1 | 45.5 | 12.9 | 15.75 | 0.64 |
| **HCC2279** | 79.4 | 5.9 | 49.3 | 7.6 | 1.25 | 0.00 |
| **HCC2429** | 63.2 | 7.8 | | | 18.36 | 10.01 |
| **HCC2935** | 17.1 | 29.7 | 70.4 | 34.5 | 3.08 | 0.00 |
| **HCC366** | | | | | | |
| **HCC4006** | 65.3 | 15.2 | 46.8 | 5.0 | 2.94 | 1.59 |
| **HCC4011** | | | 49.9 | 3.8 | 14.05 | 1.91 |
| **HCC4017** | 28.4 | 23.8 | 46.3 | 15.2 | 15.80 | 0.00 |
| **HCC4019** | 51.1 | 19.5 | 61.2 | 7.4 | | |
| **HCC44** | 96.4 | 3.1 | 36.8 | 3.0 | 9.60 | 1.42 |
| **HCC515** | 34.3 | 3.9 | 39.3 | 3.0 | 3.65 | 0.42 |
| **HCC78** | 23.1 | 13.8 | 38.7 | 6.8 | | |
| **HCC827** | 29.1 | 6.4 | 44.5 | 13.4 | 8.07 | 0.97 |
| **HCC95** | 79.9 | 9.7 | 40.6 | 3.5 | 1.12 | 0.08 |
| **HOP62** | 36.2 | 11.9 | 30.3 | 7.3 | | |

# BIBLIOGRAPHY


Aberle, D. R., C. D. Berg, et al. (2011). "The National Lung Screening Trial: overview and study design." Radiology **258**(1): 243-253.

Ahrendt, S. A., P. A. Decker, et al. (2001). "Cigarette smoking is strongly associated with mutation of the K-ras gene in patients with primary adenocarcinoma of the lung." Cancer **92**(6): 1525-1530.

Akiyama, M., T. Hideshima, et al. (2003). "Effects of oligonucleotide N3'-->P5' thio-phosphoramidate (GRN163) targeting telomerase RNA in human multiple myeloma cells." Cancer Res **63**(19): 6187-6194.

Armanios, M. and C. W. Greider (2005). "Telomerase and cancer stem cells." Cold Spring Harb Symp Quant Biol **70**: 205-208.

Asai, A., Y. Oshima, et al. (2003). "A novel telomerase template antagonist (GRN163) as a potential anticancer agent." Cancer Res **63**(14): 3931-3939.

Avilion, A. A., M. A. Piatyszek, et al. (1996). "Human telomerase RNA and telomerase activity in immortal cell lines and tumor tissues." Cancer Res **56**(3): 645-650.

Aylon, Y. and M. Oren (2011). "New plays in the p53 theater." Curr Opin Genet Dev **21**(1): 86-92.

Baird, D. M., J. Rowson, et al. (2003). "Extensive allelic variation and ultrashort telomeres in senescent human cells." Nat Genet **33**(2): 203-207.

Barma, D. K., A. Elayadi, et al. (2003). "Inhibition of telomerase by BIBR 1532 and related analogues." Bioorg Med Chem Lett **13**(7): 1333-1336.

Bianchi, A. and D. Shore (2007). "Increased association of telomerase with short telomeres in yeast." Genes Dev **21**(14): 1726-1730.

Bilaud, T., C. Brun, et al. (1997). "Telomeric localization of TRF2, a novel human telobox protein." Nat Genet **17**(2): 236-239.

Blackburn, E. H. and J. G. Gall (1978). "A tandemly repeated sequence at the termini of the extrachromosomal ribosomal RNA genes in Tetrahymena." J Mol Biol **120**(1): 33-53.

Bodnar, A. G., M. Ouellette, et al. (1998). "Extension of life-span by introduction of telomerase into normal human cells." Science **279**(5349): 349-352.

Bojovic, B. and D. L. Crowe "Resistance to telomerase inhibition by human squamous cell carcinoma cell lines." Int J Oncol **38**(4): 1175-1181.

Brandao, G. D., E. F. Brega, et al. (2012). "The role of molecular pathology in non-small-cell lung carcinoma-now and in the future." Curr Oncol **19**(Suppl 1): S24-32.

Britt-Compton, B., J. Rowson, et al. (2006). "Structural stability and chromosome-specific telomere length is governed by cis-acting determinants in humans." Hum Mol Genet **15**(5): 725-733.

Broccoli, D., A. Smogorzewska, et al. (1997). "Human telomeres contain two distinct Myb-related proteins, TRF1 and TRF2." Nat Genet **17**(2): 231-235.

Brownson, R. C., M. C. Alavanja, et al. (1998). "Epidemiology and prevention of lung cancer in nonsmokers." Epidemiol Rev **20**(2): 218-236.

Bruckova, L., T. Soukup, et al. "Proliferative potential and phenotypic analysis of long-term cultivated human granulosa cells initiated by addition of follicular fluid." J Assist Reprod Genet **28**(10): 939-950.

Bryan, T. M., A. Englezou, et al. (1995). "Telomere elongation in immortal human cells without detectable telomerase activity." EMBO J **14**(17): 4240-4248.

Bryan, T. M. and R. R. Reddel (1997). "Telomere dynamics and telomerase activity in in vitro immortalised human cells." Eur J Cancer **33**(5): 767-773.

Bryce, L. A., N. Morrison, et al. (2000). "Mapping of the gene for the human telomerase reverse transcriptase, hTERT, to chromosome 5p15.33 by fluorescence in situ hybridization." Neoplasia **2**(3): 197-201.

Capella, G., S. Cronauer-Mitra, et al. (1991). "Frequency and spectrum of mutations at codons 12 and 13 of the c-K-ras gene in human tumors." Environ Health Perspect **93**: 125-131.

Cawthon, R. M. (2002). "Telomere measurement by quantitative PCR." Nucleic Acids Res **30**(10): e47.

Cesare, A. J. and J. D. Griffith (2004). "Telomeric DNA in ALT cells is characterized by free telomeric circles and heterogeneous t-loops." Mol Cell Biol **24**(22): 9948-9957.

Chung, I., S. Osterwald, et al. (2012). "PML body meets telomere: the beginning of an ALTernate ending?" Nucleus **3**(3): 263-275.

Ciuleanu, T., T. Brodowicz, et al. (2009). "Maintenance pemetrexed plus best supportive care versus placebo plus best supportive care for non-small-cell lung cancer: a randomised, double-blind, phase 3 study." Lancet **374**(9699): 1432-1440.

Cong, Y. S., J. Wen, et al. (1999). "The human telomerase catalytic subunit hTERT: organization of the gene and characterization of the promoter." Hum Mol Genet **8**(1): 137-142.

Counter, C. M., A. A. Avilion, et al. (1992). "Telomere shortening associated with chromosome instability is arrested in immortal cells which express telomerase activity." EMBO J **11**(5): 1921-1929.

Damm, K., U. Hemmann, et al. (2001). "A highly selective telomerase inhibitor limiting human cancer cell proliferation." EMBO J **20**(24): 6958-6968.

de Lange, T. (2002). "Protection of mammalian telomeres." Oncogene **21**(4): 532-540.

de Lange, T. (2004). "T-loops and the origin of telomeres." Nat Rev Mol Cell Biol **5**(4): 323-329.

de Lange, T. (2005). "Shelterin: the protein complex that shapes and safeguards human telomeres." Genes Dev **19**(18): 2100-2110.

de Lange, T., L. Shiue, et al. (1990). "Structure and variability of human chromosome ends." Mol Cell Biol **10**(2): 518-527.

Dikmen, Z. G., G. C. Gellert, et al. (2005). "In vivo inhibition of lung cancer by GRN163L: a novel human telomerase inhibitor." Cancer Res **65**(17): 7866-7873.

Dikmen, Z. G., W. E. Wright, et al. (2008). "Telomerase targeted oligonucleotide thio-phosphoramidates in T24-luc bladder cancer cells." J Cell Biochem **104**(2): 444-452.

Djojosubroto, M. W., A. C. Chin, et al. (2005). "Telomerase antagonists GRN163 and GRN163L inhibit tumor growth and increase chemosensitivity of human hepatoma." Hepatology **42**(5): 1127-1136.

Downward, J. (1998). "Signal transduction. New exchange, new target." Nature **396**(6710): 416-417.

Downward, J. (2003). "Targeting RAS signalling pathways in cancer therapy." Nat Rev Cancer **3**(1): 11-22.

Dunham, M. A., A. A. Neumann, et al. (2000). "Telomere maintenance by recombination in human cells." Nat Genet **26**(4): 447-450.

Euhus, D. M., C. Hudd, et al. (1986). "Tumor measurement in the nude mouse." J Surg Oncol **31**(4): 229-234.

Feldser, D. M., J. A. Hackett, et al. (2003). "Telomere dysfunction and the initiation of genome instability." Nat Rev Cancer **3**(8): 623-627.

Feng, J., W. D. Funk, et al. (1995). "The RNA component of human telomerase." Science **269**(5228): 1236-1241.

Gadgeel, S. M., S. S. Ramalingam, et al. "Treatment of lung cancer." Radiol Clin North Am **50**(5): 961-974.

Gazdar, A. F., B. Gao, et al. (2010). "Lung cancer cell lines: Useless artifacts or invaluable tools for medical science?" Lung Cancer **68**(3): 309-318.

Gazdar, A. F., L. Girard, et al. (2010). "Lung cancer cell lines as tools for biomedical discovery and research." J Natl Cancer Inst **102**(17): 1310-1321.

Gazdar, A. F. and J. D. Minna (1996). "NCI series of cell lines: an historical perspective." J Cell Biochem Suppl **24**: 1-11.

Gellert, G. C., Z. G. Dikmen, et al. (2006). "Effects of a novel telomerase inhibitor, GRN163L, in human breast cancer." Breast Cancer Res Treat **96**(1): 73-81.

Goldstraw, P. (2010). The International Staging System for Lung Cancer. Principles and Practice of Lung Cancer. H. I. Pass. Philadelphia, PA, Lippincott Williams and Wilkins**:** 437-352.

Gomes, N. M., O. A. Ryder, et al. "Comparative biology of mammalian telomeres: hypotheses on ancestral states and the roles of telomeres in longevity determination." Aging Cell **10**(5): 761-768.

Gomez, D., M. F. O'Donohue, et al. (2006). "The G-quadruplex ligand telomestatin inhibits POT1 binding to telomeric sequences in vitro and induces GFP-POT1 dissociation from telomeres in human cells." Cancer Res **66**(14): 6908-6912.

Govindan, R., N. Page, et al. (2006). "Changing epidemiology of small-cell lung cancer in the United States over the last 30 years: analysis of the surveillance, epidemiologic, and end results database." J Clin Oncol **24**(28): 4539-4544.

Griffith, J. D., L. Comeau, et al. (1999). "Mammalian telomeres end in a large duplex loop." Cell **97**(4): 503-514.

Grobelny, J. V., A. K. Godwin, et al. (2000). "ALT-associated PML bodies are present in viable cells and are enriched in cells in the G(2)/M phase of the cell cycle." J Cell Sci **113 Pt 24**: 4577-4585.

Hahn, W. C., S. A. Stewart, et al. (1999). "Inhibition of telomerase limits the growth of human cancer cells." Nat Med **5**(10): 1164-1170.

Halvorsen, T. L., G. Leibowitz, et al. (1999). "Telomerase activity is sufficient to allow transformed cells to escape from crisis." Mol Cell Biol **19**(3): 1864-1870.

Harley, C. B. (1991). "Telomere loss: mitotic clock or genetic time bomb?" Mutat Res **256**(2-6): 271-282.

Harley, C. B., A. B. Futcher, et al. (1990). "Telomeres shorten during ageing of human fibroblasts." Nature **345**(6274): 458-460.

Harrington, L., W. Zhou, et al. (1997). "Human telomerase contains evolutionarily conserved catalytic and structural subunits." Genes Dev **11**(23): 3109-3115.

Hayflick, L. and P. S. Moorhead (1961). "The serial cultivation of human diploid cell strains." Exp Cell Res **25**: 585-621.

Hemann, M. T., M. A. Strong, et al. (2001). "The shortest telomere, not average telomere length, is critical for cell viability and chromosome stability." Cell **107**(1): 67-77.

Henderson, S., R. Allsopp, et al. (1996). "In situ analysis of changes in telomere size during replicative aging and cell transformation." J Cell Biol **134**(1): 1-12.

Henson, J. D., Y. Cao, et al. (2009). "DNA C-circles are specific and quantifiable markers of alternative-lengthening-of-telomeres activity." Nat Biotechnol **27**(12): 1181-1185.

Herbert, B., A. E. Pitts, et al. (1999). "Inhibition of human telomerase in immortal human cells leads to progressive telomere shortening and cell death." Proc Natl Acad Sci U S A **96**(25): 14276-14281.

Herbert, B. S., G. C. Gellert, et al. (2005). "Lipid modification of GRN163, an N3'-->P5' thio-phosphoramidate oligonucleotide, enhances the potency of telomerase inhibition." Oncogene **24**(33): 5262-5268.

Herbert, B. S., J. W. Shay, et al. (2003). "Analysis of telomeres and telomerase." Curr Protoc Cell Biol **Chapter 18**: Unit 18 16.

Hiyama, E., K. Hiyama, et al. (1995). "Correlating telomerase activity levels with human neuroblastoma outcomes." Nat Med **1**(3): 249-255.

Hochreiter, A. E., H. Xiao, et al. (2006). "Telomerase template antagonist GRN163L disrupts telomere maintenance, tumor growth, and metastasis of breast cancer." Clin Cancer Res **12**(10): 3184-3192.

Hockemeyer, D., W. Palm, et al. (2007). "Telomere protection by mammalian Pot1 requires interaction with Tpp1." Nat Struct Mol Biol **14**(8): 754-761.

Horikawa, I., P. L. Cable, et al. (1999). "Cloning and characterization of the promoter region of human telomerase reverse transcriptase gene." Cancer Res **59**(4): 826-830.

Huffman, K. E., S. D. Levene, et al. (2000). "Telomere shortening is proportional to the size of the G-rich telomeric 3'-overhang." J Biol Chem **275**(26): 19719-19722.

Jackson, S. R., C. H. Zhu, et al. (2007). "Antiadhesive effects of GRN163L--an oligonucleotide N3'->P5' thio-phosphoramidate targeting telomerase." Cancer Res **67**(3): 1121-1129.

Januszkiewicz, D., J. Wysoki, et al. (2003). "Lack of correlation between telomere length and telomerase activity and expression in leukemic cells." Int J Mol Med **12**(6): 935-938.

Jett, J. (2012). "Screening for lung cancer: who should be screened?" Arch Pathol Lab Med **136**(12): 1511-1514.

Kelland, L. R. (2005). "Overcoming the immortality of tumour cells by telomere and telomerase based cancer therapeutics--current status and future prospects." Eur J Cancer **41**(7): 971-979.

Kilian, A., D. D. Bowtell, et al. (1997). "Isolation of a candidate human telomerase catalytic subunit gene, which reveals complex splicing patterns in different cell types." Hum Mol Genet **6**(12): 2011-2019.

Kim, N. W., M. A. Piatyszek, et al. (1994). "Specific association of human telomerase activity with immortal cells and cancer." Science **266**(5193): 2011-2015.

Kim, S. H., C. Beausejour, et al. (2004). "TIN2 mediates functions of TRF2 at human telomeres." J Biol Chem **279**(42): 43799-43804.

Kipling, D. and H. J. Cooke (1990). "Hypervariable ultra-long telomeres in mice." Nature **347**(6291): 400-402.

Kreuzer, M., L. Kreienbrock, et al. (1999). "Histologic types of lung carcinoma and age at onset." Cancer **85**(9): 1958-1965.

Lam, Y. C., S. Akhter, et al. (2010). "SNMIB/Apollo protects leading-strand telomeres against NHEJ-mediated repair." EMBO J **29**(13): 2230-2241.

Lane, D. P. (1992). "Cancer. p53, guardian of the genome." Nature **358**(6381): 15-16.

Lansdorp, P. M., N. P. Verwoerd, et al. (1996). "Heterogeneity in telomere length of human chromosomes." Hum Mol Genet **5**(5): 685-691.

Lee, K. M., K. H. Choi, et al. (2004). "Use of exogenous hTERT to immortalize primary human cells." Cytotechnology **45**(1-2): 33-38.

Levine, A. J. and M. Oren (2009). "The first 30 years of p53: growing ever more complex." Nat Rev Cancer **9**(10): 749-758.

Levy, M. Z., R. C. Allsopp, et al. (1992). "Telomere end-replication problem and cell aging." J Mol Biol **225**(4): 951-960.

Li, B., S. Oestreich, et al. (2000). "Identification of human Rap1: implications for telomere evolution." Cell **101**(5): 471-483.

Lin, K. W. and J. Yan (2005). "The telomere length dynamic and methods of its assessment." J Cell Mol Med **9**(4): 977-989.

Lustig, A. J. (1999). "Crisis intervention: the role of telomerase." Proc Natl Acad Sci U S A **96**(7): 3339-3341.

Maemondo, M., A. Inoue, et al. (2010). "Gefitinib or chemotherapy for non-small-cell lung cancer with mutated EGFR." N Engl J Med **362**(25): 2380-2388.

Marcand, S., V. Brevet, et al. (1999). "Progressive cis-inhibition of telomerase upon telomere elongation." EMBO J **18**(12): 3509-3519.

Marian, C. O., S. K. Cho, et al. "The telomerase antagonist, imetelstat, efficiently targets glioblastoma tumor-initiating cells leading to decreased proliferation and tumor growth." Clin Cancer Res **16**(1): 154-163.

Marian, C. O. and J. W. Shay (2009). "Prostate tumor-initiating cells: a new target for telomerase inhibition therapy?" Biochim Biophys Acta **1792**(4): 289-296.

Marian, C. O., W. E. Wright, et al. "The effects of telomerase inhibition on prostate tumor-initiating cells." Int J Cancer **127**(2): 321-331.

Martens, U. M., J. M. Zijlmans, et al. (1998). "Short telomeres on human chromosome 17p." Nat Genet **18**(1): 76-80.

McGrath, M., J. Y. Wong, et al. (2007). "Telomere length, cigarette smoking, and bladder cancer risk in men and women." Cancer Epidemiol Biomarkers Prev **16**(4): 815-819.

Meyerson, M., C. M. Counter, et al. (1997). "hEST2, the putative human telomerase catalytic subunit gene, is up-regulated in tumor cells and during immortalization." Cell **90**(4): 785-795.

Morales, C. P., S. E. Holt, et al. (1999). "Absence of cancer-associated changes in human fibroblasts immortalized with telomerase." Nat Genet **21**(1): 115-118.

Moyzis, R. K., J. M. Buckingham, et al. (1988). "A highly conserved repetitive DNA sequence, (TTAGGG)n, present at the telomeres of human chromosomes." Proc Natl Acad Sci U S A **85**(18): 6622-6626.

Muscat, J. E. and E. L. Wynder (1995). "Lung cancer pathology in smokers, ex-smokers and never smokers." Cancer Lett **88**(1): 1-5.

Naasani, I., H. Seimiya, et al. (1998). "Telomerase inhibition, telomere shortening, and senescence of cancer cells by tea catechins." Biochem Biophys Res Commun **249**(2): 391-396.

Nakamura, T. M., G. B. Morin, et al. (1997). "Telomerase catalytic subunit homologs from fission yeast and human." Science **277**(5328): 955-959.

Nakayama, J., H. Tahara, et al. (1998). "Telomerase activation by hTRT in human normal fibroblasts and hepatocellular carcinomas." Nat Genet **18**(1): 65-68.

Newbold, R. F. (2005). Cellular Immortalization and telomerase activation in cancer. M. a. S. Knowles, P, Oxford Univeristy Press**:** 107-185.

Oie, H. K., E. K. Russell, et al. (1996). "Cell culture methods for the establishment of the NCI series of lung cancer cell lines." J Cell Biochem Suppl **24**: 24-31.

Ozawa, T., S. M. Gryaznov, et al. (2004). "Antitumor effects of specific telomerase inhibitor GRN163 in human glioblastoma xenografts." Neuro Oncol **6**(3): 218-226.

Pao, W., V. A. Miller, et al. (2005). "Acquired resistance of lung adenocarcinomas to gefitinib or erlotinib is associated with a second mutation in the EGFR kinase domain." PLoS Med **2**(3): e73.

Pao, W., T. Y. Wang, et al. (2005). "KRAS mutations and primary resistance of lung adenocarcinomas to gefitinib or erlotinib." PLoS Med **2**(1): e17.

Park, J. I., A. S. Venteicher, et al. (2009). "Telomerase modulates Wnt signalling by association with target gene chromatin." Nature **460**(7251): 66-72.

Pennarun, G., C. Granotier, et al. (2008). "Role of ATM in the telomere response to the G-quadruplex ligand 360A." Nucleic Acids Res **36**(5): 1741-1754.

Phatak, P., J. C. Cookson, et al. (2007). "Telomere uncapping by the G-quadruplex ligand RHPS4 inhibits clonogenic tumour cell growth in vitro and in vivo consistent with a cancer stem cell targeting mechanism." Br J Cancer **96**(8): 1223-1233.

Phelps, R. M., B. E. Johnson, et al. (1996). "NCI-Navy Medical Oncology Branch cell line data base." J Cell Biochem Suppl **24**: 32-91.

Pongracz, K. (1999). "Oligonucleotide N3'--P5' thiophosphoramidates: synthesis and properties." Tetrahedron Letters **40**(43): 7661-7664.

Poremba, C., H. Willenbring, et al. (1999). "Telomerase activity distinguishes between neuroblastomas with good and poor prognosis." Ann Oncol **10**(6): 715-721.

Radzikowska, E., P. Glaz, et al. (2002). "Lung cancer in women: age, smoking, histology, performance status, stage, initial treatment and survival. Population-based study of 20 561 cases." Ann Oncol **13**(7): 1087-1093.

Raz, D. J., D. V. Glidden, et al. (2007). "Clinical characteristics and survival of patients with surgically resected, incidentally detected lung cancer." J Thorac Oncol **2**(2): 125-130.

Reddel, R. R. (2000). "The role of senescence and immortalization in carcinogenesis." Carcinogenesis **21**(3): 477-484.

Reddel, R. R. (2003). "Alternative lengthening of telomeres, telomerase, and cancer." Cancer Lett **194**(2): 155-162.

Riely, G. J., J. Marks, et al. (2009). "KRAS mutations in non-small cell lung cancer." Proc Am Thorac Soc **6**(2): 201-205.

Rodenhuis, S. and R. J. Slebos (1990). "The ras oncogenes in human lung cancer." Am Rev Respir Dis **142**(6 Pt 2): S27-30.

Roth, A., C. B. Harley, et al. "Imetelstat (GRN163L)--telomerase-based cancer therapy." Recent Results Cancer Res **184**: 221-234.

Sabourin, M., C. T. Tuzon, et al. (2007). "Telomerase and Tel1p preferentially associate with short telomeres in S. cerevisiae." Mol Cell **27**(4): 550-561.

Scagliotti, G., N. Hanna, et al. (2009). "The differential efficacy of pemetrexed according to NSCLC histology: a review of two Phase III studies." Oncologist **14**(3): 253-263.

Seimiya, H., T. Oh-hara, et al. (2002). "Telomere shortening and growth inhibition of human cancer cells by novel synthetic telomerase inhibitors MST-312, MST-295, and MST-1991." Mol Cancer Ther **1**(9): 657-665.

Shammas, M. A., R. J. Shmookler Reis, et al. (2004). "Telomerase inhibition and cell growth arrest after telomestatin treatment in multiple myeloma." Clin Cancer Res **10**(2): 770-776.

Sharma, H. W., R. Hsiao, et al. (1996). "Telomerase as a potential molecular target to study G-quartet phosphorothioates." Antisense Nucleic Acid Drug Dev **6**(1): 3-7.

Sharma, S. V., D. W. Bell, et al. (2007). "Epidermal growth factor receptor mutations in lung cancer." Nat Rev Cancer **7**(3): 169-181.

Shay, J. W. and W. E. Wright (2001). "Aging. When do telomeres matter?" Science **291**(5505): 839-840.

Shields, J. M., K. Pruitt, et al. (2000). "Understanding Ras: 'it ain't over 'til it's over'." Trends Cell Biol **10**(4): 147-154.

Shigematsu, H. and A. F. Gazdar (2006). "Somatic mutations of epidermal growth factor receptor signaling pathway in lung cancers." Int J Cancer **118**(2): 257-262.

Siegel, R., D. Naishadham, et al. (2012). "Cancer statistics, 2012." CA Cancer J Clin **62**(1): 10-29.

Stockwell, H. G., A. L. Goldman, et al. (1992). "Environmental tobacco smoke and lung cancer risk in nonsmoking women." J Natl Cancer Inst **84**(18): 1417-1422.

Strahl, C. and E. H. Blackburn (1994). "The effects of nucleoside analogs on telomerase and telomeres in Tetrahymena." Nucleic Acids Res **22**(6): 893-900.

Strahl, C. and E. H. Blackburn (1996). "Effects of reverse transcriptase inhibitors on telomere length and telomerase activity in two immortalized human cell lines." Mol Cell Biol **16**(1): 53-65.

Suda, K., K. Tomizawa, et al. (2010). "Biological and clinical significance of KRAS mutations in lung cancer: an oncogenic driver that contrasts with EGFR mutation." Cancer Metastasis Rev **29**(1): 49-60.

Sullivan, J. P. and J. D. Minna (2010). "Tumor oncogenotypes and lung cancer stem cell identity." Cell Stem Cell **7**(1): 2-4.

Sullivan, J. P., M. Spinola, et al. (2010). "Aldehyde dehydrogenase activity selects for lung adenocarcinoma stem cells dependent on notch signaling." Cancer Res **70**(23): 9937-9948.

Sun, S., J. H. Schiller, et al. (2007). "Lung cancer in never smokers--a different disease." Nat Rev Cancer **7**(10): 778-790.

Teixeira, M. T., M. Arneric, et al. (2004). "Telomere length homeostasis is achieved via a switch between telomerase- extendible and -nonextendible states." Cell **117**(3): 323-335.

Toh, C. K., F. Gao, et al. (2006). "Never-smokers with lung cancer: epidemiologic evidence of a distinct disease entity." J Clin Oncol **24**(15): 2245-2251.

Triano, L. R., H. Deshpande, et al. (2010). "Management of patients with advanced non-small cell lung cancer: current and emerging options." Drugs **70**(2): 167-179.

Ulaner, G. A., J. F. Hu, et al. (1998). "Telomerase activity in human development is regulated by human telomerase reverse transcriptase (hTERT) transcription and by alternate splicing of hTERT transcripts." Cancer Res **58**(18): 4168-4172.

Valdes, A. M., T. Andrew, et al. (2005). "Obesity, cigarette smoking, and telomere length in women." Lancet **366**(9486): 662-664.

van Staveren, W. C., D. Y. Solis, et al. (2009). "Human cancer cell lines: Experimental models for cancer cells in situ? For cancer stem cells?" Biochim Biophys Acta **1795**(2): 92-103.

Vojtek, A. B. and C. J. Der (1998). "Increasing complexity of the Ras signaling pathway." J Biol Chem **273**(32): 19925-19928.

Wang, E. S., K. Wu, et al. (2004). "Telomerase inhibition with an oligonucleotide telomerase template antagonist: in vitro and in vivo studies in multiple myeloma and lymphoma." Blood **103**(1): 258-266.

Wang, S. J., T. Sakamoto, et al. (2002). "The relationship between telomere length and telomerase activity in gynecologic cancers." Gynecol Oncol **84**(1): 81-84.

Ward, R. J. and C. Autexier (2005). "Pharmacological telomerase inhibition can sensitize drug-resistant and drug-sensitive cells to chemotherapeutic treatment." Mol Pharmacol **68**(3): 779-786.

Watson, J. D. (1972). "Origin of concatemeric T7 DNA." Nat New Biol **239**(94): 197-201.

Weinrich, S. L., R. Pruzan, et al. (1997). "Reconstitution of human telomerase with the template RNA component hTR and the catalytic protein subunit hTRT." Nat Genet **17**(4): 498-502.

Wright, W. E., O. M. Pereira-Smith, et al. (1989). "Reversible cellular senescence: implications for immortalization of normal human diploid fibroblasts." Mol Cell Biol **9**(7): 3088-3092.

Wright, W. E., M. A. Piatyszek, et al. (1996). "Telomerase activity in human germline and embryonic tissues and cells." Dev Genet **18**(2): 173-179.

Wright, W. E. and J. W. Shay (2002). "Historical claims and current interpretations of replicative aging." Nat Biotechnol **20**(7): 682-688.

Wright, W. E., V. M. Tesmer, et al. (1997). "Normal human chromosomes have long G-rich telomeric overhangs at one end." Genes Dev **11**(21): 2801-2809.

Wu, P., M. van Overbeek, et al. (2010). "Apollo contributes to G overhang maintenance and protects leading-end telomeres." Mol Cell **39**(4): 606-617.

Xin, H., D. Liu, et al. (2007). "TPP1 is a homologue of ciliate TEBP-beta and interacts with POT1 to recruit telomerase." Nature **445**(7127): 559-562.

Ye, J. Z., J. R. Donigian, et al. (2004). "TIN2 binds TRF1 and TRF2 simultaneously and stabilizes the TRF2 complex on telomeres." J Biol Chem **279**(45): 47264-47271.

Ye, J. Z., D. Hockemeyer, et al. (2004). "POT1-interacting protein PIP1: a telomere length regulator that recruits POT1 to the TIN2/TRF1 complex." Genes Dev **18**(14): 1649-1654.

Yeager, T. R., A. A. Neumann, et al. (1999). "Telomerase-negative immortalized human cells contain a novel type of promyelocytic leukemia (PML) body." Cancer Res **59**(17): 4175-4179.

Zhang, A., C. Zheng, et al. (2000). "Frequent amplification of the telomerase reverse transcriptase gene in human tumors." Cancer Res **60**(22): 6230-6235.

Zhang, X., V. Mar, et al. (1999). "Telomere shortening and apoptosis in telomerase-inhibited human tumor cells." Genes Dev **13**(18): 2388-2399.

Zhang, Z., J. C. Lee, et al. "Activation of the AXL kinase causes resistance to EGFR-targeted therapy in lung cancer." Nat Genet **44**(8): 852-860.

Zhong, Z., L. Shiue, et al. (1992). "A mammalian factor that binds telomeric TTAGGG repeats in vitro." Mol Cell Biol **12**(11): 4834-4843.

Zimmermann, S. and U. M. Martens (2007). "Telomeres and telomerase as targets for cancer therapy." Cell Mol Life Sci **64**(7-8): 906-921.